

Quantum Nature of the Big Bang: An Analytical and Numerical Investigation I

Abhay Ashtekar^{1,2,3,*}, Tomasz Pawłowski^{1,†} and Parampreet Singh^{1,2‡}

¹*Institute for Gravitational Physics and Geometry
Physics Department, Penn State, University Park, PA 16802, U.S.A.*

²*Inter-University Centre for Astronomy and Astrophysics
post bag 4, Ganeshkhind, Pune 411 017, India*

³*Isaac Newton Institute for Mathematical Sciences,
20 Clarkson Road, Cambridge CB3 0EH, UK*

Abstract

Analytical and numerical methods are developed to analyze the quantum nature of the big bang in the setting of loop quantum cosmology. They enable one to explore the effects of quantum geometry both on the gravitational and matter sectors and significantly extend the known results on the resolution of the big bang singularity. Specifically, the following results are established for the homogeneous isotropic model with a massless scalar field: i) the scalar field is shown to serve as an internal clock, thereby providing a detailed realization of the ‘emergent time’ idea; ii) the physical Hilbert space, Dirac observables and semi-classical states are constructed rigorously; iii) the Hamiltonian constraint is solved numerically to show that *the big bang is replaced by a big bounce*. Thanks to the non-perturbative, background independent methods, unlike in other approaches the quantum evolution is *deterministic across the deep Planck regime*. Our constructions also provide a conceptual framework and technical tools which can be used in more general models. In this sense, they provide foundations for analyzing physical issues associated with the Planck regime of loop quantum cosmology as a whole.

PACS numbers: 04.60.Kz, 04.60Pp, 98.80Qc, 03.65.Sq

*Electronic address: ashtekar@gravity.psu.edu

†Electronic address: pawłowsk@gravity.psu.edu

‡Electronic address: singh@gravity.psu.edu

I. INTRODUCTION

Loop quantum gravity (LQG) is a background independent, non-perturbative approach to quantum gravity [1, 2, 3]. It is therefore well-suited for the analysis of certain long standing questions on the quantum nature of the big bang. Examples of such questions are:

- How close to the Big Bang does a smooth space-time of general relativity make sense? In particular, can one show from first principles that this approximation is valid at the onset of inflation?
- Is the Big-Bang singularity naturally resolved by quantum gravity? Or, is some external input such as a new principle or a boundary condition at the Big Bang essential?
- Is the quantum evolution across the ‘singularity’ deterministic? Since one needs a fully non-perturbative framework to answer this question in the affirmative, in the Pre-Big-Bang [4] and Ekpyrotic/Cyclic [5, 6] scenarios, for example, the answer is in the negative [7, 10].
- If the singularity is resolved, what is on the ‘other side’? Is there just a ‘quantum foam’, far removed from any classical space-time (as suggested, e.g., in [11]), or, is there another large, classical universe (as suggested, e.g., in [4, 5, 6])?

Over the years, these and related issues had been generally relegated to the ‘wish list’ of what one would like the future, satisfactory quantum gravity theory to eventually address. However, over the past five years, thanks to the seminal ideas introduced by Bojowald and others, notable progress was made on such questions in the context of symmetry reduced, minisuperspaces [12]. In particular, it was found that Riemannian quantum geometry, which comes on its own in the Planck regime, has just the right features to resolve the big-bang singularity [13] in a precise manner [14]. However, the physical ramifications of this resolution—in particular the answer to what is ‘on the other side’—have not been worked out. It is therefore natural to ask whether one can complete that analysis and systematically address the questions listed above, at least in the limited context of simple cosmological models. It turns out that the answer is in fact in the affirmative. A brief summary of arguments leading to this conclusion appeared in [15]. The purpose of this paper is to provide the detailed constructions and numerical simulations that underlie those results.

Let us begin with a brief summary of the main results of loop quantum cosmology (LQC). (For a comprehensive survey, see, e.g., [12].) They can be divided in two broad classes:
i) singularity resolution based on exact quantum equations (see e.g. [13, 14, 16, 17, 18, 19, 20]), and,
ii) phenomenological predictions based on ‘effective’ equations (see e.g. [21, 22, 23, 24, 25, 26, 27, 28, 29, 30, 31, 32, 33]).

Results in the first category make a crucial use of the effects of quantum geometry on the *gravitational part* of the Hamiltonian constraint. Because of these effects, the quantum ‘evolution’ is now dictated by a second order *difference equation* rather than the second order differential equation of the Wheeler-DeWitt (WDW) theory. Nonetheless, the intuitive idea of regarding the scale factor a as ‘internal time’ was maintained. The difference is that the ‘evolution’ now occurs in discrete steps. As explained in detail in Sec. II B, this discreteness descends directly from the quantum nature of geometry in LQG; in particular, the step size is dictated by the lowest non-zero eigenvalue of the area operator. When the universe is large, the WDW differential equation is an excellent approximation to the ‘more fundamental’ difference equation. However, in the Planck regime, there are major deviations. In particular, while the classical singularity generically persists in the WDW theory without additional inputs, this is not the case in LQG. This difference does *not* arise simply because

the discrete ‘evolution’ enables one to ‘jump over’ the classical singularity. Indeed, even when the discrete evolution passes *through* the point $a = 0$, the difference equation remains well-defined and enables one to ‘evolve’ *any* initial data across this classically singular point. It is in this sense that the singularity was said to be resolved.

In the second category of results, by and large the focus was on quantum geometry modifications of the *matter part* of the Hamiltonian constraint. The main idea is to work with approximation schemes which encode the idea of semi-classicality and to incorporate quantum geometry effects on the matter Hamiltonian by adding suitable ‘effective’ terms to the classical Hamiltonian constraint. The hope is that dynamics generated by the ‘quantum-corrected’ classical Hamiltonian would have a significant domain of validity and provide a physical understanding of certain aspects of the full quantum evolution. This strategy has led to a number of interesting insights. For example, using effective equations, it was argued that the singularity resolution is generic for all homogeneous models; that there is an early phase of inflation driven by quantum gravity effects; that this phase leads to a reduction of power spectrum in CMB at large angular scales; and that quantum geometry effects suppress the classical chaotic behavior of Bianchi IX models near classical singularity.

Attractive as these results are, important limitations have persisted. Let us begin with the results on singularity resolution. As in all non-trivially constrained systems, solutions to the quantum constraint fail to be normalizable in the kinematical Hilbert space on which the constraint operators are well-defined. Therefore one has to endow physical states (i.e. solutions to the Hamiltonian constraint) with a new, *physical inner product*. Systematic strategies —e.g., the powerful ‘group averaging procedure’ [34, 35]— typically require that the constraint be represented by a self-adjoint operator on the kinematic Hilbert space while, so far, most of the detailed discussions of singularity resolution are based on Hamiltonian constraints which do not have this property. Consequently, the space of solutions was not endowed with a Hilbert space structure. This in turn meant that one could not introduce Dirac observables nor *physical* semi-classical states. Therefore, as pointed out, e.g. in [36], the physical meaning of singularity resolution remained somewhat obscure. In particular, even in simple models, there was no clear-cut answer as to what the universe did ‘before’ the big-bang. Was there a genuine ‘quantum foam’ or was the quantum state peaked at a large classical universe on the ‘other side’? In absence of a physical Hilbert space, the second and the third questions posed in the beginning of this section could only be answered partially and the first and the fourth remained unanswered.

The phenomenological predictions have physically interesting features and serve as valuable guides for future research. However, the current form of this analysis also faces some important limitations. Many of these discussions focus only on the quantum geometry modifications of the matter Hamiltonian. This strategy has provided new insights and does serve as a useful starting point. However, there is no *a priori* reason to believe that it is consistent to ignore modifications of the gravitational part of the Hamiltonian and retain only the matter modifications. Conclusions drawn from such analysis can be taken as attractive suggestions, calling for more careful investigations, rather than firm predictions of LQC, to be compared with observations. On the conceptual side, a number of semi-classical approximations are made while deriving the effective equations. Many of them are largely violated in the Planck regime. Therefore it is difficult to regard conclusions drawn from effective equations on singularity avoidance, and on the fate of the universe beyond, as reliable. It does happen surprisingly often in physics that approximation schemes turn out to work even outside the regimes for which they were originally intended. But there is no *a priori* reason

to think that this *must* happen. To develop intuition on the validity of approximations, it is essential to make, in at least a few simple models, detailed comparisons of predictions of effective equations with those of quantum equations that are being approximated. To summarize, while LQC has led to significant progress by opening new avenues and by indicating how qualitatively new and physically desirable results can arise, the program has remained incomplete even within the realm of symmetry reduced, mini-superspace models.

The goal of this paper is to complete the program in the simplest of models by using a combination of analytical and numerical methods. The resulting theory will enable us to answer, in the context of these models, the questions raised in the beginning of this section. Specifically, we will show from first principles that: i) a classical space-time continuum is an excellent approximation till very early times, in particular at the onset of inflation; ii) the singularity is resolved in the sense that a complete set of *Dirac observables* on the *physical* Hilbert space remains well-defined throughout the evolution; iii) the big-bang is replaced by a big-bounce in the *quantum* theory; iv) there is a large classical universe on the ‘other side’, and, v) the evolution bridging the two classical branches is deterministic, thanks to the background independence and non-perturbative methods. While the paper is primarily concerned with basic conceptual and computational issues, our constructions also provide some tools for a more systematic analysis of phenomenological questions. Finally, our approach can be used in more general models. In particular, our constructions can be used also for anisotropic models and for models in which the scalar field has a potential, although certain conceptual subtleties have to be handled carefully and, more importantly, the subsequent numerical analysis is likely to be significantly more complicated. Nonetheless, in a rather well defined sense, these constructions provide a foundation from which one can systematically analyze the Planck regime in LQC well beyond the specific model discussed in detail.

The main ideas of our analysis can be summarized as follows. First, our Hamiltonian constraint is self-adjoint on the kinematical (more precisely, auxiliary) Hilbert space. Second, we use the scalar field as ‘internal time’. In the classical theory of $k = 0$ models with a massless scalar field ϕ , the scale factor a as well as ϕ are monotonic functions of time in any given solution. In the $k = 1$ case, on the other hand, since the universe recollapses, only ϕ has this property. Therefore, it seems more natural to use ϕ as ‘internal time’, which does not refer to coordinates or any other auxiliary structure. It turns out that ϕ is well-suited to be ‘*emergent time*’ also in the quantum theory. Indeed, our self-adjoint Hamiltonian constraint is of the form

$$\frac{\partial^2 \Psi}{\partial \phi^2} = -\Theta \Psi \quad (1.1)$$

where Θ does not involve ϕ and is a positive, self-adjoint, difference operator on the auxiliary Hilbert space of quantum geometry. Hence, the quantum Hamiltonian constraint can be readily regarded as a means to ‘evolve’ the wave function with respect to ϕ . Moreover, this interpretation makes the group averaging procedure similar to that used in the quantization of a ‘free’ particle in a static space-time, and therefore conceptually more transparent. Third, we can carry out the group averaging and arrive at the physical inner product. Fourth, we identify complete sets of Dirac observables on the physical Hilbert space. One such observable is provided by the momentum \hat{p}_ϕ conjugate to the scalar field ϕ and a set of them by $\hat{a}|_{\phi_o}$, the scale factor at the ‘instants of emergent time’ ϕ_o . Fifth, we construct semi-classical states which are peaked at values of these observables at late times, when the universe is large. Finally we ‘evolve’ them backwards using the Hamiltonian constraint

using the adaptive step, 4th order Runge-Kutta method. The numerical tools are adequate to keep track not only of how the peak of the wave function ‘evolves’ but also of fluctuations in the Dirac observables in the course of ‘evolution’. A variety of numerical simulations have been performed and the existence of the bounce is robust.

The paper is organized as follows. In section II we summarize the framework of LQC in the homogeneous, isotropic setting, keeping the matter field generic. We first summarize the kinematical structure [14], highlighting the origin of the qualitative difference between the WDW theory and LQC already at this level. We then provide a self-contained and systematic derivation of the quantum Hamiltonian constraint, spelling out the underlying assumptions. In section III we restrict the matter field to be a massless scalar field, present the detailed WDW theory and show that the singularity is not resolved. The choice of a massless scalar field in the detailed analysis was motivated by two considerations. First, it makes the basic constructions easier to present and the numerical simulations are substantially simpler. More importantly, in the massless case *every* classical solution is singular, whence the singularity resolution by LQC is perhaps the clearest illustration of the effects of quantum geometry. In section IV we discuss this model in detail within the LQC framework, emphasizing the dynamical differences from the WDW theory. Specifically, we present the general solution to the quantum constraint, construct the physical Hilbert space and introduce operators corresponding to Dirac observables. In section V we present the results of our numerical simulations in some detail. Solutions to the Hamiltonian constraint are constructed using two different methods, one using a Fast Fourier Transform and another by ‘evolving’ initial data using the adaptive step, 4th order Runge-Kutta method. To further ensure the robustness of conclusions, the initial data (at late ‘times’ when the universe is large) is specified in three different ways, reflecting three natural choices in the construction of semi-classical states. In all cases, the classical big-bang is replaced by a quantum big-bounce and the two ‘classical branches’ are joined by a deterministic quantum evolution. Section VI compares and contrasts the main results with those in the literature.

Issues which are closely related to (but are not an integral part of) the main results are discussed in three appendices. Appendix A is devoted to certain heuristics on effective equations and uncertainty relations which provide a physical intuition for ‘mechanisms’ underlying certain constructions and results. In Appendix B we discuss technical aspects of numerical simulations which are important but whose inclusion in the main text would have broken the flow of the argument. Finally in Appendix C we present an alternate physical Hilbert space which can be constructed by exploiting certain special features of LQC which are not found in the general setting of constrained systems. This space is more closely related to the WDW theory and could exist also in more general contexts. Its existence illustrates an alternate way to address semi-classical issues which may well be useful in full LQG.

II. LQC IN THE $k=0$ HOMOGENEOUS, ISOTROPIC SETTING

This section is divided into three parts. To make the paper self-contained, in the first we provide a brief summary of the kinematical framework, emphasizing the conceptual structure that distinguishes LQC from the WDW theory. In the second, we introduce the self-adjoint Hamiltonian constraints and their WDW limits. By spelling out the underlying assumptions clearly, we also pave the way for the construction of a more satisfactory Hamiltonian

constraint in [37].¹ In the third part, we first list issues that must be addressed to extract physics from this general program and then spell out the model considered in the rest of the paper.

A. Kinematics

1. Classical phase space

In the $k=0$ case, the spatial 3-manifold M is topologically \mathbb{R}^3 , endowed with the action of the Euclidean group. This action can be used to introduce on M a fiducial, flat metric ${}^0q_{ab}$ and an associated constant orthonormal triad ${}^0e_i^a$ and co-triad ${}^0\omega_a^i$. In full general relativity, the gravitational phase space consists of pairs (A_a^i, E_i^a) of fields on M , where A_a^i is an SU(2) connection and E_i^a an orthonormal triad (or moving frame) with density weight 1 [1]. As one would expect, in the present homogeneous, isotropic context, one can fix the gauge and spatial diffeomorphism freedom in such a way that A_a^i has only one independent component, \tilde{c} , and E_i^a , only one independent component, \tilde{p} :

$$A = \tilde{c} {}^0\omega^i \tau_i, \quad E = \tilde{p} \sqrt{{}^0q} {}^0e_i \tau^i, \quad (2.1)$$

where \tilde{c} and \tilde{p} are constants and the density weight of E has been absorbed in the determinant of the fiducial metric.² Denote by Γ_{grav}^S the subspace of the gravitational phase space Γ_{grav} defined by (2.1). Because M is non-compact and our fields are spatially homogeneous, various integrals featuring in the Hamiltonian framework of the full theory diverge. However, the presence of spatial homogeneity enables us to bypass this problem in a natural fashion: Fix a ‘cell’ \mathcal{V} adapted to the fiducial triad and restrict all integrations to this cell. (For simplicity, we will assume that this cell is cubical with respect to ${}^0q_{ab}$.) Then the gravitational symplectic structure Ω_{grav} on Γ_{grav} and fundamental Poisson brackets are given by [14]:

$$\Omega_{\text{grav}}^S = \frac{3V_o}{8\pi\gamma G} d\tilde{c} \wedge d\tilde{p}, \quad \text{and} \quad \{\tilde{c}, \tilde{p}\} = \frac{8\pi\gamma G}{3V_o} \quad (2.2)$$

where V_o is the volume of \mathcal{V} with respect to the auxiliary metric ${}^0q_{ab}$. Finally, there is a freedom to rescale the fiducial metric ${}^0q_{ab}$ by a constant and the canonical variables \tilde{c}, \tilde{p} fail to be invariant under this rescaling. But one can exploit the availability of the elementary cell \mathcal{V} to eliminate this additional ‘gauge’ freedom. For,

$$c = V_o^{\frac{1}{3}} \tilde{c} \quad \text{and} \quad p = V_o^{\frac{2}{3}} \tilde{p} \quad (2.3)$$

¹ Our conventions are somewhat different from those in the literature, especially [14]. First, we follow the standard quantum gravity convention and set $\ell_{\text{Pl}}^2 = G\hbar$ (rather than $8\pi G\hbar$). Second, we follow the general convention in geometry and set the volume element e on M to be $e := \sqrt{|\det E|}$ (rather than $e := \sqrt{|\det E|} \text{sgn}(\det E)$). This gives rise to some differences in factors of $\text{sgn} p$ in various terms in the expression of the Hamiltonian constraint. Finally, the role of the the minimum non-zero eigenvalue of area is spelled out in detail, and the typographical error in the expression of μ_o that features in the Hamiltonian constraint is corrected.

² Our conventions are such that $\tau_i \tau_j = \frac{1}{2} \varepsilon_{ijk} \tau^k - \frac{1}{4} \delta_{ij}$. Thus, $2i\tau_k = \sigma_k$, where σ_i are the Pauli matrices.

are independent of the choice of the fiducial metric ${}^0q_{ab}$. Using (c, p) , the symplectic structure and the fundamental Poisson bracket can be expressed as

$$\Omega_{\text{grav}}^S = \frac{3}{8\pi\gamma G} \, dc \wedge dp \quad \text{and} \quad \{c, p\} = \frac{8\pi\gamma G}{3}. \quad (2.4)$$

Since these expressions are now independent of the volume V_o of the cell \mathcal{V} and make no reference to the fiducial metric ${}^0q_{ab}$, it is natural to regard the pair (c, p) as the basic canonical variables on Γ_{grav}^S . In terms of p , the physical triad and co-triad are given by:

$$e_i^a = (\text{sgn } p)|p|^{-\frac{1}{2}} (V_o^{\frac{1}{3}} {}^0e_i^a), \quad \text{and} \quad \omega_a^i = (\text{sgn } p)|p|^{\frac{1}{2}} (V_o^{-\frac{1}{3}} {}^0\omega_a^i) \quad (2.5)$$

The function $\text{sgn } p$ arises because in connection-dynamics the phase space contains triads with both orientations, and since we have fixed a fiducial triad ${}^0e_i^a$, the orientation of the physical triad e_i^a is captured in the sign of p . (As in the full theory, we also allow degenerate co-triads which now correspond to $p = 0$, for which the triad vanishes.)

Finally, note that although we have introduced an elementary cell \mathcal{V} and restricted all integrals to this cell, the spatial topology is still \mathbb{R}^3 and not \mathbb{T}^3 . Had the topology been toroidal, connections with non-trivial holonomy around the three circles would have enlarged the configuration space and the phase space would then have inherited additional components.

2. Quantum kinematics

To construct quantum kinematics, one has to select a set of elementary observables which are to have unambiguous operator analogs. In non-relativistic quantum mechanics they are taken to be x, p . One might first imagine using c, p in their place. This would be analogous to the procedure adopted in the WDW theory. However, unlike in geometrodynamics, LQG now provides a well-defined kinematical framework for full general relativity, without any symmetry reduction. Therefore, in the passage to the quantum theory, we do not wish to treat the reduced theory as a system in its own right but follow the procedure used in the full theory. There, the elementary variables are: i) holonomies h_e defined by the connection A_a^i along edges e , and, ii) the fluxes of triads E_i^a across 2-surfaces S . In the present case, this naturally suggests that we use: i) the holonomies $h_k^{(\mu)}$ along straight edges $(\mu {}^0e_i^a)$ defined by the connection $A = (c/\sqrt[3]{V_o}) {}^0\omega^i \tau_i$, and ii) the momentum p itself [14]. Now, the holonomy along the k th edge is given by:

$$h_k^{(\mu)} = \cos \frac{\mu c}{2} \mathbb{I} + 2 \sin \frac{\mu c}{2} \tau_k \quad (2.6)$$

Therefore, the elementary configuration variables can be taken to be $\exp(i\mu c/2)$ of c . These are called *almost periodic* functions of c because μ is an arbitrary real number (positive if the edge is oriented along the fiducial triad vector ${}^0e_i^a$, and negative if it is oriented in the opposite direction). The theory of these functions was first analyzed by the mathematician Harold Bohr (who was Niels' brother).

Thus, in LQC one takes $e^{i\mu c/2}$ and p as the elementary classical variables which are to have unambiguous operator analogs. They are closed under the Poisson bracket on Γ_{grav}^S . Therefore, as in quantum mechanics, one can construct an abstract \star -algebra \mathfrak{a} generated

by $e^{i\mu c/2}$ and p , subject to the canonical commutation relations. The main task in quantum kinematics is to find the appropriate representation of \mathfrak{a} .

In this task, one again follows the full theory. There, surprisingly powerful theorems are now available: By appealing to the background independence of the theory, one can select an irreducible representation of the holonomy-flux algebra *uniquely* [38, 39]. The unique representation was constructed already in the mid-nineties and is therefore well understood [1, 35, 40, 41, 42, 43, 44]. In this representation, there are well defined operators corresponding to the triad fluxes and holonomies, but the connection itself does not lead to a well-defined operator. Since one follows the full theory in LQC, the resulting representation of \mathfrak{a} also has well-defined operators corresponding to p and almost periodic functions of c (and hence, holonomies), but there is no operator corresponding to c itself.

The Hilbert space underlying this representation is $\mathcal{H}_{\text{kin}}^{\text{grav}} = L^2(\mathbb{R}_{\text{Bohr}}, d\mu_{\text{Bohr}})$, where \mathbb{R}_{Bohr} is the Bohr compactification of the real line and μ_{Bohr} is the Haar measure on it. It can be characterized as the Cauchy completion of the space of continuous functions $f(c)$ on the real line with finite norm, defined by:

$$\|f\|^2 = \lim_{D \rightarrow \infty} \frac{1}{2D} \int_{-D}^D \bar{f} f \, dc. \quad (2.7)$$

An orthonormal basis in $\mathcal{H}_{\text{kin}}^{\text{grav}}$ is given by the almost periodic functions of the connection, $N_{(\mu)}(c) := e^{i\mu c/2}$. (The $N_{(\mu)}(c)$ are the LQC analogs of the spin network functions in full LQG.) They satisfy the relation

$$\langle N_{(\mu)} | N_{(\mu')} \rangle \equiv \langle e^{\frac{i\mu c}{2}} | e^{\frac{i\mu' c}{2}} \rangle = \delta_{\mu, \mu'}. \quad (2.8)$$

Note that, although the basis is of the plane wave type, the right side has a Kronecker delta, rather than the Dirac distribution. Therefore a generic element Ψ of $\mathcal{H}_{\text{kin}}^{\text{grav}}$ can be expanded as a *countable sum* $\Psi(c) = \sum_k \alpha_k N_{(\mu_k)}(c)$ where the complex coefficients α_k are subject to $\sum_k |\alpha_k|^2 < \infty$. Consequently, the intersection between $\mathcal{H}_{\text{kin}}^{\text{grav}}$ and the more familiar Hilbert space $L^2(\mathbb{R}, dc)$ of quantum mechanics (or of the WDW theory) consists only of the zero function. Thus, already at the kinematic level, the LQC Hilbert space is *very* different from that used in the WDW theory.

The action of the fundamental operators, however, is the familiar one. The configuration operator acts by multiplication and the momentum by differentiation:

$$\hat{N}_{(\mu)} \Psi(c) = \exp \frac{i\mu c}{2} \Psi(c), \quad \text{and} \quad \hat{p} \Psi(c) = -i \frac{8\pi\gamma\ell_{\text{Pl}}^2}{3} \frac{d\Psi}{dc} \quad (2.9)$$

where, as usual, $\ell_{\text{Pl}}^2 = G\hbar$. The first of these provides a 1-parameter family of unitary operators on $\mathcal{H}_{\text{kin}}^{\text{grav}}$ while the second is self-adjoint.

It is often convenient to use the Dirac bra-ket notation and set $e^{i\mu c/2} = \langle c | \mu \rangle$. In this notation, the eigenstates of \hat{p} are simply the basis vectors $|\mu\rangle$:

$$\hat{p} |\mu\rangle = \frac{8\pi\gamma\ell_{\text{Pl}}^2}{6} \mu |\mu\rangle. \quad (2.10)$$

Finally, since the operator \hat{V} representing the volume of the elementary cell \mathcal{V} is given by $\hat{V} = |\hat{p}|^{\frac{3}{2}}$, the basis vectors are also eigenstates of \hat{V} :

$$\hat{V} |\mu\rangle = \left(\frac{8\pi\gamma}{6} |\mu| \right)^{\frac{3}{2}} \ell_{\text{Pl}}^3 |\mu\rangle. \quad (2.11)$$

The algebra \mathfrak{a} , of course, also admits the familiar representation on $L^2(\mathbb{R}, dc)$. Indeed, as we will see in section III, this is precisely the ‘Schrödinger representation’ underlying the WDW theory. The LQC representation outlined above is unitarily inequivalent. This may seem surprising at first in the light of the von-Neumann uniqueness theorem of quantum mechanics. The LQG representation evades that theorem because there is no operator \hat{c} corresponding to the connection component c itself. Put differently, the theorem requires that the unitary operators $\hat{N}_{(\mu)}$ be *weakly continuous* in μ , while our operators on $\mathcal{H}_{\text{kin}}^{\text{grav}}$ are not. (For further discussion, see [45].)

B. The Hamiltonian constraint

1. Strategy

Because of spatial flatness, the gravitational part of the Hamiltonian constraint of full general relativity simplifies and assumes the form:

$$C_{\text{grav}} = -\gamma^{-2} \int_{\mathcal{V}} d^3x N \varepsilon_{ijk} F_{ab}^i e^{-1} E^{aj} E^{bk} \quad (2.12)$$

where $e := \sqrt{|\det E|}$, and where we have restricted the integral to our elementary cell \mathcal{V} . Because of spatial homogeneity the lapse N is constant and we will set it to one.

To obtain the corresponding constraint operator, we need to first express the integrand in terms of our elementary phase space functions h_e, p and their Poisson brackets. The term involving triad can be treated using the Thiemann strategy:

$$\varepsilon_{ijk} e^{-1} E^{aj} E^{bk} = \sum_k \frac{(\text{sgn } p)}{2\pi\gamma G\mu_o V_o^{1/3}} {}^o\varepsilon^{abc} {}^o\omega_c^k \text{Tr} \left(h_k^{(\mu_o)} \{ h_k^{(\mu_o)-1}, V \} \tau_i \right) \quad (2.13)$$

where $h_k^{(\mu_o)}$ is the holonomy along the edge parallel to the k th basis vector of length $\mu_o V_o^{1/3}$ with respect to ${}^oq_{ab}$, and $V = |p|^{3/2}$ is the volume function on the phase space. While the right side of (2.13) involves μ_o , it provides an exact expression for the left side which is independent of the value of μ_o .

For the field strength F_{ab}^i , we use the standard strategy used in gauge theories. Consider a square \square_{ij} in the i - j plane spanned by two of the triad vectors ${}^o\epsilon_i^a$, each of whose sides has length $\mu_o V_o^{1/3}$ with respect to the fiducial metric ${}^oq_{ab}$. Then, ‘the ab component’ of the curvature is given by:

$$F_{ab}^k = -2 \lim_{\mu_o \rightarrow 0} \text{Tr} \left(\frac{h_{\square_{ij}}^{(\mu_o)} - 1}{\mu_o^2 V_o^{2/3}} \right) \tau^k {}^o\omega_a^i {}^o\omega_b^j \quad (2.14)$$

where the holonomy $h_{\square_{ij}}^{(\mu_o)}$ around the square \square_{ij} is just the product of holonomies (2.6) along the four edges of \square_{ij} :

$$h_{\alpha_{ij}}^{(\mu_o)} = h_i^{(\mu_o)} h_j^{(\mu_o)} (h_i^{(\mu_o)})^{-1} (h_j^{(\mu_o)})^{-1}. \quad (2.15)$$

By adding the two terms and simplifying, C_{grav} can be expressed as:

$$\begin{aligned} C_{\text{grav}} &= \lim_{\mu_o \rightarrow 0} C_{\text{grav}}^{(\mu_o)}, \quad \text{where} \\ C_{\text{grav}}^{(\mu_o)} &= -\frac{4(\text{sgn } p)}{8\pi\gamma^3\mu_o^3 G} \sum_{ijk} \varepsilon^{ijk} \text{tr}(h_i^{(\mu_o)} h_j^{(\mu_o)} h_i^{(\mu_o)-1} h_j^{(\mu_o)-1} h_k^{(\mu_o)} \{h_k^{(\mu_o)-1}, V\}) \end{aligned} \quad (2.16)$$

Since $C_{\text{grav}}^{(\mu_o)}$ is now expressed entirely in terms of holonomies and p and their Poisson bracket, it is straightforward to write the corresponding quantum operator on $\mathcal{H}_{\text{kin}}^{\text{grav}}$:

$$\begin{aligned} \hat{C}_{\text{grav}}^{(\mu_o)} &= \frac{4i(\text{sgn } p)}{8\pi\gamma^3\mu_o^3\ell_{\text{Pl}}^2} \sum_{ijk} \varepsilon^{ijk} \text{Tr} \left(\hat{h}_i^{(\mu_o)} \hat{h}_j^{(\mu_o)} \hat{h}_i^{(\mu_o)-1} \hat{h}_j^{(\mu_o)-1} \hat{h}_k^{(\mu_o)} [\hat{h}_k^{(\mu_o)-1}, \hat{V}] \right) \\ &= \frac{24i(\text{sgn } p)}{8\pi\gamma^3\mu_o^3\ell_{\text{Pl}}^2} \sin^2 \mu_o c \left(\sin \frac{\mu_o c}{2} \hat{V} \cos \frac{\mu_o c}{2} - \cos \frac{\mu_o c}{2} \hat{V} \sin \frac{\mu_o c}{2} \right). \end{aligned} \quad (2.17)$$

However, the limit $\mu_o \rightarrow 0$ of this operator does not exist. This is not accidental; had the limit existed, there would be a well-defined operator corresponding to the curvature F_{ab}^i and we know that even in full LQG, while holonomy operators are well defined, there are no operators corresponding to connections and curvatures. This feature is intimately intertwined with the quantum nature of Riemannian geometry of LQG. The viewpoint in LQC is that the failure of the limit to exist is a reminder that there is an underlying *quantum* geometry where eigenvalues of the area operator are *discrete*, whence there is a smallest non-zero eigenvalue, Δ , i.e., an *area gap*. Thus, quantum geometry is telling us that it is physically incorrect to let μ_o go to zero because that limit corresponds to shrinking the area enclosed by loops \square_{ij} to zero. Rather, *the ‘correct’ field strength operator in the quantum theory is in fact non-local, given by setting μ_o in (2.14) to a non-zero value, appropriately related to Δ .* In quantum theory, we simply can not force locality by shrinking the loops \square_{ij} to zero area. In the classical limit, however, we are led to ignore quantum geometry, and recover the usual, local field F_{ab} [14, 24].

There are two ways of implementing this strategy. In this paper, we will discuss the one that has been used in the literature [12, 14, 20]. The second strategy will be discussed in [37]; it has a more direct motivation and is more satisfactory in semi-classical considerations especially in presence of a non-zero cosmological constant.

In the above discussion, μ_o enters through holonomies $h_k^{(\mu_o)}$. Now, it is straightforward to verify that (every matrix element of) $h_k^{(\mu_o)}$ is an eigenstate of the area operator $\widehat{Ar} = \widehat{|p|}$ (associated with the face of the elementary cell \mathcal{V} orthogonal to the k th direction):

$$\widehat{Ar} h_k^{(\mu_o)}(c) = \left(\frac{8\pi\gamma\mu_o}{6} \ell_{\text{Pl}}^2 \right) h_k^{(\mu_o)}(c). \quad (2.18)$$

In the first strategy, one fixes μ_o by demanding that this eigenvalue be $\Delta = 2\sqrt{3}\pi\gamma\ell_{\text{Pl}}^2$, the area gap [1, 46], so that $\mu_o = 3\sqrt{3}/2$.

To summarize, by making use of some key physical features of quantum geometry in LQG, we have arrived at a ‘quantization’ of the classical constraint C_{grav} :

$$\hat{C}_{\text{grav}} = \hat{C}_{\text{grav}}^{(\mu_o)} \big|_{\mu_o = \frac{3\sqrt{3}}{2}} \quad (2.19)$$

There are still factor ordering ambiguities which will be fixed in the section II B 2.

We will conclude our summary of the quantization strategy by comparing this construction with that used in full LQG [1, 3, 47]. As one would expect, the curvature operator there is completely analogous to (2.14). However in the subsequent discussion of the Hamiltonian constraint certain differences arise: While the full theory is diffeomorphism invariant, the symmetry reduced theory is not because of gauge fixing carried out in the beginning of section II A 1. These differences are discussed in [14]. That comparison with the full theory also brings out the fact that the ‘ μ_o -ambiguity’ encountered here can be understood as the imprint on LQC of the factor ordering ambiguity (the ‘ j ambiguity’) in full LQG. Our strategy to fix the value of μ_o further sharpens its similarity with the label j in the full theory: Fixing μ_o by appealing to the area gap is similar to the standard choice $j = 1/2$ made in the evaluation of the holonomy around the closed loop while defining the Hamiltonian constraint in the full theory [1, 3, 47, 84]. In this sense, our choice of a specific μ_o is a way of fixing a specific factor ordering ambiguity. μ_o is not a ‘regulator’ in the traditional sense because, as discussed above, the quantum nature of geometry tells us that it is *physically* incorrect to take the naive limit $\mu_o \rightarrow 0$.

2. Constraint operators and their properties

It is easy to verify that, although the classical constraint function C_{grav} we began with is real on the phase space Γ_{grav}^S , the operator $\hat{C}_{\text{grav}}^{(\mu_o)}$ is not self-adjoint on $\mathcal{H}_{\text{kin}}^{\text{grav}}$. This came about just because of the standard factor ordering ambiguities of quantum mechanics and there are two natural re-orderings that can rectify this situation.

First, we can simply take the self-adjoint part of (2.19) on $\mathcal{H}_{\text{kin}}^{\text{grav}}$ and use it as the gravitational part of the constraint:

$$\hat{C}'_{\text{grav}} = \frac{1}{2} \left[\hat{C}_{\text{grav}} + (\hat{C}_{\text{grav}})^\dagger \right] \quad (2.20)$$

It is convenient to express its action on states $\Psi(\mu) := \langle \Psi | \mu \rangle$ in the μ —or the triad/geometry— representation. The action is given by

$$\hat{C}'_{\text{grav}} \Psi(\mu) = f'_+ \Psi(\mu + 4\mu_o) + f'_o \Psi(\mu) + f'_- \Psi(\mu - 4\mu_o) \quad (2.21)$$

where the coefficients f'_\pm, f'_o are functions of μ :

$$\begin{aligned} f'_o(\mu) &= -\sqrt{\frac{4\pi}{3}} \frac{\ell_{\text{Pl}}}{(\gamma\mu_o^2)^{\frac{3}{2}}} \left| |\mu + \mu_o|^{\frac{3}{2}} - |\mu - \mu_o|^{\frac{3}{2}} \right| \\ f'_+(\mu) &= -\frac{1}{4} (f'_o(\mu) + f'_o(\mu + 4\mu_o)) \\ f'_-(\mu) &= -\frac{1}{4} (f'_o(\mu) + f'_o(\mu - 4\mu_o)) \end{aligned} \quad (2.22)$$

By construction, this operator is self-adjoint and one can show that it is also bounded above (in particular, $\langle \Psi, \hat{C}'_{\text{grav}} \Psi \rangle < \sqrt{\pi/3} \ell_{\text{Pl}} (\gamma\mu_o)^{-\frac{3}{2}} (5^{\frac{3}{2}} - 3^{\frac{3}{2}}) \langle \Psi | \Psi \rangle$). Next, consider the ‘parity’ operator Π defined by $\Pi\Psi(\mu) := \Psi(-\mu)$. It corresponds to the flip of the orientation of the triad and thus represents a large gauge transformation. It will play an important role in section IV. Here we note that the functions f'_\pm, f'_o are such that the constraint operator \hat{C}'_{grav} commutes with Π :

$$[\hat{C}'_{\text{grav}}, \Pi] = 0 \quad (2.23)$$

Finally, for $\mu \gg \mu_o \equiv 3\sqrt{3}/2$, this difference operator can be approximated, in a well-defined sense, by a second order differential operator (a connection-dynamics analog of the WDW operator of geometrodynamics). Since \hat{C}'_{grav} is just the self-adjoint part of the operator used in [14], we can directly use results of section 4.2 of that paper. Set $p = 8\pi\gamma\mu\ell_{\text{Pl}}^2/6$ and consider functions $\Psi(p)$ which, together with their first four derivatives are bounded. On these functions, we have

$$\hat{C}'_{\text{grav}} \Psi(p) \approx \frac{64\pi^2}{3} \ell_{\text{Pl}}^4 [\sqrt{p} \frac{d^2}{dp^2} + \frac{d^2}{dp^2} \sqrt{p}] \Psi(p) =: \hat{C}'_{\text{grav}}^{\text{WDW}} \Psi(p) \quad (2.24)$$

where \approx stands for equality modulo terms of the order $o(p_o)$. That is, had we left μ_o as a free parameter, the equality would hold in the limit $\mu_o \rightarrow 0$. This is the limit in which the area gap goes to zero, i.e., quantum geometry effects can be neglected.

Let us now turn to the second natural factor ordering. The form of the expression (2.17) of \hat{C}_{grav} suggests [48] that we simply ‘re-distribute’ the $\sin^2 \mu_o c$ term in a symmetric fashion. Then this factor ordering leads to the following self-adjoint gravitational constraint:

$$\begin{aligned} \hat{C}_{\text{grav}} &= \frac{24i(\text{sgn } p)}{8\pi\gamma^3\mu_o^3\ell_{\text{Pl}}^2} \left[\sin \mu_o c \left(\sin \frac{\mu_o c}{2} \hat{V} \cos \frac{\mu_o c}{2} - \cos \frac{\mu_o c}{2} \hat{V} \sin \frac{\mu_o c}{2} \right) \sin \mu_o c \right]_{\mu_o=\frac{3\sqrt{3}}{2}} \\ &=: \left[\sin \mu_o c \hat{A} \sin \mu_o c \right]_{\mu_o=\frac{3\sqrt{3}}{2}} \end{aligned} \quad (2.25)$$

For concreteness in most of this paper we will work with this form of the constraint and, for notational simplicity, unless otherwise stated set $\mu_o = 3\sqrt{3}/2$. However, numerical simulations have been performed also using the constraint \hat{C}'_{grav} of Eq. (2.20) and the results are robust.

Properties of \hat{C}_{grav} which we will need in this paper can be summarized as follows. First, the eigenbasis $|\mu\rangle$ of \hat{p} diagonalizes the operator \hat{A} . Therefore in the p -representation, \hat{A} acts simply by multiplication:

$$\hat{A} \Psi(\mu) = -2 \sqrt{\frac{8\pi}{6}} \frac{\ell_{\text{Pl}}}{(\gamma\mu_o^2)^{\frac{3}{2}}} \left(|\mu + \mu_o|^{\frac{3}{2}} - |\mu - \mu_o|^{\frac{3}{2}} \right) \Psi(\mu) \quad (2.26)$$

By inspection, \hat{A} is self-adjoint and negative definite on $\mathcal{H}_{\text{kin}}^{\text{grav}}$. The form of \hat{C}_{grav} now implies that it is also self-adjoint and negative definite. Its action on states $\Psi(\mu)$ is given by

$$\hat{C}_{\text{grav}} \Psi(\mu) = f_+ \Psi(\mu + 4\mu_o) + f_o \Psi(\mu) + f_- \Psi(\mu - 4\mu_o) \quad (2.27)$$

where the coefficients f_{\pm}, f_o are again functions of μ :

$$\begin{aligned} f_+(\mu) &= \frac{1}{2} \sqrt{\frac{8\pi}{6}} \frac{\ell_{\text{Pl}}}{(\gamma\mu_o^2)^{\frac{3}{2}}} \left| |\mu + 3\mu_o|^{\frac{3}{2}} - |\mu + \mu_o|^{\frac{3}{2}} \right| \\ f_-(\mu) &= f_+(\mu - 4\mu_o) \\ f_o(\mu) &= -f_+(\mu) - f_-(\mu). \end{aligned} \quad (2.28)$$

It is clear from Eqs (2.25) and (2.26) that \hat{C}_{grav} commutes with the parity operator Π which flips the orientations of triads:

$$[\hat{C}_{\text{grav}}, \Pi] = 0. \quad (2.29)$$

Finally, the ‘continuum limit’ of the difference operator \hat{C}_{grav} yields a second order differential operator. Let us first set

$$\chi(\mu) = f_+(\mu - 2\mu_o)[\Psi(\mu + 2\mu_o) - \Psi(\mu - 2\mu_o)] \quad (2.30)$$

Then,

$$\hat{C}_{\text{grav}}\Psi(\mu) = \chi(\mu + 2\mu_o) - \chi(\mu - 2\mu_o) \quad (2.31)$$

Therefore, if we again set $p = 8\pi\gamma\mu\ell_{\text{Pl}}^2/6$ and consider functions $\Psi(p)$ which, together with their first four derivatives are bounded we have

$$\hat{C}_{\text{grav}}\Psi(p) \approx \frac{128\pi^2}{3}\ell_{\text{Pl}}^4 \left[\frac{d}{dp} \sqrt{p} \frac{d\Psi}{dp} \right] =: \hat{C}_{\text{grav}}^{\text{WDW}}\Psi(p) \quad (2.32)$$

where \approx again stands for equality modulo terms of the order $O(p_o)$. That is, in the limit in which the area gap goes to zero, i.e., quantum geometry effects can be neglected, the difference operator reduces to a WDW type differential operator. (As one might expect, the limiting WDW operator is independent of the Barbero-Immirzi parameter γ .) We will use this operator extensively in section III.

In much of computational physics, especially in numerical general relativity, the fundamental objects are differential equations and discrete equations are introduced to approximate them. In LQC the situation is just the opposite. The physical fundamental object is now the discrete equation (2.27) with $\mu_o = 3\sqrt{3}/2$. The differential equation is the approximation. The leading contribution to the difference between the two —i.e., to the error — is of the form $O(\mu_o)^2\Psi'''$ where the second term depends on the wave function Ψ under consideration. Therefore, the approximation is not uniform. For semi-classical states, Ψ''' can be large, of the order of $10^{16}/\mu^4$ in the examples considered in section V. In this case, the continuum approximation can break down already at $\mu \sim 10^4$.

As one might expect the two differential operators, $\hat{C}_{\text{grav}}^{\text{WDW}}$ and $\hat{C}_{\text{grav}}^{\text{grav}}$ differ only by a factor ordering:

$$\left(\hat{C}_{\text{grav}}^{\text{WDW}} - \hat{C}_{\text{grav}}^{\text{grav}} \right) \Psi(p) = -\frac{16\pi^2}{3}\ell_{\text{Pl}}^4 |p|^{-\frac{3}{2}} \Psi(p). \quad (2.33)$$

Remark: As noted in section II B 1, the ‘continuum limit’ $\mu_o \rightarrow 0$ of any of the quantum constraint operators of LQC does not exist on $\mathcal{H}_{\text{kin}}^{\text{grav}}$ because of the quantum nature of underlying geometry. To take this limit, one has to work in the setting in which the quantum geometry effects are neglected, i.e., on the WDW type Hilbert space $L^2(\mathbb{R}, dc)$. On this space, operators $\hat{C}_{\text{grav}}^{\text{grav}}$, $\hat{C}_{\text{grav}}^{\text{WDW}}$ and $\hat{C}_{\text{grav}}^{\text{WDW}}$ are all densely defined and the limit can be taken on a suitable dense domain.

C. Open issues and the model

In section II A we recalled the kinematical framework used in LQC and in II B we extended the existing results by analyzing two self-adjoint Hamiltonian constraint operators in some detail. Physical states $\Psi(\mu, \phi)$ can now be constructed as solutions of the Hamiltonian constraint:

$$(\hat{C}_{\text{grav}} + \hat{C}_{\text{matt}}) \Psi(\mu, \phi) = 0 \quad (2.34)$$

where ϕ stands for matter fields. Given any matter model, one could solve this equation numerically. However, generically, the solutions would not be normalizable in the total

kinematic Hilbert space $\mathcal{H}_{\text{kin}}^{\text{total}}$ of gravity plus matter. Therefore, although section II B goes beyond the existing literature in LQC, one still can not calculate expectation values, fluctuations and probabilities —i.e., extract physics— knowing only these solutions.

To extract physics, then, we still have to complete the following tasks:

- In the classical theory, seek a dynamical variable which is monotonically increasing on all solutions (or at least ‘large’ portions of solutions). Attempt to interpret the Hamiltonian constraint (2.34) as an ‘evolution equation’ with respect to this ‘internal time’. If successful, this strategy would provide an ‘emergent time’ in the background independent quantum theory. Although it is possible to extract physics under more general conditions, physical interpretations are easier and more direct if one can locate such an emergent time.
- Introduce an inner product on the space of solutions to (2.34) to obtain the physical Hilbert space \mathcal{H}_{phy} . The fact that the orientation reversal induced by Π is a large gauge transformation will have to be handled appropriately.
- Isolate suitable Dirac observables in the classical theory and represent them by self-adjoint operators on \mathcal{H}_{phy} .
- Use these observables to construct physical states which are semi-classical at ‘late times’, sharply peaked at a point on the classical trajectory representing a large classical universe.
- ‘Evolve’ these states using (2.34). Monitor the mean values and fluctuations of Dirac observables. Do the mean values follow a classical trajectory? Investigate if there is a drastic departure from the classical behavior. If there is, analyze what replaces the big-bang.

In the rest of the paper, we will carry out these tasks in the case when matter consists of a zero rest mass scalar field. In the classical theory, the phase space Γ_{grav}^S is now 4-dimensional, coordinatized by $(c, p; \phi, p_\phi)$. The basic (non-vanishing) Poisson brackets are given by:

$$\{c, p\} = \frac{8\pi\gamma G}{3}, \quad \text{and} \quad \{\phi, p_\phi\} = 1. \quad (2.35)$$

The symmetry reduction of the classical Hamiltonian constraint is of the form

$$C_{\text{grav}} + C_{\text{matt}} \equiv -\frac{6}{\gamma^2} c^2 \sqrt{|p|} + 8\pi G \frac{p_\phi^2}{|p|^{\frac{3}{2}}} = 0. \quad (2.36)$$

Using this constraint, one can solve for c in terms of p and p_ϕ . Furthermore, since ϕ does not enter the expression of the constraint, p_ϕ is a constant of motion. Therefore, each dynamical trajectory can be specified on the 2-dimensional (p, ϕ) plane. Typical trajectories are shown in Fig. 1. Because the phase space allows triads with both orientations, the variable p can take both positive and negative values. At $p = 0$ the physical volume of the universe goes to zero and, if the point lies on any dynamical trajectory, it is an end-point of that trajectory, depicting a curvature singularity. As the figure shows, for each fixed value of p_ϕ , there are four types of trajectories, two in the $p \geq 0$ half plane and two in the $p \leq 0$ half plane. Analytically they are given by:

$$\phi = \pm \sqrt{\frac{3}{16\pi G}} \ln \frac{|p|}{|p_\star|} + \phi_\star \quad (2.37)$$

where p_\star, ϕ_\star are integration constants. These trajectories are related by a ‘parity transformation’ on the phase space which simply reverses the orientation of the physical triad. As noted before, since the metric and the scalar field are unaffected, it represents a large

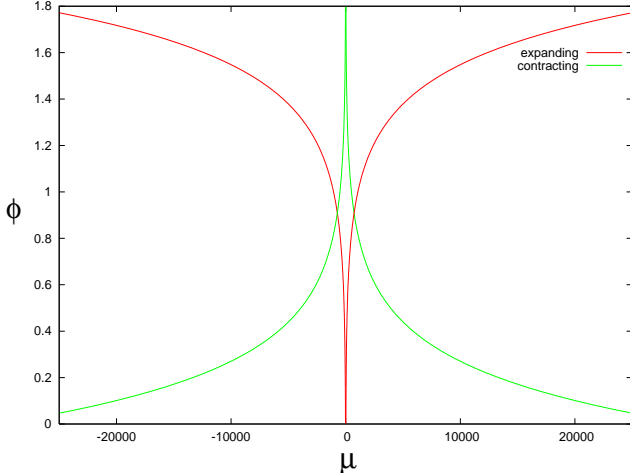


FIG. 1: Classical phase space trajectories are plotted in the $\phi, p \sim \mu$ -plane. For $\mu \geq 0$, there is a branch which starts with a big-bang (at $\mu = 0$) and expands out and a branch which contracts into a big crunch (at $\mu = 0$). Their mirror images appear in the $\mu \leq 0$ half plane.

gauge transformation. Therefore, it suffices to focus just on the portion $p \geq 0$ of figure 1. Then for each fixed value of p_ϕ , there are two solutions passing through any given point (ϕ_*, p_*) . In one, the universe begins with the big-bang and then expands and in the other the universe contracts into a big crunch. Thus *in this model, every classical solution meets the singularity*.

Finally, we can introduce a natural set of *Dirac observables*. Since p_ϕ is a constant of motion, it is obviously one. To introduce others, we note that ϕ is a monotonic function on each classical trajectory. Furthermore, in each solution, the space-time metric takes the form $ds^2 = -dt^2 + V_o^{-2/3}|p|(t)dS_o^2$ and the time dependence of the scalar field is given by

$$\frac{d\phi}{dt} = \frac{16\pi G p_\phi^*}{|p_\phi|^{3/2}} \exp \pm [\sqrt{12\pi G}(\phi - \phi_*)], \quad (2.38)$$

where p_* , ϕ_* and p_ϕ^* are constants. Thus, in every solution ϕ is a monotonic function of time and can therefore serve as a good ‘internal clock’. This interpretation suggests the existence of a natural family of Dirac observables: $p|_{\phi_o}$, the value of p at the ‘instant’ ϕ_o . The set $(p_\phi, p|_{\phi_o})$ constitutes a complete set of Dirac observables since their specification uniquely determines a classical trajectory on the symmetry reduced phase space Γ^S , i.e., a point in the reduced phase space $\tilde{\Gamma}^S$. While the interpretation of ϕ as ‘internal time’ motivates this construction and, more generally, makes physics more transparent, it is not essential. One can do all of physics on $\tilde{\Gamma}^S$: Since physical states are represented by points in $\tilde{\Gamma}^S$ and a complete set of observables is given by $(p_\phi, p|_{\phi_o})$, one can work just with this structure.

Remark: In the open i.e., $k=0$ model now under consideration, since p is also monotonic along any classical trajectory, ϕ_{p_o} is also a Dirac observable and p could also be used as an ‘internal time’. However, in LQC the expression of the gravitational part of the constraint operator makes it difficult to regard p as the ‘emergent time’ in quantum theory. Moreover even in the classical theory, since the universe expands and then recollapses in the $k=1$ case, p fails to be monotonic along solutions and cannot serve as ‘internal time’ globally.

III. WDW THEORY

The WDW theory of the model has been analyzed in some detail within geometrodynamics (see especially [49]). However, that analysis was primarily in the context of a WKB approximation. More recently, the group averaging technique was used to construct the physical Hilbert space in a general cosmological context [34, 50], an elementary example of which is provided by the present model. However, to our knowledge a systematic completion of the program outlined in section II C has not appeared in the literature.

In this section we will construct the WDW type quantum theory in the *connection dynamics*. This construction will serve two purposes. First it will enable us to introduce the key notions required for the completion of the program in a familiar and simpler context. Second, we will be able to compare and contrast the results of the WDW theory and LQC in detail, thereby bringing out the role played by quantum geometry in quantum dynamics.

A. Emergent time and the general solution to the WDW equation

Recall that the phase space of the model is 4-dimensional, coordinatized by $(c, p; \phi, p_\phi)$ and the fundamental non-vanishing Poisson brackets are given by (2.35). The Hamiltonian constraint has the form:

$$C_{\text{grav}} + C_\phi \equiv -\frac{6}{\gamma^2} c^2 \sqrt{|p|} + 8\pi G \frac{p_\phi^2}{|p|^{\frac{3}{2}}} = 0. \quad (3.1)$$

To make comparison with the standard geometrodynamical WDW theory, it is most convenient to work in the p, ϕ representation. Then, the kinematic Hilbert space is given by $\mathcal{H}_{\text{kin}}^{\text{wdw}} = L^2(\mathbb{R}^2, dp d\phi)$. Operators $\hat{p}, \hat{\phi}$ operate by multiplication while \hat{c} and \hat{p}_ϕ are represented as:

$$\hat{c} \Psi = i\hbar \frac{8\pi\gamma G}{3} \frac{\partial \Psi}{\partial p} \quad \text{and} \quad \hat{p}_\phi \Psi = -i\hbar \frac{\partial \Psi}{\partial \phi} \quad (3.2)$$

Note that, while in geometrodynamics the scale factor is restricted to be non-negative, here p ranges over the entire real line, making the specification of the Hilbert space and operators easier.

To write down the quantum constraint operator, we have to make a choice of factor ordering. Since our primary motivation behind the introduction of the WDW theory is to compare it with LQC, it is most convenient to use the factor ordering that comes from the continuum limit (2.32) of the constraint operator of LQC. Then, the WDW equation becomes:

$$\frac{2}{3}(8\pi G\hbar)^2 \frac{\partial}{\partial p} \sqrt{p} \frac{\partial \Psi}{\partial p} = 8\pi G\hbar^2 \widehat{|p|^{-\frac{3}{2}}} \frac{\partial^2 \Psi}{\partial \phi^2} =: 8\pi G\hbar^2 \underline{B}(p) \frac{\partial^2 \Psi}{\partial \phi^2}, \quad (3.3)$$

where we have denoted the eigenvalue $|p|^{-\frac{3}{2}}$ of $\widehat{|p|^{-\frac{3}{2}}}$ by $\underline{B}(p)$ to facilitate later comparison with LQC.³ The operator on the left side of this equation is self-adjoint on $L^2(\mathbb{R}, dp)$ and the equation commutes with the orientation reversal operator $\Pi \Psi(p, \phi) = \Psi(-p, \phi)$ representing a large gauge transformation. Thus, if Ψ is a solution to Eq. (3.3), so is $\Psi(-p, \phi)$.

³ Here, and in what follows, quantities with an underbar will refer to the WDW theory.

For a direct comparison with LQC, it is convenient to replace p with μ defined by $p = (8\pi\gamma G\hbar/6)\mu$. Then, (3.3) becomes:

$$\begin{aligned}\frac{\partial^2 \Psi}{\partial \phi^2} &= \frac{16\pi G}{3} [\underline{B}(\mu)]^{-1} \frac{\partial}{\partial \mu} \sqrt{\mu} \frac{\partial \Psi}{\partial \mu} \\ &=: -\underline{\Theta} \Psi\end{aligned}\tag{3.4}$$

where we have recast the equation in such a way that operators involving only ϕ appear on the left side and operators involving only μ appear on the right. The WDW equation now has the same form as the Klein-Gordon equation in a static space-time, ϕ playing the role of time and $\underline{\Theta}$ of the (elliptic operator constructed from the norm of the Killing field and the) spatial Laplacian. Thus, the form of the quantum Hamiltonian constraint is such that ϕ can be interpreted as *emergent time* in the quantum theory. In this factor ordering of the constraint operator, which emerged in the continuum limit (2.32) of LQC, it is not as convenient to regard $p \sim \mu$ as emergent time.

Physical states will be suitably regular solutions to (3.4). Since Π is a large gauge transformation, we can divide physical states into eigenspaces of \hat{P} . Physical observables will preserve each eigenspace. Since $\Pi^2 = 1$, there are only two eigenspaces, one representing the symmetric sector and the other, anti-symmetric. Since the standard WDW theory deals with geometry, it is completely insensitive to the orientation of the triad. Therefore, it is natural to work with the symmetric sector. Thus, *the physical Hilbert space will consist of suitably regular solutions $\Psi(\mu, \phi)$ to (3.3) which are symmetric under $\mu \rightarrow -\mu$.*

The mathematical similarity with the Klein Gordon equation in static space-times immediately suggests a strategy to obtain the general solution of (3.3). We first note that $d/d\mu(\sqrt{\mu}d/d\mu)$ is a negative definite, self-adjoint operator on $L_S^2(\mathbb{R}, d\mu)$, the symmetric sector of $L^2(\mathbb{R}, d\mu)$. Therefore, $\underline{\Theta}$ is a positive definite, self-adjoint operator on $L_S^2(\mathbb{R}, \underline{B}(\mu)d\mu)$. Its eigenfunctions provide us with an orthonormal basis. It is easy to verify that the eigenvectors $\underline{e}_k(\mu)$ can be labeled by $k \in \mathbb{R}$ and are given by

$$\underline{e}_k(\mu) := \frac{|\mu|^{\frac{1}{4}}}{4\pi} e^{ik \ln |\mu|} \tag{3.5}$$

Their eigenvalues are given by:

$$\underline{\Theta} \underline{e}_k(\mu) = \omega^2 \underline{e}_k(\mu), \quad \text{with } \omega^2 = \frac{16\pi G}{3} (k^2 + \frac{1}{16}); \tag{3.6}$$

(where the factor of $1/16$ is an artifact of the factor ordering choice which we were led to from LQC). The eigenfunctions satisfy the orthonormality relations:

$$\int_{-\infty}^{\infty} d\mu \underline{B}(\mu) \bar{\underline{e}}_k(\mu) \underline{e}_{k'}(\mu) = \delta(k, k'), \tag{3.7}$$

(where the right side is the standard Dirac distribution, not the Kronecker symbol as on $L^2(\mathbb{R}_{\text{Bohr}}, d\mu_{\text{Bohr}})$); and the completeness relation:

$$\int_{-\infty}^{\infty} d\mu \underline{B}(\mu) \bar{\underline{e}}_k(\mu) \Psi(\mu) = 0 \quad \forall k \quad \text{iff } \Psi(\mu) = 0 \tag{3.8}$$

for any $\Psi(\mu) \in L_S^2(\mathbb{R}, \underline{B}(\mu)d\mu)$.

With these eigenfunctions at hand, we can now write down a ‘general’ symmetric solution to (3.3). Any solution, whose initial data at $\phi = \phi_o$ is such that $\mu^{-1/4}\Psi(\mu, \phi_o)$ and $\mu^{-1/4}\dot{\Psi}(\mu, \phi_o)$ are symmetric and lie in the Schwartz space of rapidly decreasing functions, has the form:

$$\Psi(\mu, \phi) = \int_{-\infty}^{\infty} dk \tilde{\Psi}_+(k) \underline{e}_k(\mu) e^{i\omega\phi} + \tilde{\Psi}_-(k) \bar{\underline{e}}_k(\mu) e^{-i\omega\phi}, \quad (3.9)$$

for some $\tilde{\Psi}_\pm(k)$ in the Schwartz space. Following the terminology used in the Klein-Gordon theory, if $\tilde{\Psi}_\pm(k)$ have support on the negative k -axis, we will say the solution is ‘outgoing’ (or ‘expanding’) while if it has support on the positive k axis, it is ‘incoming’ (or, ‘contracting’).

If $\tilde{\Psi}_-(k)$ vanishes, the solution will be said to be *positive frequency* and if $\tilde{\Psi}_+(k)$ vanishes, it will be said to be of *negative frequency*. Thus, every solution (3.9) admits a natural decomposition into positive and negative frequency parts. Finally we note that positive (respectively negative) frequency solutions satisfy a first order (in ϕ) equation which can be regarded as the square-root of (3.4):

$$\mp i \frac{\partial \Psi_\pm}{\partial \phi} = \sqrt{\underline{\Theta}} \Psi_\pm \quad (3.10)$$

where $\sqrt{\underline{\Theta}}$ is the positive, self-adjoint operator defined via spectral decomposition of $\underline{\Theta}$ on $L^2(\mathbb{R}, \underline{B}(\mu) d\mu)$. Regarding ϕ as time, this is just a first order Schrödinger equation with a *non-local* Hamiltonian $\sqrt{\underline{\Theta}}$. Therefore, a general ‘initial datum’ $f_\pm(\mu)$ at $\phi = \phi_o$ can be ‘evolved’ to obtain a solution to (3.10) via:

$$\Psi_\pm(\mu, \phi) = e^{\pm i\sqrt{\underline{\Theta}}(\phi - \phi_o)} f_\pm(\mu, \phi_o) \quad (3.11)$$

B. The physical sector

Solutions (3.9) are not normalizable in $\mathcal{H}_{\text{kin}}^{\text{wdw}}$ (because zero is in the continuous part of the spectrum of the WDW operator). Our first task is to endow the space of these physical states with a Hilbert space structure. There are several possible avenues. We will begin with one that is somewhat heuristic but has direct physical motivation. The idea [51, 52] is to introduce operators corresponding to a complete set of Dirac observables and select the required inner product by demanding that they be self-adjoint. In the classical theory, such a set is given by p_ϕ and $\mu|_{\phi_o}$. Since \hat{p}_ϕ commutes with the WDW operator in (3.4), given a (symmetric) solution $\Psi(\mu, \phi)$ to (3.4),

$$\hat{p}_\phi \Psi(\mu, \phi) := -i\hbar \frac{\partial \Psi}{\partial \phi} \quad (3.12)$$

is again a (symmetric) solution. So, we can just retain this definition of \hat{p}_ϕ from $\mathcal{H}_{\text{kin}}^{\text{wdw}}$. The Schrödinger type evolutions (3.11) enable us to define the other Dirac observable $\hat{\mu}|_{\phi_o}$: Given a (symmetric) solution $\Psi(\mu, \phi)$ to (3.4), we can first decompose it into positive and negative frequency parts $\Psi_\pm(\mu, \phi)$, freeze them at $\phi = \phi_o$, multiply this ‘initial datum’ by μ and evolve via (3.11):

$$\widehat{\mu|_{\phi_o}} \Psi(\mu, \phi) = e^{i\sqrt{\underline{\Theta}}(\phi - \phi_o)} \mu \Psi_+(\mu, \phi_o) + e^{-i\sqrt{\underline{\Theta}}(\phi - \phi_o)} \mu \Psi_-(\mu, \phi_o) \quad (3.13)$$

The result is again a (symmetric) solution to (3.4). Now, we see that both these operators have the further property that they preserve the positive and negative frequency subspaces. Since they constitute a complete family of Dirac observables, we have *superselection*. In quantum theory we can restrict ourselves to one superselected sector. In what follows, for definiteness *we will focus on the positive frequency sector and, from now on, drop the suffix +.*

We now seek an inner product on positive frequency solutions $\Psi(\mu, \phi)$ to (3.4) (invariant under the μ reflection) which makes \hat{p}_ϕ and $\hat{\mu}|_{\phi_o}$ self-adjoint. Each of these solutions is completely determined by its initial datum $\Psi(\mu, \phi_o)$ and the Dirac observables have the following action on the datum:

$$\widehat{\mu|_{\phi_o}} \Psi(\mu, \phi_o) = \mu \Psi(\mu, \phi_o), \quad \text{and} \quad \hat{p}_\phi \Psi(\mu, \phi_o) = \hbar \sqrt{\underline{\Theta}} \Psi(\mu, \phi_o). \quad (3.14)$$

Therefore, it follows that (modulo an overall rescaling,) the unique inner product which will make these operators self-adjoint is just:

$$\langle \Psi_1 | \Psi_2 \rangle_{\text{phy}} = \int_{\phi=\phi_o} d\mu \underline{B}(\mu) \bar{\Psi}_1 \Psi_2 \quad (3.15)$$

(see e.g. [51, 52]). Note that the inner product is conserved, i.e., is independent of the choice of the ‘instant’ $\phi = \phi_o$. Thus, *the physical Hilbert space $\mathcal{H}_{\text{phy}}^{\text{wdw}}$ is the space of positive frequency wave functions $\Psi(\mu, \phi)$ which are symmetric under μ reflection and have a finite norm (3.15)*. The procedure has already provided us with a representation of our complete set of Dirac observables on this $\mathcal{H}_{\text{phy}}^{\text{wdw}}$:

$$\widehat{\mu|_{\phi_o}} \Psi(\mu, \phi) = e^{i\sqrt{\underline{\Theta}}(\phi-\phi_o)} \mu \Psi(\mu, \phi_o), \quad \text{and} \quad \hat{p}_\phi \Psi(\mu, \phi) = \hbar \sqrt{\underline{\Theta}} \Psi(\mu, \phi). \quad (3.16)$$

We will now show that the same representation of the algebra of Dirac observables can be obtained by the more systematic group averaging method [34, 50] which also brings out the mathematical inputs that go in this choice. (The two methods have been applied and compared for a non-trivially constrained system in [53]). Here, one first notes that the total constraint operator is self-adjoint on an auxiliary Hilbert space $\mathcal{H}_{\text{aux}}^{\text{wdw}} := L_S^2(\mathbb{R}^2, \underline{B}(\mu) d\mu d\phi)$, (where, as before the subscript S denotes restriction to functions which are symmetric under μ -reflection). One must then select an appropriate dense subspace Φ of $\mathcal{H}_{\text{aux}}^{\text{wdw}}$. A natural candidate is the Schwartz space of rapidly decreasing functions. One then ‘averages’ elements of Φ under the 1-parameter family group generated by the constraint operator $\hat{C} = \partial_\phi^2 + \underline{\Theta}$ to produce a solution to (3.4):

$$\begin{aligned} \Psi_f(\mu, \phi) : &= \int_{-\infty}^{\infty} d\alpha e^{i\alpha \hat{C}} f(\mu, \phi) \\ &= \int_{-\infty}^{\infty} \frac{dk}{2|\omega|} \left(\tilde{f}(k, \omega) \underline{e}_k(\mu) e^{i\omega\phi} + \tilde{f}(k, -\omega) \underline{e}_k(\mu) e^{-i\omega\phi} \right) \end{aligned} \quad (3.17)$$

where to arrive at the second step we expanded f in the eigenbasis of $\underline{\Theta}$ and \hat{p}_ϕ with \tilde{f} as the coefficients. Thus, the group averaging procedure reproduces the solution (3.9) with $\tilde{\Psi}_+(k) = \tilde{f}(k, \omega)/2|\omega|$ and $\tilde{\Psi}_-(k) = \tilde{f}(k, -\omega)/2|\omega|$. Solutions Ψ_f are regarded as ‘distributions’ or elements of the dual Φ^* of Φ and the physical norm is given by the action of this distribution, Ψ_f , on the ‘test function’ f . However, there is some freedom in the specification of this action

which generally results in seemingly different but unitarily equivalent representations of the algebra of Dirac observables. For us the most convenient choice is:

$$||\Psi||^2 := \Psi_f(f) := \int_{-\infty}^{\infty} d\phi \int_{-\infty}^{\infty} d\mu \underline{B}(\mu) \bar{\Psi}_f(\mu, \phi) \sqrt{\underline{\Theta}} f(\mu, \phi) \quad (3.18)$$

where $\Psi_f(f)$ is the action of the distribution Ψ_f on the test field f . Then, the inner product coincides with (3.15) and the representation of the Dirac observables is the same as in (3.12) and (3.13). Had we chosen to drop the factor of $\sqrt{\underline{\Theta}}$ in defining the action of Ψ_f on f , we would have obtained a unitarily equivalent representation in which the action of $\hat{\mu}|_{\phi_o}$ is more complicated.

Finally, with the physical Hilbert space and a complete set of Dirac observables at hand, we can now introduce semi-classical states and study their evolution. Let us fix a ‘time’ $\phi = \phi_o$ and construct a semi-classical state which is peaked at $p_\phi = p_\phi^*$ and $\mu|_{\phi_o} = \mu^*$. We would like the peak to be at a point that lies on a large classical universe. This implies that we should choose $\mu^* \gg 1$ and (in the natural classical units $c=G=1$), $p_\phi^* \gg \hbar$. In the closed ($k=1$) models for example, the second condition is necessary to ensure that the universe expands out to a size much larger than the Planck scale. At ‘time’ $\phi = \phi_o$, consider the state

$$\Psi(\mu, \phi_o) = \int_{-\infty}^{\infty} dk \tilde{\Psi}(k) \underline{e}_k(\mu) e^{i\omega(\phi_o - \phi^*)}, \quad \text{where } \tilde{\Psi}(k) = e^{-\frac{(k-k^*)^2}{2\sigma^2}}. \quad (3.19)$$

where $k^* = -\sqrt{3/16\pi G \hbar^2} p_\phi^*$ and $\phi^* = -\sqrt{3/16\pi G} (\ln |\mu^*|) + \phi_o$. It is easy to evaluate the integral in the approximation $\omega = -\sqrt{(16\pi G/3)} k$ (which is justified because $k^* \ll -1$) and calculate mean values of the Dirac observables and their fluctuations. One finds that, as required, the state is sharply peaked at values μ^*, p_ϕ^* . The above construction is closely related to that of coherent states in non-relativistic quantum mechanics. The main difference is that the observables of interest are not μ and its conjugate momentum but rather μ and p_ϕ —the momentum conjugate to ‘time’, i.e., the analog of the Hamiltonian in non-relativistic quantum mechanics.

We can now ask for the evolution of this state. Does it remain peaked at the classical trajectory defined by $p_\phi = p_\phi^*$ passing through μ^* at $\phi = \phi_o$? This question is easy to answer because (3.11) implies that the (positive frequency) solution to $\Psi(\mu, \phi)$ (3.4) defined by ‘initial data’ (3.19) is obtained simply by replacing ϕ_o by ϕ in (3.19)! Since the measure of dispersion σ in (3.19) does not depend on ϕ , it follows that the initial state $\Psi(\mu, \phi_o)$ which is the semi-classical, representing a large universe at ‘time’ ϕ_o continues to be peaked at a trajectory defined by:

$$\phi = \sqrt{\frac{3}{16\pi G}} \ln \frac{|\mu|}{|\mu^*|} + \phi_o. \quad (3.20)$$

This is precisely the classical trajectory with $p_\phi = p_\phi^*$, passing through μ^* at $\phi = \phi_o$. This is just as one would hope during the epoch in which the universe is large. However, this holds also in the Planck regime and, in the backward evolution, the semi-classical state simply follows the classical trajectory into the big-bang singularity. (Had we worked the positive k^* , we would have obtained a contracting solution and then the forward evolution would have followed the classical trajectory into the big-crunch singularity.) In this sense, the WDW evolution does not resolve the classical singularity.

Remark: In the above discussion for simplicity we restricted ourselves to eigenfunctions $\underline{e}_k(\mu)$ which are symmetric under $\mu \rightarrow -\mu$ from the beginning. Had we dropped this

requirement, we would have found that there is a 4-fold (rather than 2-fold) degeneracy in the eigenfunctions of $\underline{\Theta}$. Indeed, if $\theta(\mu)$ is the step function ($\theta(\mu) = 0$ if $\mu < 0$ and $= 1$ if $\mu > 0$), then $\theta(\mu)\underline{e}_{|k|}$, $\theta(\mu)\underline{e}_{-|k|}$, $\theta(-\mu)\underline{e}_{|k|}$, $\theta(-\mu)\underline{e}_{-|k|}$ are all continuous functions of μ which satisfy the eigenvalue equation (in the distributional sense) with eigenvalue $\omega^2 = (16\pi G/3)(k^2 + 1/16)$. This fact will be relevant in the next section.

IV. ANALYTICAL ISSUES IN LOOP QUANTUM COSMOLOGY

We will now analyze the model within LQG. We will first observe that the form of the Hamiltonian constraint is such that the scalar field ϕ can again be used as emergent time. Since the form of the resulting ‘evolution equation’ is very similar in the WDW theory, we will be able to construct the physical Hilbert space and Dirac observables following the ideas introduced in section III B.

A. Emergent time and the general solution to the LQC Hamiltonian constraint

The quantum constraint has the form

$$\hat{C}_{\text{grav}} + \hat{C}_\phi = 0 \quad (4.1)$$

where \hat{C}_{grav} is given by (2.27). Since $\hat{C}_\phi = (8\pi G) \widehat{(1/p^{3/2})} (\hat{p}_\phi^2)$, the constraint becomes:

$$8\pi G \hat{p}_\phi^2 \Psi(\mu, \phi) = [\tilde{B}(p)]^{-1} \hat{C}_{\text{grav}} \Psi(\mu, \phi) \quad (4.2)$$

where $\tilde{B}(p)$ is the eigenvalue of the operator $\widehat{1/|p|^{3/2}}$:

$$\tilde{B}(p) =: \left(\frac{6}{8\pi\gamma\ell_{\text{Pl}}^2} \right)^{3/2} B(\mu), \text{ where } B(\mu) = \left(\frac{2}{3\mu_o} \right)^6 \left[|\mu + \mu_o|^{\frac{3}{4}} - |\mu - \mu_o|^{\frac{3}{4}} \right]^6. \quad (4.3)$$

Thus, we now have a separation of variables. Both the classical and the WDW theory suggests that ϕ could serve as emergent time. To implement this idea, let us introduce an appropriate kinematical Hilbert space for both geometry and the scalar field: $\mathcal{H}_{\text{kin}}^{\text{total}} := L^2(\mathbb{R}_{\text{Bohr}}, B(\mu) d\mu_{\text{Bohr}}) \otimes L^2(\mathbb{R}, d\phi)$. Since ϕ is to be thought of as ‘time’ and μ as the genuine, physical degree of freedom which evolves with respect to this ‘time’, we chose the standard Schrödinger representation for ϕ but the ‘polymer representation’ for μ which correctly captures the quantum geometry effects. This is a conservative approach in that the results will directly reveal the manifestations of quantum geometry; had we chosen a non-standard representation for the scalar field, these effects would have been mixed with those arising from an unusual representation of ‘time evolution’. Comparison with the WDW theory would also become more complicated. (However, the use of a ‘polymer representation’ for ϕ may become necessary to treat inhomogeneities in an adequate fashion.)

On $\mathcal{H}_{\text{kin}}^{\text{total}}$, the constraint takes the form:

$$\begin{aligned} \frac{\partial^2 \Psi}{\partial \phi^2} &= [B(\mu)]^{-1} (C^+(\mu)\Psi(\mu + 4\mu_o, \phi) + C^o(\mu)\Psi(\mu, \phi) + C^-(\mu)\Psi(\mu - 4\mu_o, \phi)) \\ &= -\Theta\Psi(\mu, \phi) \end{aligned} \quad (4.4)$$

were the functions C^\pm, C^o are given by:⁴

$$\begin{aligned} C^+(\mu) &= \frac{\pi G}{9|\mu_o|^3} \mid |\mu + 3\mu_o|^{\frac{3}{2}} - |\mu + \mu_o|^{\frac{3}{2}} \mid \\ C^-(\mu) &= C^+(\mu - 4\mu_o) \\ C^o(\mu) &= -C^+(\mu) - C^-(\mu). \end{aligned} \quad (4.5)$$

The form of (4.4) is the same as that of the WDW constraint (3.4), the only difference is that the ϕ -independent operator Θ is now a difference operator rather than a differential operator. Thus, the the LQC quantum Hamiltonian constraint can also be regarded as an ‘evolution equation’ which evolves the quantum state in the emergent time ϕ .

However, since Θ is a difference operator, an important difference arises from the WDW analysis. For, now the space physical states, i.e. of appropriate solutions to the constraint equation, is naturally divided into sectors each of which is preserved by the ‘evolution’ and by the action of our Dirac observables. Thus, there is super-selection. Let $\mathcal{L}_{|\varepsilon|}$ denote the ‘lattice’ of points $\{|\varepsilon| + 4n\mu_o, n \in \mathbb{Z}\}$ on the μ -axis, $\mathcal{L}_{-|\varepsilon|}$ the ‘lattice’ of points $\{-|\varepsilon| + 4n\mu_o, n \in \mathbb{Z}\}$ and let $\mathcal{L}_\varepsilon = \mathcal{L}_{|\varepsilon|} \cup \mathcal{L}_{-|\varepsilon|}$. Let $\mathcal{H}_{|\varepsilon|}^{\text{grav}}$, $\mathcal{H}_{-|\varepsilon|}^{\text{grav}}$ and $\mathcal{H}_\varepsilon^{\text{grav}}$ denote the subspaces of $L^2(\mathbb{R}_{\text{Bohr}}, B(\mu)d\mu_{\text{Bohr}})$ with states whose support is restricted to lattices $\mathcal{L}_{|\varepsilon|}$, $\mathcal{L}_{-|\varepsilon|}$ and \mathcal{L}_ε . Each of these three subspaces is mapped to itself by Θ . Since \hat{C}_{grav} is self-adjoint and positive definite on $\mathcal{H}_{\text{kin}}^{\text{grav}} \equiv L^2(\mathbb{R}_{\text{Bohr}}, d\mu_{\text{Bohr}})$, it follows that Θ is self-adjoint and positive definite on all three Hilbert spaces.

Note however that since $\mathcal{H}_{|\varepsilon|}^{\text{grav}}$ and $\mathcal{H}_{-|\varepsilon|}^{\text{grav}}$ are mapped to each other by the operator Π , only $\mathcal{H}_\varepsilon^{\text{grav}}$ is left invariant by Π . Now, because Π reverses the triad orientation, it represents a large gauge transformation. In gauge theories, we have to restrict ourselves to sectors, each consisting of an eigenspace of the group of large gauge transformations. (In QCD in particular this leads to the θ sectors.) The group generated by Π is just \mathbb{Z}_2 , whence there are only two eigenspaces, with eigenvalues ± 1 . Since there are no fermions in our theory, there are no parity violating processes whence we are led to choose the symmetric sector with eigenvalue $+1$. (Also, in the anti-symmetric sector all states are forced to vanish at the ‘singularity’ $\mu = 0$ while there is no such a priori restriction in the symmetric sector.) Thus, we are primarily interested in the symmetric subspace of $\mathcal{H}_\varepsilon^{\text{grav}}$; the other two Hilbert spaces will be useful only in the intermediate stages of our discussion.

Our first task is to explore properties of the operator Θ . Since it is self-adjoint and positive definite, its spectrum is non-negative. Therefore, as in the WDW theory, we will denote its eigenvalues by ω^2 . Let us first consider a generic ε , i.e., not equal to 0 or $2\mu_o$. Then, on each of the two Hilbert spaces $\mathcal{H}_{\pm|\varepsilon|}^{\text{grav}}$, we can solve for the eigenvalue equation $\Theta e_\omega(\mu) = \omega^2 e_\omega(\mu)$, i.e.,

$$C^+(\mu)e_\omega(\mu + 4\mu_o) + C^o(\mu)e_\omega(\mu) + C^-(\mu)e_\omega(\mu - 4\mu_o) = \omega^2 B(\mu)e_\omega(\mu) \quad (4.6)$$

Since this equation has the form of a recursion relation and since the coefficients $C^\pm(\mu)$ never vanish on the ‘lattices’ under consideration, it follows that we will obtain an eigenfunction by

⁴ Note that this fundamental evolution equation makes no reference to the Barbero-Immirzi parameter γ .

If we set $\tilde{\mu} = \mu/\mu_o$ and $\tilde{\Psi}(\tilde{\mu}, \phi) = \Psi(\mu, \phi)$, the equation satisfied by $\tilde{\Psi}(\tilde{\mu}, \phi)$ makes no reference to μ_o either. *This is the equation used in numerical simulations.* To interpret the results in terms of scale factor, however, values of γ and μ_o become relevant.

freely specifying, say, $\Psi(\mu^*)$ and $\Psi(\mu^* + 4\mu_o)$ for any μ^* on the ‘lattice’ $\mathcal{L}_{|\varepsilon|}$ or $\mathcal{L}_{-|\varepsilon|}$. Hence the eigenfunctions are 2-fold degenerate on each of $\mathcal{H}_{|\varepsilon|}^{\text{grav}}$ and $\mathcal{H}_{-|\varepsilon|}^{\text{grav}}$. On $\mathcal{H}_{\varepsilon}^{\text{grav}}$ therefore, the eigenfunctions are 4-fold degenerate as in the WDW theory. Therefore, $\mathcal{H}_{\varepsilon}^{\text{grav}}$ admits an orthonormal basis e_{ω}^I where the degeneracy index I ranges from 1 to 4, such that

$$\langle e_{\omega}^I | e_{\omega'}^{I'} \rangle = \delta_{I,I'} \delta(\omega, \omega'). \quad (4.7)$$

(The Hilbert space $\mathcal{H}_{\varepsilon}^{\text{grav}}$ is separable and the spectrum is equipped with the standard topology of the real line. Therefore we have the Dirac distribution $\delta(\omega, \omega')$ rather than the Kronecker delta $\delta_{\omega,\omega'}$.) As usual, every element $\Psi(\mu)$ of $\mathcal{H}_{\varepsilon}^{\text{grav}}$ can be expanded as:

$$\Psi(\mu) = \int_{\text{sp}\Theta} d\omega \tilde{\Psi}_I(\omega) e^I(\omega) \quad \text{where } \tilde{\Psi}_I(\omega) = \langle e_{\omega}^I | \Psi \rangle, \quad (4.8)$$

where the integral is over the spectrum of Θ . The numerical analysis of section V and comparison with the WDW theory are facilitated by making a convenient choice of this basis in $\mathcal{H}_{\varepsilon}^{\text{grav}}$, i.e., by picking specific vectors from each 4 dimensional eigenspace spanned by e_{ω}^I . To do so, note first that, as one might expect, every eigenvector $e_{\omega}^I(\mu)$ has the property that it approaches unique eigenvectors $\underline{e}^{\pm}(\omega)$ of the WDW differential operator $\underline{\Theta}$ as $\mu \rightarrow \pm\infty$. The precise rate of approach is discussed in section VA. In general, the two WDW eigenfunctions $\underline{e}^{\pm}(\omega)$ are distinct. Indeed, because of the nature of the WDW operator $\underline{\Theta}$, its eigenvectors can be chosen to vanish on the entire negative (or positive) μ -axis; their behavior on the two half lines is uncorrelated. (See the remark at the end of section III B.) Eigenvectors of the LQC Θ on the other hand are rigid; their values at any two lattice points determine their values on the entire lattice $\mathcal{L}_{\pm|\varepsilon|}$. Second, recall that the spectrum of the WDW operator $\underline{\Theta}$ is bounded below by $\omega^2 \geq \pi G/3$, whence \underline{e}_{ω} with $\omega^2 < \pi G/3$ does not appear in the spectral decomposition of $\underline{\Theta}$. Note however that solutions to the eigenvalue equation $\underline{\Theta} \underline{e}_{\omega} = \omega^2 \underline{e}_{\omega}$ continue to exist even for $\omega^2 < \pi G/3$. But such eigenfunctions diverge so fast as $\mu \rightarrow \infty$ or as $\mu \rightarrow -\infty$ that $\langle \underline{e}_{\omega} | \Psi \rangle$ fails to converge for all $\Psi \in L^2(\mathbb{R}, \underline{B}(\mu) d\mu)$, whence they do not belong to the basis. What is the situation with eigenvectors of the LQC Θ ? Since eigenvectors e_{ω} of Θ approach those of $\underline{\Theta}$, $\langle e_{\omega} | \Psi \rangle$ again fails to converge for all $\Psi \in \mathcal{H}_{\varepsilon}^{\text{grav}}$ if $\omega^2 < \pi G/3$. Thus the spectrum of Θ is again bounded below by $\pi G/3$.⁵ Therefore, to facilitate comparison with the WDW theory we will introduce a variables k via $\omega^2 - \pi G/3 = (16\pi G/3)k^2$ and use k in place of ω to label the orthonormal basis. To be specific, let us

- i) Denote by $e_{-|k|}^{\pm}(\mu)$ the basis vector in $\mathcal{H}_{\pm|\varepsilon|}^{\text{grav}}$ with eigenvalue ω^2 , which is proportional to the WDW $\underline{e}_{-|k|}$ as $\mu \rightarrow \infty$; (i.e., it has only ‘outgoing’ or ‘expanding’ component in this limit);
- ii) Denote by $e_{|k|}^{\pm}(\mu)$ the basis vector in $\mathcal{H}_{\pm|\varepsilon|}^{\text{grav}}$ with eigenvalue ω^2 which is orthogonal to $e_{-|k|}^{\pm}(\mu)$, i.e., (since eigenvectors are 2-fold degenerate in each of $\mathcal{H}_{\pm|\varepsilon|}^{\text{grav}}$, the vector $e_{|k|}^{\pm}(\mu)$ is uniquely determined up to a multiplicative phase factor.)

As we will see in section VA, this basis is well-suited for numerical analysis.

We thus have an orthonormal basis e_k^{\pm} in $\mathcal{H}_{\varepsilon}^{\text{grav}}$ with $k \in \mathbb{R}$: $\langle e_k^{\pm} | e_{k'}^{\pm} \rangle = \delta(k, k')$, and $\langle e_k^+ | e_{k'}^- \rangle = 0$. The four eigenvectors with eigenvalue ω^2 are now $e_{|k|}^+, e_{-|k|}^+$ which have support

⁵ A rigorous version of this argument can be constructed e.g. by using the Gel’fand triplet [54] associated with the operator Θ . However, this step has not been carried out.

on the ‘lattice’ $\mathcal{L}_{|\varepsilon|}$, and $e_{|k|}^-, e_{-|k|}^-$ which have support on the ‘lattice’ $\mathcal{L}_{-|\varepsilon|}$. We will be interested only in the symmetric combinations:

$$e_k^{(s)}(\mu) = \frac{1}{2} (e_k^+(\mu) + e_k^+(-\mu) + e_k^-(\mu) + e_k^-(-\mu)) \quad (4.9)$$

which are invariant under Π . Finally we note that any symmetric element $\Psi(\mu)$ of $\mathcal{H}_\varepsilon^{\text{grav}}$ can be expanded as

$$\Psi(\mu) = \int_{-\infty}^{\infty} dk \tilde{\Psi}(k) e_k^{(s)}(\mu) \quad (4.10)$$

We can now write down the general symmetric solution to the quantum constraint (4.4) with initial data in $\mathcal{H}_\varepsilon^{\text{grav}}$:

$$\Psi(\mu, \phi) = \int_{-\infty}^{\infty} dk [\tilde{\Psi}_+(k) e_k^{(s)}(\mu) e^{i\omega\phi} + \tilde{\Psi}_-(k) \bar{e}_k^{(s)}(\mu) e^{-i\omega\phi}] \quad (4.11)$$

where $\tilde{\Psi}_\pm(k)$ are in $L^2(\mathbb{R}, dk)$. As $\mu \rightarrow \pm\infty$, these approach solutions (3.9) to the WDW equation. However, the approach is not uniform in the Hilbert space but varies from solution to solution. As indicated in section II B, the LQC solutions to (4.4) which are semi-classical at late times can start departing from the WDW solutions for relatively large values of μ , say $\mu \sim 10^4 \mu_o$.

As in the WDW theory, if $\Psi_-(k)$ vanishes, we will say that the solution is of positive frequency and if $\Psi_+(k)$ vanishes we will say it is of negative frequency. Thus, every solution to (4.4) admits a natural positive and negative frequency decomposition. The positive (respectively negative) frequency solutions satisfy a Schrödinger type first order differential equation in ϕ :

$$\mp i \frac{\partial \Psi_\pm}{\partial \phi} = \sqrt{\Theta} \Psi_\pm \quad (4.12)$$

but with a Hamiltonian $\sqrt{\Theta}$ (which is non-local in μ). Therefore the solutions with initial datum $\Psi(\mu, \phi_o) = f_\pm(\mu)$ are given by:

$$\Psi_\pm(\mu, \phi) = e^{\pm i\sqrt{\Theta}(\phi - \phi_o)} f_\pm(\mu, \phi) \quad (4.13)$$

Remark: In the above discussion, we considered a generic ε . We now summarize the situation in the special cases, $\varepsilon = 0$ and $\varepsilon = 2\mu_o$. In these cases, differences arise because the individual lattices are invariant under the reflection $\mu \rightarrow -\mu$, i.e., the lattices $\mathcal{L}_{|\varepsilon|}$ and $\mathcal{L}_{-|\varepsilon|}$ coincide. As before, there is a 2-fold degeneracy in the eigenvectors of Θ on any one lattice. For concreteness, let us label the Hilbert spaces $\mathcal{H}_{|\varepsilon|}^{\text{grav}}$ and choose the basis vectors $e_k^+(\mu)$, with $k \in \mathbb{R}$ as above. Now, symmetrization can be performed on each of these Hilbert spaces by itself. So, we have:

$$e_k^{(s)}(\mu) = \frac{1}{\sqrt{2}} (e_k^+(\mu) + e_k^+(-\mu)) \quad (4.14)$$

However, the vector $e_{|k|}^{(s)}(\mu)$ coincides with the vector $e_{-|k|}^{(s)}(\mu)$ so there is only one symmetric eigenvector per eigenvalue. This is not surprising: the original degeneracy was 2-fold (rather than 4-fold) and so there is one symmetric and one anti-symmetric eigenvector per eigenvalue. Nonetheless, it is worth noting that there is a precise sense in which the Hilbert

space of symmetric states is only ‘half as big’ in these exceptional cases as they are for a generic ε .

For $\varepsilon = 2\mu_o$, there is a further subtlety because C^+ vanishes at $\mu = -2\mu_o$ and C^- vanishes at $\mu = 2\mu_o$. Thus, in this case, as in the WDW theory, there is a decoupling and the knowledge of the eigenfunction $e_k^+(\mu)$ on the positive μ -axis does not suffice to determine it on the negative μ axis and vice-versa. However, the degeneracy of the eigenvectors does not increase but remains 2-fold because (4.4) now introduces two new constraints: $C^+(2\mu_o)e_k^+(\pm 6\mu_o) = [\omega^2 B(\pm 2\mu_o) - C^o(\pm 2\mu_o)]e_k^+(\pm 2\mu_o) = 0$. Conceptually, this difference is not significant; there is again a single symmetric eigenfunction for each eigenvalue.

B. The Physical sector

Results of section IV A show that while the LQC operator Θ differs from the WDW operator $\underline{\Theta}$ in interesting ways, the structural form of the two Hamiltonian constraint equations is the same. Therefore, apart from the issue of superselection sectors which arise from the fact that Θ is discrete, introduction of the Dirac observables and determination of the inner product either by demanding that the Dirac observables be self-adjoint or by carrying out group averaging is completely analogous in the two cases. Therefore, we will not repeat the discussion of section III B but only summarize the final structure.

The sector of physical Hilbert space $\mathcal{H}_{\text{phy}}^\varepsilon$ labeled by $\varepsilon \in [0, 2\mu_o]$ consists of positive frequency solutions $\Psi(\mu, \phi)$ to (4.4) with initial data $\Psi(\mu, \phi_o)$ in the symmetric sector of $\mathcal{H}_{\text{grav}}^\varepsilon$. Eq. (4.11) implies that they have the explicit expression in terms of our eigenvectors $e_k^{(s)}(\mu)$

$$\Psi(\mu, \phi) = \int_{-\infty}^{\infty} dk \tilde{\Psi}(k) e_k^{(s)}(\mu) e^{i\omega\phi}, \quad (4.15)$$

where, as before, $\omega^2 = (16\pi G/3)(k^2 + 1/16)$ and $e_k^{(s)}(\mu)$ is given by (4.9) and (4.14). By choosing appropriate functions $\tilde{\Psi}(k)$, this expression will be evaluated in section V A using Fast Fourier Transforms. The resulting $\Psi(\mu, \phi)$ will provide, numerically, quantum states which are semi-classical for large μ . The physical inner product is given by:

$$\langle \Psi_1 | \Psi_2 \rangle_\varepsilon = \sum_{\mu \in \{\pm|\varepsilon| + 4n\mu_o; n \in \mathbb{Z}\}} B(\mu) \bar{\Psi}_1(\mu) \Psi_2(\mu) \quad (4.16)$$

The action of the Dirac observables is independent of ε , and has the same form as in the WDW theory:

$$\widehat{\mu|_{\phi_o}} \Psi(\mu, \phi) = e^{i\sqrt{\Theta}(\phi - \phi_o)} \mu \Psi(\mu, \phi_o), \quad \text{and} \quad \hat{p}_\phi \Psi(\mu, \phi) = -i\hbar \frac{\partial \Psi(\mu, \phi)}{\partial \phi}. \quad (4.17)$$

The kinematical Hilbert space $\mathcal{H}_{\text{kin}}^{\text{total}}$ is non-separable but, because of super-selection, each physical sector $\mathcal{H}_{\text{phy}}^\varepsilon$ is separable. Eigenvalues of the Dirac observable $\widehat{\mu|_{\phi_o}}$ constitute a discrete subset of the real line in each sector. In the kinematic Hilbert space $\mathcal{H}_{\text{kin}}^{\text{grav}}$, the spectrum of \hat{p} is discrete in a subtler sense: while every real value is allowed, the spectrum has discrete topology, reflecting the fact that each eigenvector has a finite norm in $\mathcal{H}_{\text{kin}}^{\text{grav}}$. Thus, the more delicate discreteness of the spectrum of \hat{p} on $\mathcal{H}_{\text{kin}}^{\text{grav}}$ descends to the standard type of discreteness of Dirac observables. Question is often raised whether the kinematic

discreteness in LQG will have strong imprints in the physical sector or if they will be washed away in the passage to the physical Hilbert space. A broad answer—illustrated by the area eigenvalues of isolated horizons [55, 56]—is that the discreteness will generically descend to the physical sector at least in cases where one can construct Dirac observables directly from the kinematical geometrical operators [1]. The present discussion provides another illustration of this situation.

Note that the eigenvalues of $\widehat{\mu|_{\phi_o}}$ in distinct sectors are distinct. Therefore which sector actually occurs is a question that can be in principle answered experimentally, provided one has access to microscopic measurements which can distinguish between values of the scale factor which differ by $\sim 10\ell_{\text{Pl}}$. This will not be feasible in the foreseeable future. Of greater practical interest are the coarse-grained measurements, where the coarse graining occurs at significantly greater scales. For these measurements, different sectors would be indistinguishable and one could work with any one.

The group averaging procedure used in this section is quite general in the sense that it is applicable for a large class of systems, including full LQG if, e.g., its dynamics is formulated using Thiemann’s master constraint program [57]. In this sense, the physical Hilbert spaces $\mathcal{H}_{\text{phy}}^{\varepsilon}$ constructed here are natural. However, using the special structures available in this model, one can also construct an inequivalent representation which is closer to that used in the WDW theory. The main results on the bounce also hold in that representation. Although that construction appears to have an ad-hoc element, it may well admit extensions and be useful in more general models. Therefore, it is presented in Appendix C.

V. NUMERICS IN LOOP QUANTUM COSMOLOGY

In this section, we will find physical states of LQG and analyze their properties numerically. This section is divided into three parts. In the first we study eigenfunctions $e_k^{\pm}(\mu)$ of Θ and then use them to directly evaluate the right side of (4.15), thereby obtaining a ‘general’ physical state. In the second part we solve the initial value problem starting from initial data at $\phi = \phi_o$, thereby obtaining a ‘general’ solution to the difference equation (4.4). In the third we summarize the main results and compare the outcome of the two methods. Readers who are not interested in the details of simulations can go directly to the third subsection.

A large number of simulations were performed within each of the approaches by varying the parameters in the initial data and working with different lattices $\mathcal{L}_{\varepsilon}$. They show that the final results are robust. To avoid the making the paper excessively long, we will only show illustrative plots.

A. Direct evaluation of the integral representation (4.15) of solutions

The goal of this sub-section is to evaluate the right side of (4.15) using suitable momentum profiles $\tilde{\Psi}(k)$. This calculation requires the knowledge of eigenfunctions $e_k^{(s)}(\mu)$ of Θ . Therefore, we will first have to make a somewhat long detour to numerically calculate the basis functions $e_k^{\pm}(\mu)$ and $e_k^{(s)}(\mu)$ introduced in section IV A. The integral in (4.15) will be then evaluated using a fast Fourier transform.

1. General eigenfunctions of the Θ operator: asymptotics

We will first establish properties of the general eigenfunctions $e_\omega(\mu)$ of Θ that were used in section IV A.

Let us fix a ‘lattice’, say $\mathcal{L}_{|\varepsilon|}$. Since the left side of (4.6) approaches $\hat{C}_{\text{grav}}^{\text{WDW}} e_\omega(\mu)$ as $|\mu| \rightarrow \infty$, in this limit one would expect each e_ω to converge to an eigenfunction \underline{e}_ω of $\underline{\Theta}$ with the same eigenvalue. Numerical simulations have shown that this expectation is correct and have also provided the rate of approach.

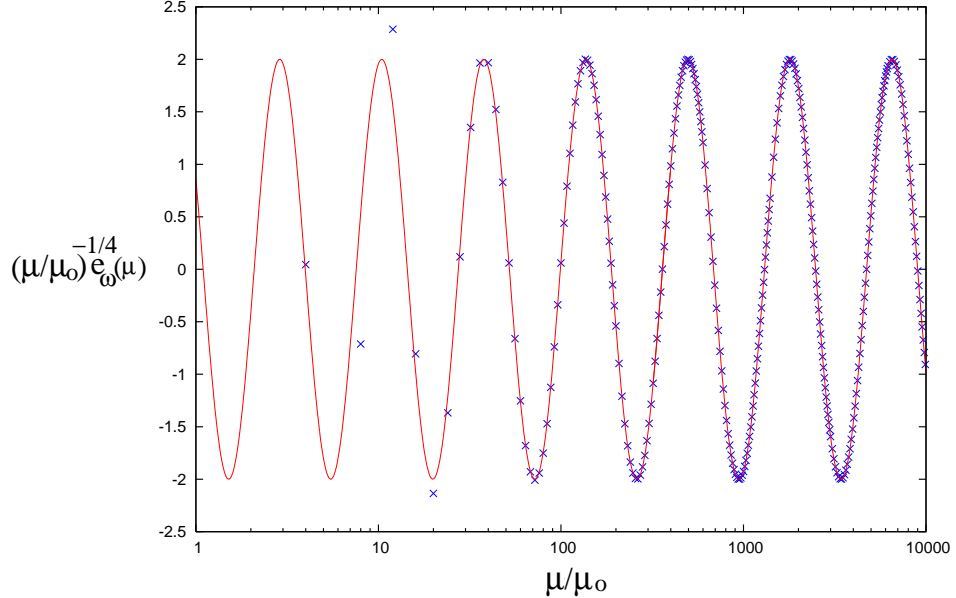


FIG. 2: Crosses denote the values of an eigenfunction $e_\omega(\mu)$ of Θ for $\varepsilon = 0$ and $\omega = 20$. The solid curve is the eigenfunction $\underline{e}_\omega(\mu)$ of the WDW $\underline{\Theta}$ to which $e_\omega(\mu)$ approaches at large positive μ . As μ increases, the set of points on \mathcal{L}_ε becomes denser and fill the solid curve. For visual clarity only some of these points are shown for $\mu > 100$.

Recall that each WDW eigenfunction e_ω is a linear combination of basis functions $e_{|k|}$, $e_{-|k|}$ defined in section III A. Therefore, given an e_ω it suffices to calculate the coefficients of the decomposition of e_ω with respect to this basis. The method of finding these coefficients is presented in detail in Appendix B.⁶ Once the limiting $e_\omega(\mu)$ were found, they were compared with the original eigenfunction $e_\omega(\mu)$ for a variety of values of ω . An illustrative plot comparing $e_\omega(\mu)$ with its limit is shown in Fig. 2. In general, each $e_\omega(\mu)$ approaches distinct eigenfunctions $\underline{e}_{\omega,\pm}(\mu)$ of $\underline{\Theta}$ in the limits $\mu \rightarrow \pm\infty$. The rate of approach is given

⁶ If $\omega^2 < \pi G/3$, then ω^2 is not part of the spectrum of the self-adjoint operator $\underline{\Theta}$. Nonetheless, by directly solving the eigenvalue equation $\underline{\Theta}e_\omega = \omega^2 e_\omega$ one can introduce an analogous decomposition onto fixed eigenfunctions, $\underline{e}_{\pm|k'|} := |\mu|^{\frac{1}{4} \pm k'} e_{\pm|k'|}$, $k'^2 = 1/16 - 3/(16\pi G)\omega^2$ and also write the limit of e_ω in terms of coefficients in this ‘basis’.

by:

$$\mu^{-\frac{1}{4}} e_\omega(\mu) = \begin{cases} \mu^{-\frac{1}{4}} \underline{e}_{\omega,+}(\mu) + O\left(\frac{1}{\mu^2}\right), & \text{for } \mu > 0, \\ \mu^{-\frac{1}{4}} \underline{e}_{\omega,-}(\mu) + O\left(\frac{1}{\mu^2}\right), & \text{for } \mu < 0. \end{cases} \quad (5.1)$$

Numerical tests were performed up to $|\mu| = 10^6 \mu_o$. The quantity $\mu^{7/4} |e_\omega - \underline{e}_{\omega,\pm}|(\mu)$ was found to be bounded. The bound decreases with μ . For the case $\varepsilon = 0$, $\omega = 20$ depicted in Fig. 2 the absolute bound in the interval $(\mu = 10^2 \mu_o, 10^6 \mu_o)$ was less than 90.

Because the eigenfunctions $e_\omega(\mu)$ of Θ are determined on the entire lattice $\mathcal{L}_{|\varepsilon|}$ by their values on (at most) two points, the WDW limits for positive and negative μ are not independent. Thus, if the limits are expressed as

$$e_\omega(\mu) \xrightarrow{\mu \gg 1} A \underline{e}_{|k|}(\mu) + B \underline{e}_{-|k|}(\mu), \quad e_\omega(\mu) \xrightarrow{\mu \ll -1} C \underline{e}_{|k|}(\mu) + D \underline{e}_{-|k|}(\mu) \quad (5.2)$$

the coefficients C, D are uniquely determined by values of A, B (and vice versa). One relation, suggested by analytical considerations involving the physical inner product, was verified in detail numerically:

$$|A|^2 - |B|^2 = |C|^2 - |D|^2. \quad (5.3)$$

It will be useful in the analysis of basis functions in the next two sub-sections.

2. Construction of the basis $e_{-|k|}^\pm$

In section IV A we introduced a specific basis of \mathcal{H}_ε which is well adapted for comparison with the WDW theory. We will now use numerical methods to construct this basis and analyze its properties. Our investigation will be restricted to the vectors $e_{-|k|}^\pm(\mu)$ because, the physical states $\Psi(\mu, \phi)$ of Eq. (4.15) we are interested will have negligible projections on the vectors $e_{|k|}^\pm(\mu)$. (Recall that in general $\Psi \in \mathcal{H}_\varepsilon$ has support on $\mathcal{L}_{|\varepsilon|} \cup \mathcal{L}_{-|\varepsilon|}$. $e_{-|k|}^+(\mu)$ has support on $\mathcal{L}_{+|\varepsilon|}$ and $e_{-|k|}^-(\mu)$ on $\mathcal{L}_{-|\varepsilon|}$.)

Each of the eigenfunctions $e_{-|k|}^\pm(\mu)$ is calculated as follows. To solve (4.6), we need to specify initial conditions at two points on each of the two lattices. We fix large positive $\mu_\pm^* \in \mathcal{L}_{\pm|\varepsilon|}$ and demand that the values of $e_{-|k|}^\pm(\mu)$ agree with those of $\underline{e}_{-|k|}(\mu)$ at the points μ_\pm^* and $\mu_\pm^* + 4\mu_o$. Then $e_{-|k|}^\pm$ are evaluated separately on finite domains $\mathcal{L}_{\pm|\varepsilon|} \cap [-\mu_\pm^*, \mu_\pm^*]$ of each of the two lattices. For large negative μ , these eigenfunctions are linear combinations of the WDW basis functions $C^\pm \underline{e}_{|k|} + D^\pm \underline{e}_{-|k|}$. The coefficients C^\pm, D^\pm are evaluated using the method specified in Appendix B.

Eigenfunctions $e_{-|k|}^\pm(\mu)$ were calculated for approximately 2×10^4 different $|k|$'s in the range $5 \leq \omega \leq 10^3$. They revealed the following properties:

- (i) Each $e_{-|k|}^\pm(\mu)$ is well approximated by a WDW eigenfunction until one reaches the ‘genuinely quantum region’. In this region the absolute value $|e_{-|k|}^\pm|$ grows very quickly as μ decreases: $|e_{-|k|}^\pm| \propto e^{-\text{sgn}(\mu) \alpha \sqrt{\omega |\mu|}}$, where $\alpha \equiv \alpha(\varepsilon)$ is a constant on any given lattice. This property is illustrated by Fig. 3. This region of rapid growth is symmetric about $\mu = 0$ and its size depends linearly on ω (the square-root of the eigenvalue of Θ); its boundary lies at $\mu \approx 0.5\omega \mu_o$. (However, this region excludes the interval $[-4\mu_o, 4\mu_o]$ where $B(\mu)$ decreases and goes to zero, departing significantly from its WDW analog $\underline{B}(\mu)$.)

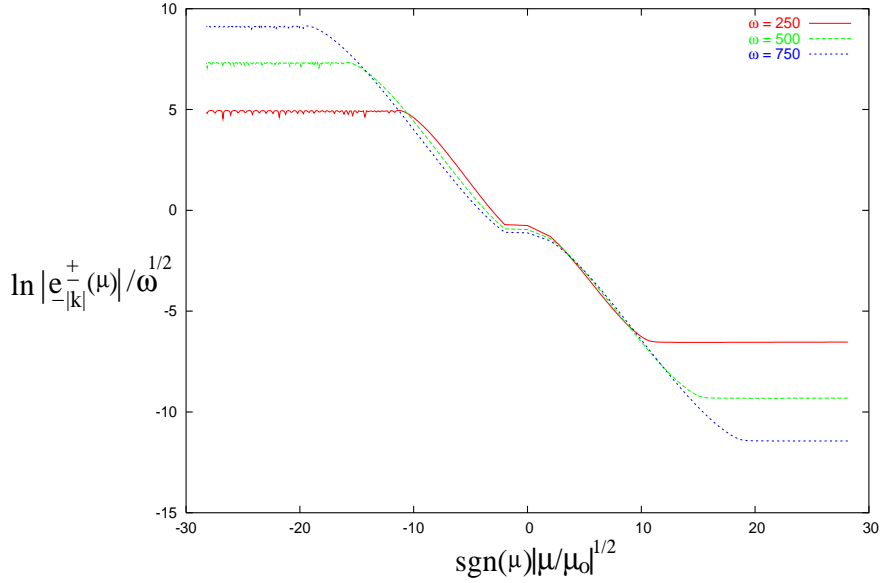


FIG. 3: The exponential growth of $|e_{-|k|}^{\pm}(\mu)|$ in the ‘genuinely quantum region’ is shown for three different values of ω , where ω is given by $\Theta e_{-|k|}^{\pm} = \omega^2 e_{-|k|}^{\pm}$.

(ii) After leaving this region of growth, the basis function $e_{-|k|}^{\pm}(\mu)$ again approaches some WDW eigenfunction

$$e_{-|k|}^{\pm} \xrightarrow{\mu \ll -1} C^{\pm} e_{|k|} + D^{\pm} e_{-|k|} . \quad (5.4)$$

where the coefficients C^{\pm}, D^{\pm} are large. Their absolute values grow exponentially with ω . To investigate this property qualitatively we defined an ‘amplification factor’

$$\lambda^{\pm} := \frac{1}{2} (|C^{\pm}|^2 + |D^{\pm}|^2) \quad (5.5)$$

The numerical calculations show that $\lambda^+ = \lambda^-$, so parts of $e_{-|k|}^{\pm}$ supported on $\mathcal{L}_{+|\varepsilon|}$ and $\mathcal{L}_{-|\varepsilon|}$ are amplified equally. The dependence of λ^{\pm} on ω and ε is shown in Fig. 4. Almost everywhere it can be well approximated by the function

$$\lambda^{\pm}(\omega, \varepsilon) \approx e^{a\omega+b} . \quad (5.6)$$

where a, b are rather complicated functions of ε . The fits of $a(\varepsilon), b(\varepsilon)$ are presented in Fig. 5 and Fig. 6. The actual simulations were carried out for various values of $p_{\phi} = \hbar\omega$, up to $p_{\phi} = 10^3$.

(iii) The general relation (5.3) holds in our case with $|B| = 0$. Existence of the tremendous amplification now implies that the absolute values of C and D are almost equal (with differences of the order of $1/\lambda^{\pm}$)

$$|C^{\pm}| \approx |D^{\pm}| . \quad (5.7)$$

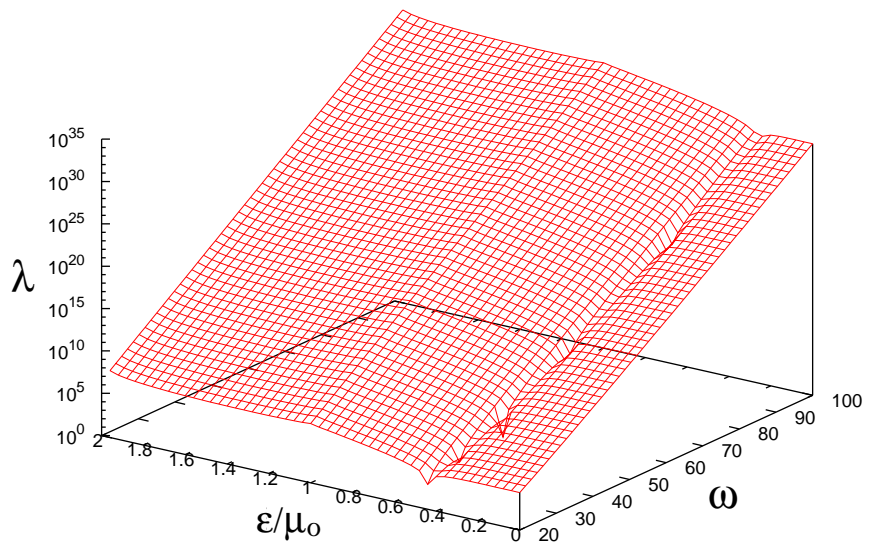


FIG. 4: The amplification factor λ^\pm in the ‘genuinely quantum region is shown as a function of the parameter ε labeling the lattice and ω .

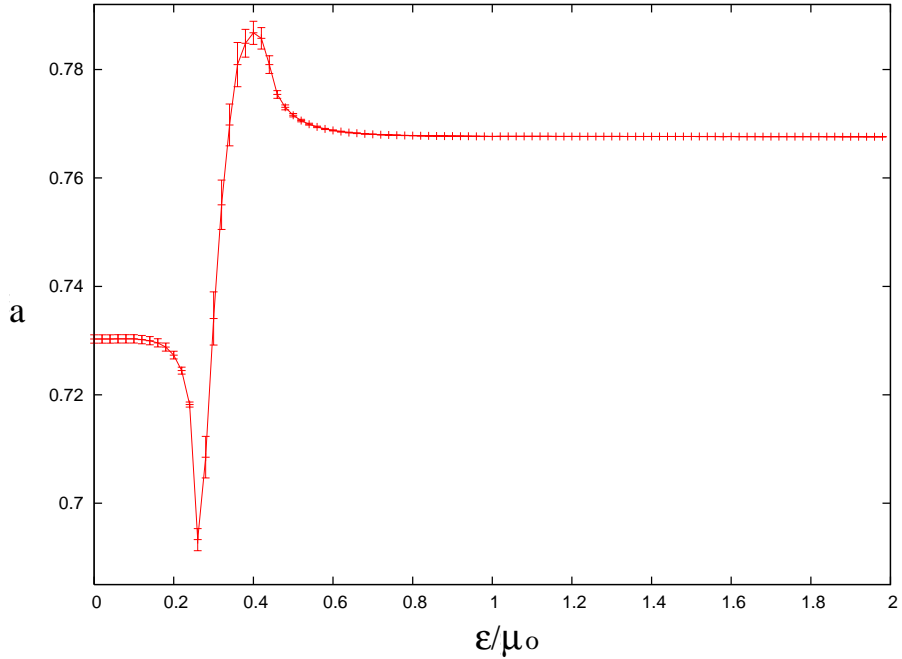


FIG. 5: The function $a(\varepsilon)$ of Eq 5.6 is plotted by connecting numerically calculated data points.

Thus for negative μ , eigenfunctions asymptotically approach WDW eigenfunctions

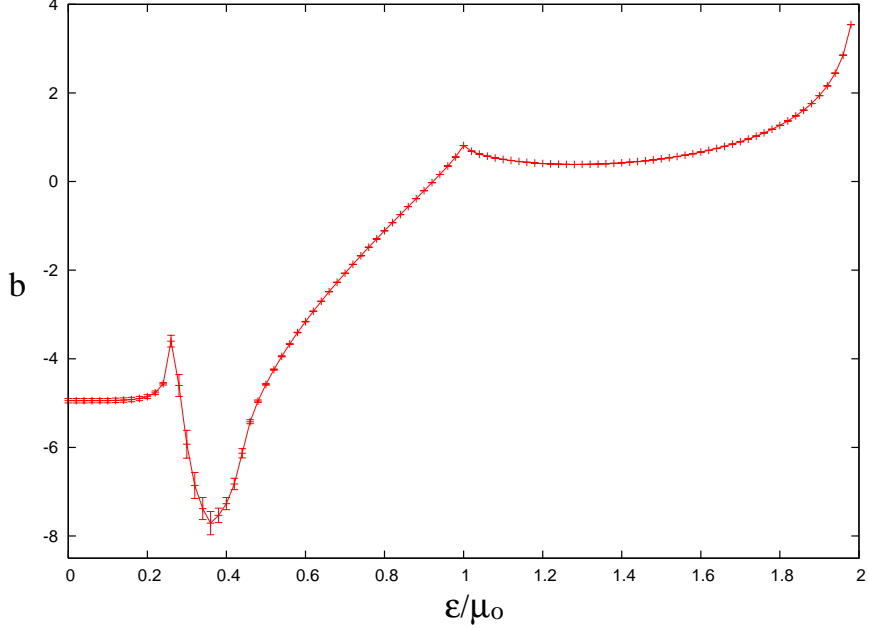


FIG. 6: The function $b(\varepsilon)$ of Eq 5.6 is plotted by connecting numerically calculated data points.

and are almost equally composed of incoming and outgoing waves.

3. Basis for the symmetric sector

Once the basis functions $e_{-|k|}^\pm$ are known one can readily use (4.9) to construct the basis $e_{-|k|}^{(s)}$ for solutions to (4.6) which are symmetric under $\mu \rightarrow -\mu$. Due to strong amplification in the region around $\mu = 0$ the behavior of $e_{-|k|}^{(s)}$ is dominated by properties of $e_{-|k|}^\pm$ for $\mu < 0$. The numerical calculations show the following properties:

- (i) Each symmetric basis eigenfunction is strongly suppressed in the ‘genuinely quantum region’ around to $\mu = 0$. The behavior of $e_{-|k|}^\pm$ in this region implies that $|e_{-|k|}^{(s)}| \propto \cosh(\alpha\sqrt{\omega\mu})$, where α is a function of ε only.
- (ii) Outside the ‘genuinely quantum region’ $e_{-|k|}^{(s)}$ quickly approaches the WDW eigenfunction almost equally composed of incoming and outgoing ‘plane waves’ ($e_{|k|}$ and $e_{-|k|}$). In the exceptional cases $\varepsilon = 0$ or $2\mu_o$ the two contributions are exactly equal. To establish this result, note first that the symmetry requirement and the fact that $C^+(-2\mu_o) = C^-(2\mu_o) = 0$ imply that in both cases the value of $e_{-|k|}^{(s)}$ at one point already determines the complete ‘initial data’ (i.e., values at some μ_* and $\mu_* + 4\mu_o$) and hence the eigenfunction on the entire \mathcal{L}_ε :

$$e_{-|k|}^{(s)}(4\mu_o) = e_{-|k|}^{(s)}(-4\mu_o) = e_{-|k|}^{(s)}(0) , \quad \text{for } \varepsilon = 0 , \quad (5.8a)$$

$$e_{-|k|}^{(s)}(6\mu_o) = \frac{\omega^2 B(2\mu_o) - C^o(2\mu_o)}{C^+(2\mu_o)} e_{-|k|}^{(s)}(2\mu_o) , \quad \text{for } \varepsilon = 2\mu_o . \quad (5.8b)$$

Because of the reality of coefficients of Eq. (4.6), this implies that the phase of $e_{-|k|}^{(s)}$ is exactly constant, whence contributions of $\underline{e}_{|k|}$ and $\underline{e}_{-|k|}$ are also exactly equal.

(iii) On each lattice $\mathcal{L}_{\pm|\varepsilon|}$ the incoming and outgoing components are rotated with respect to each other by an angle α^\pm

$$e_{-|k|}^{(s)} |_{\mathcal{L}_{\pm|\varepsilon|}} \xrightarrow{\mu \rightarrow \infty} z^\pm (e^{i\alpha^\pm} \underline{e}_{|k|} + e^{-i\alpha^\pm} \underline{e}_{-|k|}), \quad (5.9)$$

where z^\pm are some complex *constants* satisfying $|z^+| \approx |z^-|$, while the phases α^\pm are functions of ε and ω . In general, for $\varepsilon \neq 0$ or $\varepsilon \neq 2\mu_o$, α_+ need not equal α_- .

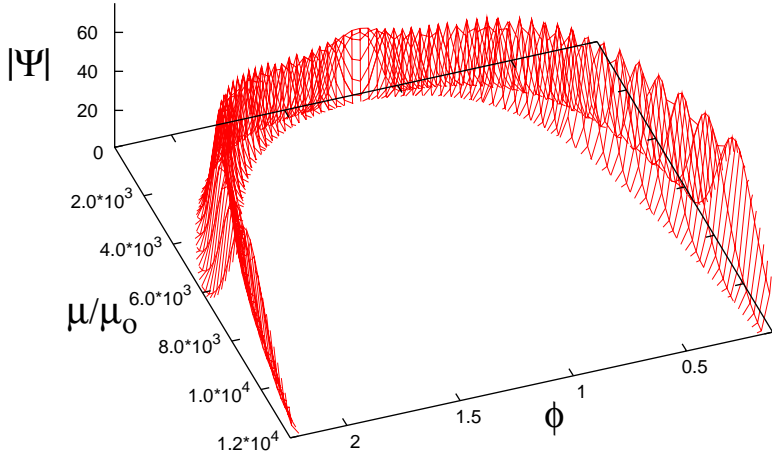


FIG. 7: Plot of the wave function $\Psi(\mu, \phi)$ obtained by directly evaluating the right side of (4.15). Parameters are $p_\phi = 500$, $\Delta p_\phi/p_\phi = 0.05$ and $\varepsilon = \mu_o$.

4. Evaluation of the integral in (4.15)

Now that we have the symmetric basis functions $e_{-|k|}^{(s)}$ at our disposal, we can obtain the desired physical states by directly evaluating the integral in (4.15).

We wish to construct physical states which are sharply peaked at a phase space point on a classical trajectory of the expanding universe at a late time (e.g., ‘now’). The form of the integrand in (4.15), the expression (4.16) of the physical inner product, the functional form of $\omega(k)$ and standard facts about coherent and squeezed states in quantum mechanics provide a natural strategy to select an appropriate $\tilde{\Psi}(k)$. If we set

$$\tilde{\Psi}(k) = e^{-\frac{(k-k^*)^2}{2\sigma^2}} e^{-i\omega\phi^*} \quad (5.10)$$

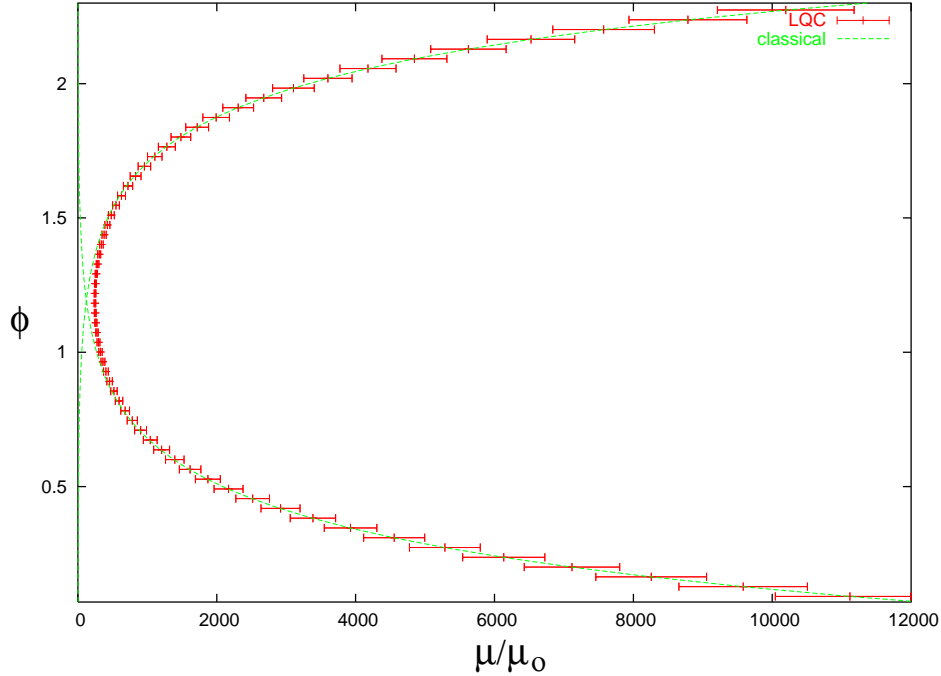


FIG. 8: Expectation values and dispersion of $\widehat{\mu|\phi}$ for wave function presented in Fig. 7 are compared with classical trajectories.

with suitably small σ , the final state will be sharply peaked at $p_\phi = p_\phi^*$

$$p_\phi^* = - \left(\frac{16\pi G \hbar^2}{3} \right)^{\frac{1}{2}} k^* \quad (5.11)$$

and the parameter ϕ^* will determine the value μ^* of the Dirac observable $\widehat{\mu|\phi_o}$ at which the state will be peaked at ‘time’ ϕ_o . As mentioned in section III B, to obtain a state which is semi-classical at a late time, we need a large value of p_ϕ : $p_\phi^* \gg \hbar$ in the classical units, $c=G=1$. Therefore, we need $k^* \ll -1$, whence the functions $\tilde{\Psi}(k)$ of interest will be negligibly small for $k > 0$. Therefore, without loss of physical content, we can set them to zero on the positive k axis. This is why the explicit form of eigenfunctions $e_{|k|}^{(s)}$ is not required in our analysis.

Thus, the integral we wish to evaluate is:

$$\Psi(\mu, \phi) = \int_0^\infty dk e^{-\frac{(k-k^*)^2}{2\sigma^2}} e_k^{(s)}(\mu) e^{i\omega(k)(\phi-\phi^*)}, \quad (5.12)$$

where σ is the spread of the Gaussian. The details of the numerical evaluation can be summarized as follows.

- For a generic ε , the $e_{-|k|}^{(s)}$ were found numerically following the procedure specified in sections V A 2 and V A 3. For the exceptional cases, $\varepsilon = 0, 2\mu_o$, in order to avoid loss of precision in the region where $e_{-|k|}^{(s)}$ is very small, we provided ‘initial values’ of $e_{k_j}^{(s)}$

at $\mu = \pm \varepsilon$ and $\mu = \pm \varepsilon + 4\mu_o$ using (5.8). On the k axis we chose a set $\{k_j\}$ of points which are uniformly distributed across the interval $[k^* - 10\sigma, k^* + 10\sigma]$. In numerical simulations, the number l of points in the set $\{k_j\}$ ranged between 2^{11} and 2^{13} .

- Next, for each k_j , we calculated $e_{-|k_j|}^{(s)}(\mu_i)$ for $\mu \in \{\pm \varepsilon + 4n\mu_o : n \in \{-N, \dots, N\}\}$ where N is a large constant ($\sim 50p_\phi^*$).
- Finally, we evaluated (5.12) using discrete Fourier transform (FFT). The result was a set of profiles $\Psi(\mu_i, \phi_j)$ where $\phi_j = \sqrt{3\pi/(4G)}(j - l/2)/(k_l - k_1)$. This is a positive frequency solution to the LQC equation (4.4).

Our next task is to analyze properties of these solution. Given any one $\Psi(\phi_j, \mu_i)$, we chose ‘instants of time’ ϕ and calculated the norm and the expectation values of our Dirac observable $\hat{\mu}|_\phi$ and \hat{p}_ϕ using:

$$\|\Psi\|^2 = \sum_{\mu_i \in \mathcal{L}_\varepsilon} B(\mu_i) |\Psi(\phi, \mu_i)|^2, \quad (5.13a)$$

$$\langle \widehat{|\mu|_\phi} \rangle = \frac{1}{\|\Psi\|^2} \sum_{\mu \in \mathcal{L}_\varepsilon} B(\mu_i) |\mu_i| |\Psi(\phi, \mu_i)|^2, \quad (5.13b)$$

$$\langle \hat{p}_\phi \rangle = \frac{1}{\|\Psi\|^2} \sum_{\mu \in \mathcal{L}_\varepsilon} B(\mu_i) \bar{\Psi}(\phi, \mu_i) \frac{\hbar}{i} \partial_\phi \Psi(\phi, \mu_i). \quad (5.13c)$$

Finally, the dispersions were evaluated using their definitions:

$$\langle \Delta \widehat{|\mu|_\phi} \rangle^2 = |\langle \widehat{|\mu^2|_\phi} \rangle - \langle \widehat{|\mu|_\phi} \rangle^2|, \quad \langle \Delta \hat{p}_\phi \rangle^2 = |\langle \hat{p}_\phi^2 \rangle - \langle \hat{p}_\phi \rangle^2|. \quad (5.14)$$

These calculations were performed for 16 different choices of ε and for ten values of p_ϕ up to a maximum of $p_\phi = 10^3$, and for 5 different choices of the dispersion parameter σ . Fig. 7 provides an example of a state constructed via this method. The expectation values of $\langle \widehat{|\mu|_\phi} \rangle$ are shown in Fig. 8.

Results are discussed in section VC below.

B. Evolution in ϕ

We can also regard the quantum constraint (4.4) as an initial value problem in ‘time’ ϕ and solve it by carrying out the ϕ -evolution. Conceptually, this approach is simpler since it does not depend on the properties of the eigenfunctions of Θ . However, compared to the direct evaluation of the integral (4.15), this method is technically more difficult because it entails solving a large number of coupled differential equations. Nonetheless, to demonstrate the robustness of results, we carried out the ϕ -evolution as well. This sub-section summarizes the procedure.

1. Method of integration

At large $|\mu|$ the difference equation is well approximated by the WDW equation which is a hyperbolic partial differential equation (PDE). However since Θ couples μ in discrete

steps, for a given ε -sector (4.4) is just a system of a countable number of coupled ordinary differential equations (ODEs) of the 2nd order.⁷

Technical limitations require restriction of the domain of integration to a set $|\mu - \varepsilon| \leq 4N\mu_o$, where $1 \ll N \in \mathbb{N}$. This restriction makes the number of equations finite. However one now needs to introduce appropriate boundary conditions. The fundamental equation on the boundary is $i\partial_\phi\Psi = s\sqrt{\Theta}\Psi$, where $s = +1$ (-1) for the forward (backward) evolution in ϕ . It is difficult to calculate $\sqrt{\Theta}\Psi$ at each time step. Therefore, *just on the boundary itself*, this equation was simplified to:

$$\partial_\phi\Psi(\mu, \phi) = s\sqrt{\pi G/3}(|\mu| - 2\mu_o)(\Psi(\mu, \phi) - \Psi(\mu - 4\operatorname{sgn}(\mu)\mu_o, \phi)). \quad (5.15)$$

This is the discrete approximation of the continuum operator $\partial_\phi\Psi = s(\sqrt{16\pi G}/3)\mu\partial_\mu\Psi$ which itself is an excellent approximation to the fundamental equation when the boundary is far. The boundary condition requires the solution to leave the domain of integration. (For, to make the evolution deterministic in the domain of interest, it is important to avoid waves entering the integration domain from the boundary.) The boundary was chosen to lie sufficiently far from the location (in μ) of the peak of the initial wave packet. Its position was determined by requiring that the value of the wave function at the boundary be less than 10^{-n} times that at its value of the peak, and n ranged between 9 and 24 in different numerical simulations.

Three different methods were used to specify the initial data Ψ and $\partial_\phi\Psi$ at $\phi = \phi_o$. These are described in section V B 2. The data were then evolved using the fourth order adaptive Runge-Kutta method (RK4). To estimate the numerical error due to discretization of time evolution, two sup-norms were used:

$$|\Psi_1 - \Psi_2|_I(\phi) = \frac{\sup_{|\mu_i - \varepsilon| \leq N\mu_o} |\Psi_1 - \Psi_2|(\phi)}{\sup_{|\mu_i - \varepsilon| \leq N\mu_o} |\Psi_2|(\phi)}. \quad (5.16)$$

and

$$|\Psi_1 - \Psi_2|_{II}(\phi) = \frac{\sup_{|\mu_i - \varepsilon| \leq N\mu_o} ||\Psi_1| - |\Psi_2||(\phi)}{\sup_{|\mu_i - \varepsilon| \leq N\mu_o} |\Psi_2|(\phi)}. \quad (5.17)$$

Fig. 9 shows an example of the results of convergence tests for the solution corresponding to $p_\phi = 10^3$ with initial spread in p_ϕ of 3% (used in figures 12 — 15). One can see that the phase of Ψ is more sensitive to numerical errors than its absolute value. Therefore, although the accuracy is high for the solution $\Psi(\mu, \phi)$ itself, it is even higher for the mean values and dispersions of $\widehat{\mu}|_{\phi_o}$ and \widehat{p}_ϕ .

2. Initial data

Although we are interested in positive frequency solutions, to avoid having to take square-roots of Θ at each ‘time step’, the second order evolution equation (4.4) was used. Thus, the initial data, consist of the pair Ψ and its time derivative $\partial_\phi\Psi$, specified at some ‘time’

⁷ Unfortunately for the $\varepsilon = 0$ sector the equation is singular at $\mu = 0$, so the analysis of this sub-section will not go through. This sector was handled by the direct evaluation of the integral representation of the solution, presented in the last sub-section.

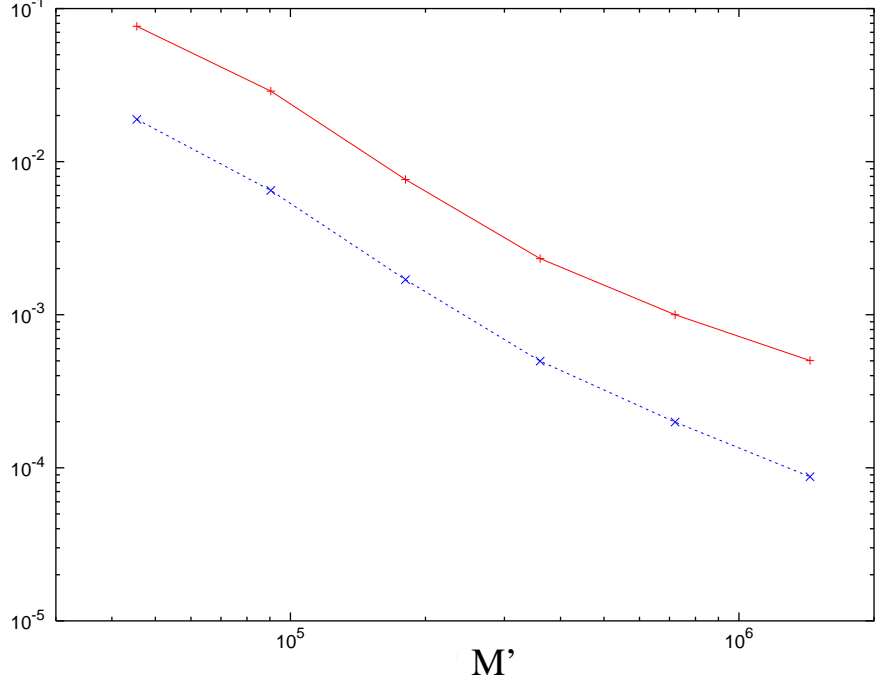


FIG. 9: Error functions $|\Psi_{(M')} - \Psi_{(M)}|_I$ (upper curve) and $|\Psi_{(M')} - \Psi_{(M)}|_{II}$ (lower curve) are plotted as a function of time steps. Here $\Psi_{(M')}$ refers to final profile of wave function for simulation with M' time steps. $\Psi_{(M)}$ refers to the final profile for the finest evolution (approximately 2.88×10^6 time steps). In both cases, the evolution started at $\phi = 0$ and the final profile refers to $\phi = -1.8$.

ϕ_o . The positive frequency condition was incorporated by specifying, in the initial data, the time derivative of Ψ in terms of Ψ . The idea is to choose semi-classical initial data peaked at a point (p_ϕ^*, μ^*) on a classical trajectory at ‘time’ $\phi = \phi_o$, with $(p_\phi^* \gg \sqrt{G\hbar^2}, \mu^* \gg 1)$, and evolve them. To avoid philosophical prejudices on what the state should do at or near the big bang, we specify the data on the expanding classical trajectory at ‘late time’ (i.e., ‘now’) and ask it to be semi-classical like the observed universe.

The idea that the data be semi-classical was incorporated in three related but distinct ways.

1. *Method I*: This procedure mimics standard quantum mechanics. Since (c, μ) are canonically conjugate on the phase space, we chose $\Psi(\mu)$ to be a Gaussian (with respect to the measure defined by the WDW inner product) and peaked at large μ^* and the value c^* of c at the point on the classical trajectory determined by $(\mu^*, p_\phi^*, \phi_o)$:

$$\Psi|_{\phi_o} := N |\mu|^{\frac{3}{4}} e^{-\frac{(\mu-\mu^*)^2}{2\tilde{\sigma}^2}} e^{-i\frac{c^*(\mu-\mu^*)}{2}} . \quad (5.18)$$

where N is a normalization constant. The initial value of $\partial_\phi \Psi|_{\phi_o}$ was calculated using the classical Hamilton’s equations of motion

$$\partial_\phi \Psi|_{\phi_o} = \left(-\text{sgn}(k^*) \sqrt{\frac{16\pi G}{3}} \frac{(\mu - \mu^*)\mu^*}{\tilde{\sigma}^2} + i\omega^* \frac{\mu}{\mu^*} \right) \Psi|_{\phi_o} , \quad (5.19)$$

where $\omega^* = p_\phi^*/\hbar$.

2. *Method II*: This procedure takes advantage of the fact that (3.19) provides a WDW physical state which is semi-classical at late times. The idea is to calculate Ψ and $\partial_\phi \Psi$ at $\phi = \phi_o$ and use their restrictions to lattices \mathcal{L}_ε as the initial data for LQC, setting $\omega = \sqrt{16\pi G/3} |k|$ as in the discussion following (3.19). Thus the initial data used in the simulations were of the form:

$$\Psi|_{\phi_o} = \left(\frac{\mu}{\mu^*} \right)^{\frac{1}{4}} e^{-\frac{\sigma^2}{2} \ln^2 \frac{|\mu|}{|\mu^*|}} e^{ik^* \ln \frac{|\mu|}{|\mu^*|}}, \quad (5.20)$$

$$\partial_\phi \Psi|_{\phi_o} = \left(-\text{sgn}(k^*) \sqrt{\frac{16\pi}{3}} \sigma^2 \ln \frac{|\mu|}{|\mu^*|} + i\omega(k^*) \right) \Psi|_{\phi_o} \quad (5.21)$$

This choice is best suited to comparing the LQC results with those of the WDW theory. The spreads $\tilde{\sigma}$ of *Method I* and σ of *Method II* are related to the initial spread $\Delta\mu|_{\phi_o}$ as follows

$$\tilde{\sigma} = \frac{\mu^*}{\sigma} = \sqrt{2} \Delta\mu|_{\phi_o}. \quad (5.22)$$

3. *Method III*: To facilitate comparison with the direct evaluation of the integral solution described in section V A, a variation was made on *Method II*. Specifically, in the expression (3.19) of Ψ , the WDW basis eigenfunctions $\underline{e}_k(\mu)$ were rotated by multiplying them with a k and ε dependent phase factor defined in Eq. (5.9)

$$\underline{e}_{-|k|} \mapsto e^{-i\alpha^+} \underline{e}_{-|k|}. \quad (5.23)$$

These phases were first found numerically using the method specified in appendix B and then functions of the form

$$\alpha^+ = A \ln(Bk + C)k + D, \quad (5.24)$$

(where A, B, C, D are real constants) were fitted to the results. After subtraction of the 0th and the 1st order terms in the expansion in k around k^* (which respectively correspond to a constant phase and a shift of origin of ϕ) the resulting function was used to rotate the basis $\underline{e}_k(\mu)$ appearing in (3.19) via (5.23)). The expression on the right side of Eq (3.19) and its ϕ -derivative were then integrated numerically at $\phi = \phi_o$.

In the simulations, 15 different values of p_ϕ^* were used ranging between 10^2 and 10^5 . μ^* was always greater than $2.5p_\phi$. The dispersion σ was allowed to have five different values. These simulations involved four different, randomly chosen values of ε .

C. Results and Comparisons

We now summarize the results obtained by using the two constructions specified in sections V A and V B. The qualitative results are robust and differences lie in the finer structure. In particular, evolutions of initial data constructed from the three methods described in section V B 2 yield physical states $\Psi(\mu, \phi)$ which are virtually identical except for small differences in the behavior of relative dispersions of the Dirac observables. The numerical

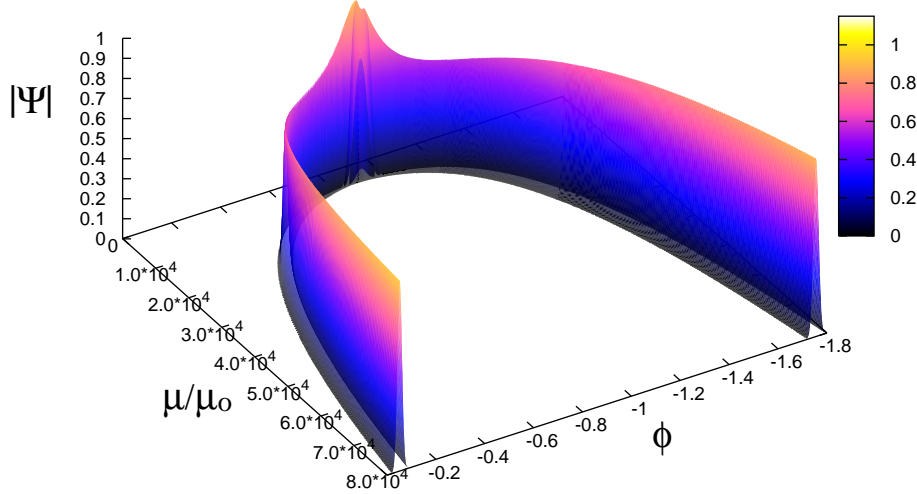


FIG. 10: The absolute value of the wave function obtained by evolving an initial data of *Method II*. For clarity of visualization, only the values of $|\Psi|$ greater than 10^{-4} are shown. Being a physical state, Ψ is symmetric under $\mu \rightarrow -\mu$. In this simulation, the parameters were: $\varepsilon = 2\mu_o$, $p_\phi^* = 10^4$, and $\Delta p_\phi/p_\phi^* = 7.5 \times 10^{-3}$.

evaluation of the integral (4.15) in section V A 4 yielded results very similar to those obtained in V B 2 using initial data of *Method III*. An example of results is presented in Fig. 10 and Fig. 11.

Highlights of the results can be summarized as follows:

- (1) The state remains sharply peaked throughout the evolution. However, as shown in Fig. 16, while the product $\Delta\phi \Delta p_\phi$ is nearly constant for large μ , there is a substantial increase near $\mu = 0$.
- (2) The expectation values of $\hat{\mu}_\phi$ and \hat{p}_ϕ are in good agreement with the classical trajectories, until the increasing matter density approaches a critical value. Then, the state bounces from the expanding branch to a contracting branch with the same value of $\langle \hat{p}_\phi \rangle$. (See Fig. 11). This phenomena occurs *universally*, i.e., in every ε -sector, for all three methods of choosing the initial data and for any choice of $p_\phi \gg \sqrt{G\hbar^2}$. *In this sense the classical big-bang is replaced by a quantum bounce.* Note that this is in striking contrast with the situation with the WDW theory we encountered in section III B, even when the initial data is chosen using *Method II* which is tailored to the WDW theory. As indicated in Appendix A, the existence of the bounce can be heuristically understood from an ‘effective theory’. The detailed numerical work supports that description, thereby providing a justification for the approximation involved.
- (3) If the state is peaked on the expanding branch $\mu(\phi) = \mu^* \exp(\sqrt{16\pi G/3}(\phi - \phi_o))$ in the distant future, due to the bounce it is peaked on a contracting branch in the

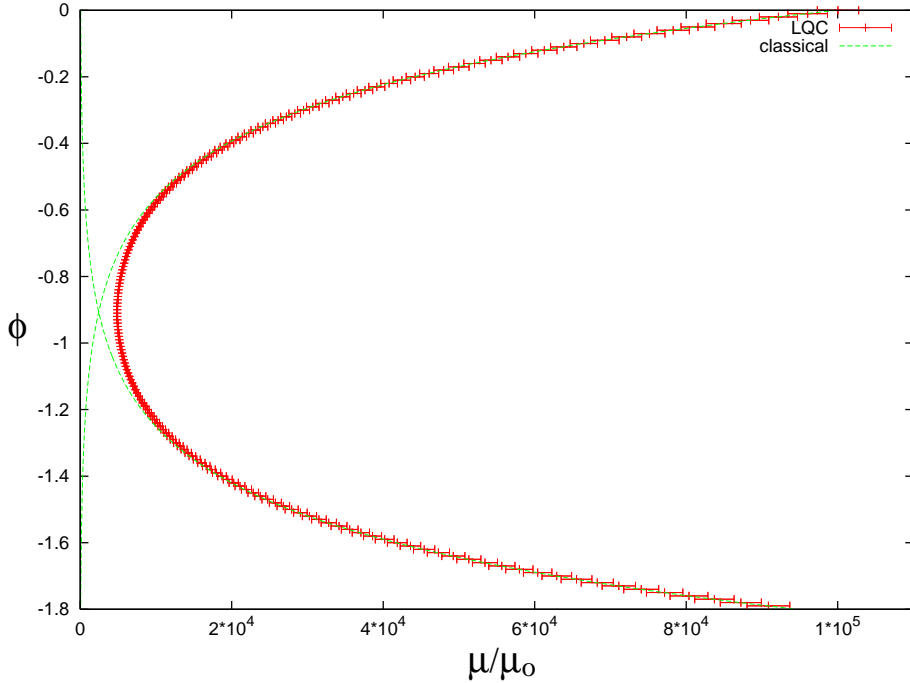


FIG. 11: The expectation values (and dispersions) of $\widehat{|\mu|_\phi}$ are plotted for the wavefunction in Fig. 10 and compared with expanding and contracting classical trajectories.

distant past, given by $\mu(\phi) = D(p_\phi^*) \mu^* \exp(-\sqrt{16\pi G/3}(\phi - \phi_o))$, where $D(p_\phi) = \mu_o^2 p_\phi^2 / 12\pi G \hbar^2$. Thus, for large $|\mu|$ the solution $\Psi(\mu, \phi)$ exhibits reflection symmetry (about $\phi = \phi_o - \frac{1}{2} \ln D(p_\phi^*)$). However, it is not exactly reflection symmetric (compare [58]).

(4) As a consistency check, we verified that the norm and the expectation value $\langle \hat{p}_\phi \rangle$ are preserved during the entire evolution. Furthermore, the dispersion also remains small throughout the evolution, although the precise behavior depends on the method of specification of the initial data. Differences arise primarily near the bounce point and manifest themselves through the behavior of the relative dispersion $\Delta\mu/\mu$ as a function of ϕ . These are illustrated (for all three methods as well as for the direct evaluation of section V A) in Fig. 12. Finally, as argued in Appendix A, since the state is sharply peaked, the value of $\Delta\mu/\mu$ can be related to $\Delta\phi$ via Eq A13. One finds that the product $\Delta\phi\Delta p_\phi$ is essentially constant in the region away from the bounce but grows near the bounce.

The differences can be summarized as follows:

(i) In *Method I* the initial state is a minimum uncertainty state in (μ, c) but doesn't minimize the uncertainty in (ϕ, p_ϕ) at any value of ϕ . The relative spread in μ remains approximately constant in the regions where $\langle \hat{\mu}_\phi \rangle$ is large and increases near the bounce point monotonically. The wave function interpolates 'smoothly' between expanding and contracting branches (see Fig. 13). On the other hand

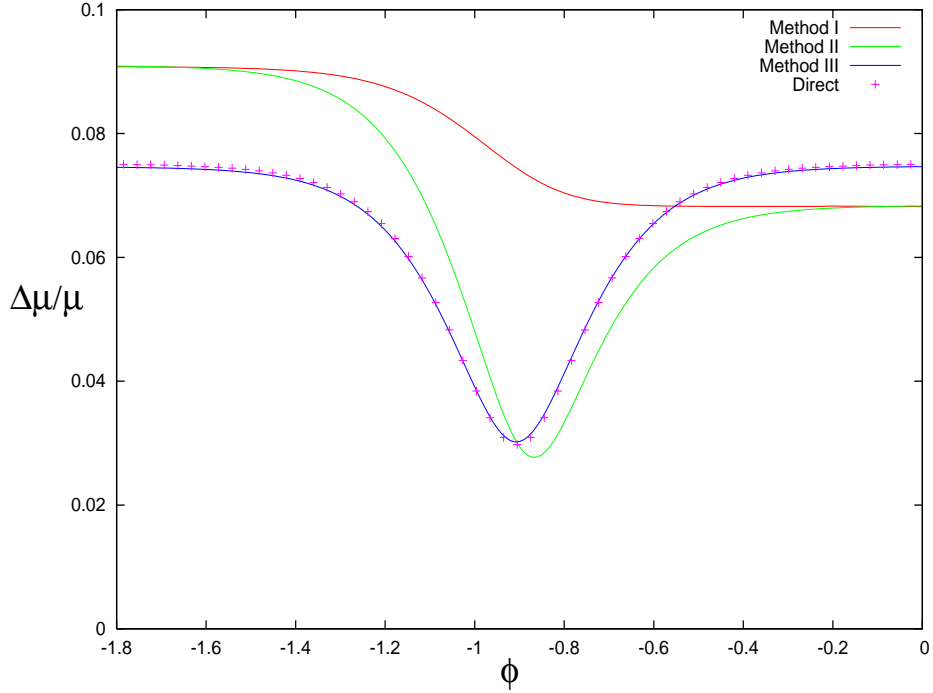


FIG. 12: Comparisons between the relative dispersions $\Delta\mu/\mu$ as functions of ϕ for all three methods specifying initial data and the result of direct construction.

the product $\Delta\phi\Delta p_\phi$ of uncertainties has a value much higher than $1/2$, grows quickly near the bounce and settles down to constant value after it. See Fig. 16.

- (ii) The state obtained by evolving the initial data constructed from *Method II* has minimal uncertainty in (ϕ, p_ϕ) . $\Delta\mu/\mu$ is approximately constant for large $\langle\widehat{\mu}|\phi\rangle$ and it decreases quickly near the bounce point, reaching its minimal value shortly before the bounce point. After the bounce it grows and stabilizes at the value of the relative spread found for data constructed using *Method I* (for the same values of p_ϕ^* and initial $\Delta\mu/\mu$). Behavior of the wave function is also different from that in the previous case. Near the bounce point its value grows to form a bulge (see Fig. 14). The product $\Delta\phi\Delta p_\phi$ remains almost constant for as long as the results of the numerical measurement are reliable (see Fig. 16) approaching a constant after the bounce, with a somewhat higher value. The heuristic estimate on $\Delta\phi\Delta p_\phi$ (see Appendix A) agrees with these results. Finally, we also found that the increase of the relative spread depends on p_ϕ^* and initial $\Delta\mu/\mu$.
- (iii) The state obtained by evolving the initial data constructed from *Method III* does not have minimum uncertainty in (ϕ, p_ϕ) . The behavior of $\Delta\mu/\mu$ is similar to the previous case except that it becomes equal to $\Delta p_\phi/p_\phi$ at the bounce point and its asymptotic value in the contracting branch is same as its starting value. Thus the spread is symmetric with respect to reflection in ϕ around the bounce point. The difference between the value of $\Delta\mu/\mu$ for large $\langle\widehat{\mu}|\phi\rangle$ and the one corresponding to the minimum uncertainty state (for the same p_ϕ^* and Δp_ϕ) is a function of p_ϕ and Δp_ϕ . The wave function forms a symmetric bulge near the

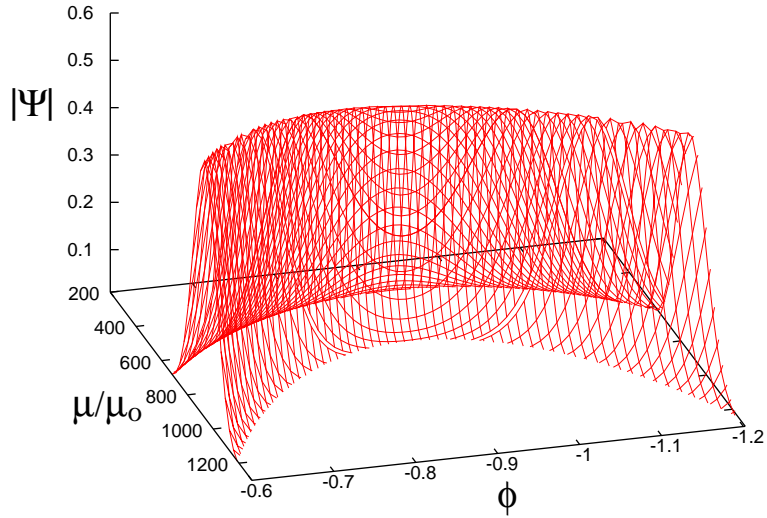


FIG. 13: A zoom on the absolute value of the wave function near the bounce point. Initial data was specified using *Method I*.

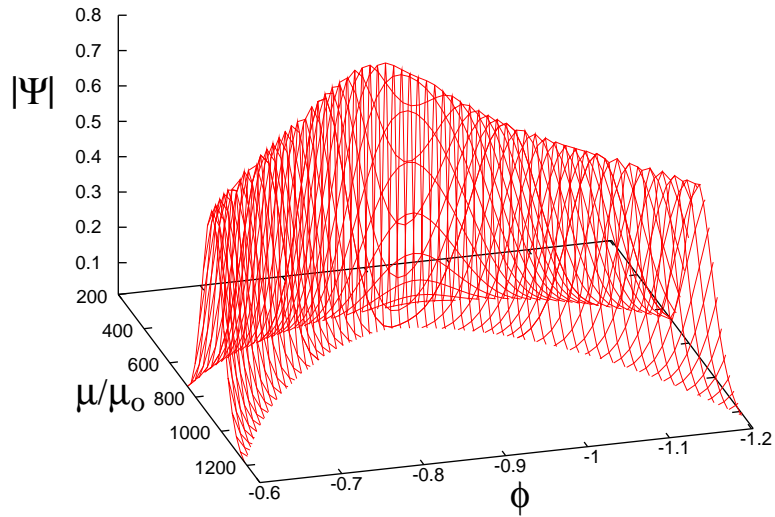


FIG. 14: A zoom on the absolute value of the wave function near the bounce point. Initial data was specified using *Method II*.

bounce point and the value $\Delta\phi\Delta p_\phi$ remains constant within regime of validity of

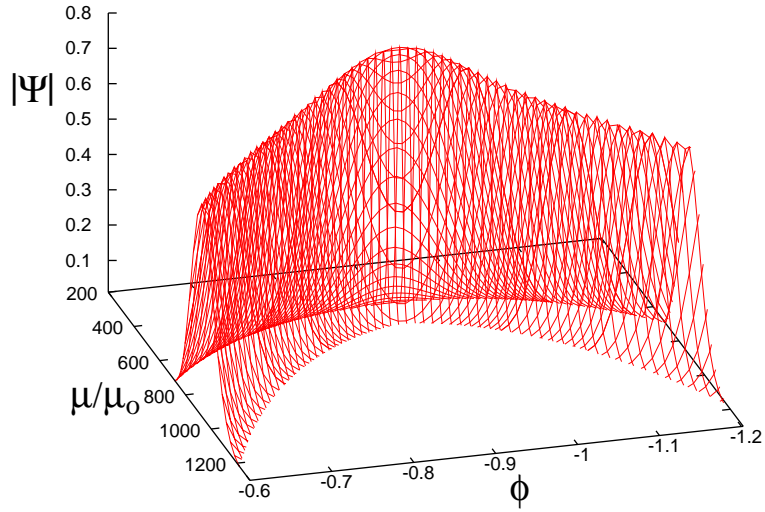


FIG. 15: A zoom on the absolute value of the wave function near the bounce point. Initial data was specified using *Method III*.

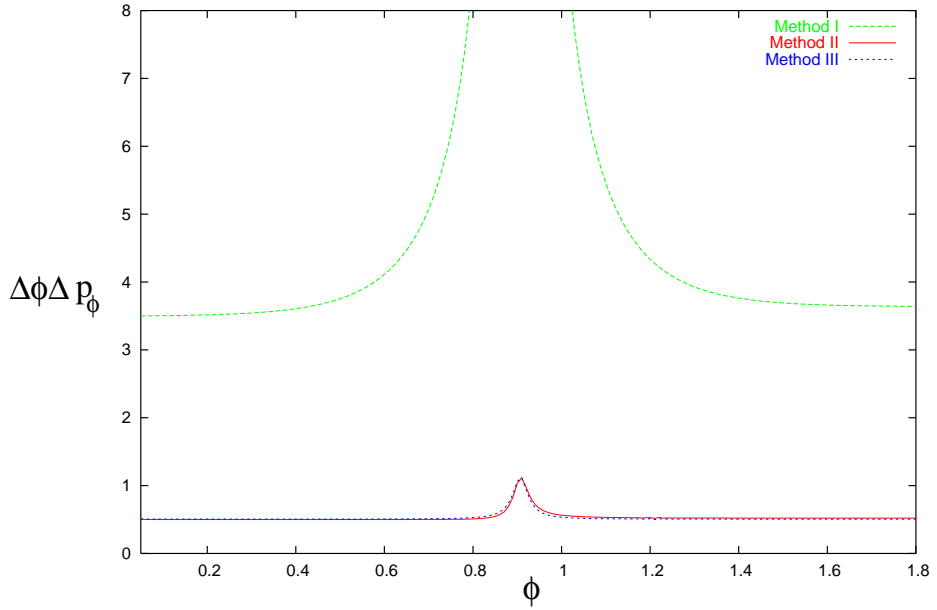


FIG. 16: The uncertainty product $\Delta\phi\Delta p_\phi$ for three methods of specifying the initial data.

its estimation (see Fig.16).

(iv) The direct construction of section V A yields results similar to those obtained by

using the third method to choose the initial data for the ϕ evolution.

(v) The differences between the relative dispersion $\Delta\mu/\mu$ resulting from different methods of choosing initial data can also be estimated using the solutions to the effective dynamical equations (for details of the method see Appendix A).

We will conclude with two remarks.

(i) Let us return to the comparison between the results of LQC and the WDW theory in light of our numerical results. As remarked in section II B, on functions $\Psi(\mu)$ which we used to construct the semi-classical initial data, the leading term in the difference $(\hat{C}_{\text{grav}} - \hat{C}_{\text{grav}}^{\text{wdw}})\Psi$ between the actions of the two constraint operators goes as $O(\mu_o^2)\Psi'''$. Now, in LQC μ_o is fixed, ($\mu_o = 3\sqrt{3}/2$), and on semi-classical states $\Psi''' \sim k^{*2}/\mu^4 \Psi$. Hence the difference is negligible only in the regime $k^{*4}/\mu^4 \ll 1$. In our simulations, $k^* \sim 10^4$ whence the differences are guaranteed to be negligible only for $\mu \gg 10^4$, i.e., well away from the bounce. But let us probe the situation in greater detail. Let us regard μ_o as a mathematical parameter which can be varied and shrink it. In the limit $\mu_o \rightarrow 0$, $(\hat{C}_{\text{grav}} - \hat{C}_{\text{grav}}^{\text{wdw}})\Psi$ should tend to zero. Since there is no bounce in the WDW theory, we are led to ask: Would the LQC bounce continue to exist all the way to $\mu_o = 0$ or is there a critical value at which the bounce stops? The answer is that for any finite value of μ_o there is a bounce. However, if we keep the *physical* initial data the same, we find that as we decrease μ_o the solution follows the classical trajectory into the past more and more and bounce is pushed further and further in to the past. In the limit as μ_o goes to zero, the wave function follows the classical trajectory into infinite past, i.e., the bounce never occurs. This is the sense in which the WDW result is recovered in the limit $\mu_o \rightarrow 0$.

(ii) Numerical simulations show that the matter density at the bounce points is inversely proportional to the expectation value $\langle \hat{p}_\phi \rangle \equiv p_\phi^*$ of the Dirac observable \hat{p}_ϕ : Given two semi-classical states with $\langle \hat{p}_\phi \rangle = p_\phi^*$ and \bar{p}_ϕ^* , we have $\rho_{\text{crit}}/\bar{\rho}_{\text{crit}} = \bar{p}_\phi^*/p_\phi^*$. Therefore, this density can be made small by choosing sufficiently large p_ϕ^* . Physically, this is unreasonable because one would not expect departures from the classical theory until matter density becomes comparable to the Planck density. This is a serious weakness of our framework. Essentially every investigation within LQC we are aware of has this—or a similar—drawback but it did not become manifest before because the physics of the singularity resolution had not been analyzed systematically. The origin of this weakness can be traced back to details of the construction of the Hamiltonian constraint operator, specifically the precise manner in which the operator corresponding to the classical field strength F_{ab}^i was introduced. The physical idea that in LQC the operator corresponding to the field strength F_{ab}^i should be defined through holonomies, and that quantum geometry does not allow us to shrink the loop to zero size, seem compelling. However, the precise manner in which the value of μ_o was determined using the area gap Δ is not as systematic and represents only a ‘first stab’ at the problem. In [37] we will discuss an alternate and more natural way of implementing this idea. The resulting Hamiltonian constraint has a similar form but also important differences. Because of similarities the qualitative conclusions of this analysis—including the occurrence of the quantum bounce—are retained but the differences are sufficiently important to replace the expression of the critical density by $\rho'_{\text{crit}} = (3/8\pi G\gamma^2\Delta)$ where, as before, $\Delta = 2\sqrt{3}\pi\gamma\ell_{\text{Pl}}^2$ is the area gap. Since ρ'_{crit} is of Planck scale and is independent of

parameters associated with the semi-classical state, such as p_ϕ^* , the departures from classical theory now appear only in the Planck regime. This issue is discussed in detail in [37].

VI. DISCUSSION

We will first present a brief summary and then compare our analysis with similar constructions and results which have appeared in the literature. However, since this literature is vast, to keep the discussion to a manageable size, these comparisons will be illustrative rather than exhaustive.

In general relativity, gravity is encoded in space-time geometry. A basic premise of LQG is that geometry is fundamentally quantum mechanical and its quantum aspects are central to the understanding of the physics of the Planck regime. In the last three sections, we saw that LQC provides a concrete realization of this paradigm. In our model every classical solution is singular and the singularity persists in the WDW theory. The situation is quite different in LQC. As in full LQG, the kinematical framework of LQC forces us to define curvature in terms of holonomies around closed loops and the underlying quantum geometry makes it impossible to shrink the loops to zero size because of the ‘area gap’ Δ . This leads to a replacement of the WDW differential equation by a difference equation whose step size are dictated by Δ . Careful numerical simulations demonstrated in a robust fashion that the classical big-bang is now replaced by a quantum bounce. Thus, with hindsight, one can say that although the WDW theory is quite similar to LQC in its structure, the singularity persists in the WDW theory because it ignores the quantum nature of geometry.⁸

Emergent time

In this paper we isolated the scalar field ϕ as the emergent time and used it to motivate and simplify various constructions. However, we would like to emphasize that this—or indeed any other—choice of emergent time is not *essential* to the final results. In the classical theory (for any given value of the constant of motion p_ϕ), we can draw dynamical trajectories in the $\mu - \phi$ plane without singling out an internal clock. A complete set of Dirac observables can be taken to be p_ϕ , and either $\mu|_{\phi_o}$ or $\phi|_{\mu_o}$.⁹ What these observables measure is correlations and their specification singles out a point in the reduced phase space. However, we do not have to single out a time variable to define them. The same is true in quantum theory. To have complete control of physics, we need to construct the physical Hilbert space \mathcal{H}_{phy} and introduce on it a complete set of Dirac observables. Again, both these steps can be carried out without singling out ϕ as emergent time. For example, the scalar product can be constructed using group averaging which requires only the knowledge

⁸ Differences arise in two places. The first occurs in the matter part of the constraint and stems from the fact that the functions $B(\mu)$ representing the eigenvalues of the operator $1/\widehat{|p|^3/2}$ in LQG is different from the corresponding $\underline{B}(\mu)$ of the WDW theory. The second comes from the role of quantum geometry in the gravitational part of the Hamiltonian constraint, emphasized above. In our model, qualitatively new features of the LQG quantum dynamics can be traced back to the second. In particular, the bounce would have persisted even if we had used $\underline{B}(\mu)$ in place of $B(\mu)$ in the analysis presented in this paper.

⁹ In the closed models, care is needed to specify the latter because they can not be defined globally. But this issue is well-understood in the literature, especially through Rovelli’s contributions [59]. See also [34].

of the full quantum constraint and its properties, and not its decomposition into a ‘time evolution part’ ∂_ϕ^2 and an operator Θ on the ‘true degrees of freedom’. Once the scalar product is constructed, we can introduce a complete set of Dirac observables consisting of \hat{p}_ϕ , and $\hat{\mu}|_{\phi_o}$ or $\hat{\phi}|_{\mu_o}$. Again, what matters is the correlations. This and related issues have been discussed exhaustively in the quantum gravity literature in relativity circles. In particular, a major part of a conference proceedings [60] was devoted to it in the late eighties and several exhaustive reviews also appeared in the nineties (see in particular [61, 62]).

However, thanks to our knowledge of how quantum theory works in static space-times, singling out ϕ as the emergent time turned out to be extremely useful in practice because it provided guidance at several intermediate steps. In particular, it directly motivated our choice of $L^2(\mathbb{R}_{\text{Bohr}}, B(\mu)d\mu_{\text{Bohr}}) \otimes L^2(\mathbb{R}, d\phi)$ as our auxiliary Hilbert space; stream-lined the detailed definition of operators representing the Dirac observables; and facilitated the subsequent selection of the inner product by demanding that these be self-adjoint. More importantly, by enabling us to regard the constraint as an evolution equation, it transformed the ‘frozen formalism’ to a familiar language of ‘evolution’ and enabled us to picture and interpret the bounce and associated physics more easily. Indeed, following the lead of early LQC papers, initially we tried to use μ as time and ran into several difficulties: specification of physically interesting data became non-intuitive and cumbersome; one could not immediately recognize the occurrence of the bounce; and the physics of the singularity resolution remained obscure.

Our specific identification and use of emergent time differs in some respects from that introduced earlier in the literature. For example, in the context of the WDW theory, there is extensive work on isolating time in the WKB approximation (see e.g., [49, 63]). By contrast, a key feature of our emergent time is that it is not restricted to semi-classical regimes: We first isolated the scalar field ϕ as a variable which serves as a good internal clock away from the singularity in the classical theory, but then showed that the form of the *quantum* Hamiltonian constraint is such that ϕ can be regarded as emergent time in the *full* quantum theory, without a restriction that the states be semi-classical or stay away from the singularity. The idea of identifying an emergent time and exploiting the resulting ‘deparametrization’ to select an inner product on the space of solutions to the Hamiltonian constraint is not new [34, 50, 51, 60, 61, 62]. However, several of the concrete proposals turn out to have serious deficiencies (for a further discussion see, e.g., [64, 65]). The idea of using a matter field to define emergent time is rather old. In the framework of geometrodynamics, it was carried out in detail for dust in [66]. A proposal to use a massless scalar field as time was also made in the framework of LQG [67] but its implementation remained somewhat formal. In particular, it is unlikely that the required gauge conditions can be imposed globally in the phase space and the modifications in the construction of the physical scalar product that are necessary to accommodate a more local constructions were not spelled out. More recently, a massless scalar field was used as the internal clock in quantum cosmology in the connection dynamics framework [68]. However, the focus of discussion there is on the Kodama state in inflationary models. Because of the inflationary potential, the quantum constraint has explicit time dependence and the construction of the physical inner product is technically much more subtle. In particular, a viable inner product cannot depend on any auxiliary structure such as the choice of an ‘instant of time’. These issues do not appear to have been fully addressed in [68].

The issue of obtaining singularity free cosmological models has drawn much attention over the years. The discovery of singularity theorems sharpened this discussion and there is a large body of literature on how one may violate one or more assumptions of these theorems, thereby escaping the big bang. Proposals include the use of matter which violate the standard energy conditions, addition of higher derivative corrections to Einstein-Hilbert action and introduction of higher dimensional scenarios inspired by string theory. To facilitate comparison with the model discussed in this paper, we will restrict ourselves to spatially non-compact situations.

Already in the seventies, Bekenstein investigated a model where the matter source consisted of incoherent radiation and dust, interacting with a conformal massless scalar field (which can have a negative energy density). He showed that Einstein's equations admit solutions which are free of singularities [69]. In the eighties, Narlikar and Padmanabhan found a singularity free solution to Einstein's equation with radiation and a *negative energy* massless scalar field (called the 'creation field') as source, and argued that the resulting model was consistent with the then available observations [70]. Such investigations were carried out entirely in the paradigm of classical relativity and the key difference from the standard Friedmann-Robertson-Walker models arose from the use of 'non-standard' matter sources. Our analysis, by contrast, uses a standard massless scalar field and *every* solution is singular in the classical theory. The resolution of the singularity occurs due to genuinely quantum effects.

Another class of investigations starts with actions containing higher derivative terms which are motivated by suitable fundamental considerations. For example, to guide the search for an effective theory of gravity which is viable close to the Planck scale, Mukhanov and Brandenberger proposed an action with higher order curvature terms for which all isotropic cosmological solutions are non-singular, even when coupled to matter [71]. The modifications to Einstein's equations are thought of as representing quantum corrections. However one continues to work with differential equations formulated in the continuum. By contrast, our investigation is carried out in the framework of a genuine quantum theory with a physical Hilbert space, Dirac observables and detailed calculations of expectation values and fluctuations. Departures from classical general relativity arise directly from the quantum nature of geometry. The final results are also different: While solutions in [71] asymptotically approach de Sitter space, in our analysis the classical big-bang is replaced by a quantum bounce.

Perhaps the most well-known discussions of bounces come from the pre-big-bang cosmology and Ekpyrotic/Cyclic models. The pre-big-bang model uses the string dilaton action and exploits the scale factor duality to postulate the existence of a super-inflating pre-big-bang branch of the Universe, joined to the radiation dominated post-big-bang branch [4]. However, the work was carried out in the framework of perturbative string theory and the transition from the pre-big-bang to post-big-bang was *postulated*. The initial hope was that non-perturbative stringy effects would enforce such a transition. However, as of now, such mechanisms have not been found [7]. Although subsequent investigations have shown that a bounce can occur in simplified models [8] or by using certain effective equations (see, e.g., [9]), it is not yet clear that this is a consequence of the fundamental theory. The Ekpyrotic and the more recent Cyclic models [5, 6] are motivated by certain compactifications in string theory and feature a five dimensional bulk space-time with a 4-d branes as boundaries. In the Ekpyrotic model, the collision between a bulk brane with a boundary brane is envisioned as a big bang. A key difficulty is the singularity associated with this collision [10]

(which can be avoided but the cost of violating the null energy condition [6]). In the Cyclic model, collision occurs between the boundary branes [6], however it has been shown that the singularity problems persists [72]. Thus, a common limitation of these models is that the branch on ‘our side’ of the big-bang is not joined deterministically to the branch on the ‘other side’. In LQC by contrast, the quantum evolution is fully deterministic. This is possible because the approach is non-perturbative and does not require a space-time continuum in the background.

Finally, the idea of a bounce has been pursued also in the context of braneworld models. In the original Randall-Sundrum scenario, the Friedmann equation *is* modified by addition of a term on the right side which is quadratic in density: $\dot{a}^2/a^2 = (8\pi G/3) \rho(1 + \rho/(2\sigma))$ where σ is brane tension. However, since $\sigma > 0$, the sign of quadratic term in ρ is positive whence \dot{a} can not vanish and there is no bounce. To obtain a bounce, the correction should be negative, i.e., make a ‘repulsive’ contribution. One way to reverse the sign is to introduce a second time-like dimension in the bulk [73]. However, this strategy does not appear to descend from fundamental considerations and the physical meaning of the second time-like direction is also unclear. Another avenue is to consider a bulk with a charged black hole. A non-vanishing charge leads to terms in the modified Friedmann equation which are negative. \dot{a} can now vanish and a bounce can occur [74]. However it was shown that transition from contraction to expansion for the brane trajectory occurs in the Cauchy horizon of the bulk which is unstable to small excitations, thus the brane encounters singularity before bouncing [75]. In LQC, by contrast, while the Friedmann equation *is* effectively modified, the corrections come from quantum geometry and they are automatically negative, without any new input.

Extensions

The main weakness of our results is that they have been obtained in a specific mini-superspace model. Thus their domain of validity is extremely restricted. In particular, in more complicated models, the full solution is not likely to remain so sharply peaked on the classical trajectory till the bounce point. Indeed, even the existence of a bounce is not *a priori* guaranteed, especially when inhomogeneities are added.

However, the *methods* developed in the paper can be applied to more general situations. First, one could consider anisotropies. Now, the main structural difference is that the operator Θ will no longer be positive definite. However, a detailed analysis shows that what matters is just the operator $|\Theta|$, obtained by projecting the action of Θ to the positive eigenspace in its spectral decomposition. Therefore, our analytical considerations should go through without a major modification. The numerical simulations will be more complicated because we have to solve a higher dimensional difference equation (involving 4 variables in place of 2). Another extension will involve the inclusion of non-trivial potentials for the scalar field. Now, generically ϕ will no longer be a monotonic function on the classical trajectories and one would not be able to use it as ‘internal time’ globally. In the quantum theory, the operator Θ becomes ‘time-dependent’ (i.e. depends on ϕ) and the mathematical analogy between the quantum constraint and the Klein-Gordon equation in a static space-time is no longer valid. Nonetheless, one can still use the group averaging procedure [34, 50] to construct the physical Hilbert space. For a general potential, a useful notion of time will naturally emerge only in the semi-classical regimes. For specific potentials (such as the quadratic one used in chaotic inflation) one should be able to use methods that have been successfully employed in the quantization of model systems [52, 53] (in particular, a pair of harmonic oscillators constrained to have a fixed total energy).

Incorporation of spherical inhomogeneities seems to be within reach since significant amount of technical groundwork has already been laid [76]. Incorporation of general inhomogeneities, on the other hand, will be substantially more difficult. Background dependent treatments have suggested that results obtained in the mini-superspace approximation may be qualitatively altered once field theoretical complications are unleashed (see, e.g., [77]). However, already in the anisotropic case, there is a qualitative difference between perturbative and non-perturbative treatments. Specifically, if anisotropies are treated as perturbations of a background isotropic model, the big-bang singularity is not resolved while if one treats the whole problem non-perturbatively, it is [78]. Therefore definitive conclusions can not be reached until detailed calculations have been performed in inhomogeneous models. However, if a quantum bounce does generically replace the big bang singularity, it would be possible to explore the relation between the effective descriptions of LQG and the Hartle-Hawking ‘no boundary’ proposal [79]. For, in the effective description, the extrinsic curvature would vanish at the bounce. Therefore generically it may be possible to attach to the Lorentzian, post-bounce effective solution representing the universe at late times, a *Riemannian* pre-bounce solution without boundary. If so, it would be very interesting to analyze the sense in which this Riemannian solution captures the physics of the pre-bounce branch of the full quantum evolution.

Finally, it is instructive to recall the situation with singularities in classical general relativity. There, singularities first appeared in highly symmetric situations. For a number of years, arguments were advanced that this is an artifact of symmetry reduction and generic, non-symmetric solutions will be qualitatively different. However, singularity theorems by Penrose, Hawking, Geroch and others showed that this is not correct. An astute use of the *differential geometric* Raychaudhuri equation revealed that singularities first discovered in the simple, symmetric solutions are in fact a generic feature of classical general relativity. A fascinating question is whether the singularity resolution due to quantum geometry is also generic in an appropriate sense [80]. Is there a general equation in *quantum geometry* which implies that gravity effectively becomes repulsive near generic space-like singularities, thereby halting the classical collapse? If so, one could construct robust arguments, now establishing general ‘singularity resolution theorems’ for broad classes of situations in quantum gravity, without having to analyze models, one at a time.

Acknowledgments: We would like to thank Martin Bojowald, Jim Hartle and Pablo Laguna for discussions. This work was supported in part by the NSF grants PHY-0354932 and PHY-0456913, the Alexander von Humboldt Foundation, and the Eberly research funds of Penn State.

APPENDIX A: HEURISTICS

Quantum corrections to the classical equations can be calculated using ideas from a geometric formulation of quantum mechanics where the Hilbert space is regarded as (an infinite dimensional) phase space, the symplectic structure being given by the imaginary part of the Hermitian inner product (see, e.g., [81]). This ‘quantum phase space’ has the structure of a bundle with the classical phase space as the base space, and all states with the same expectation values for the canonically conjugate operators (\hat{q}^i, \hat{p}_i) as an (infinite dimensional) fiber. Thus, any horizontal section provides an embedding of the classical phase space into the ‘quantum phase space’. In the case of a harmonic oscillator (or free quantum fields)

coherent states constitute horizontal sections which are furthermore preserved by the full quantum dynamics. In the semi-classical sector defined by these coherent states, the effective Hamiltonian coincides with the classical Hamiltonian and there are no quantum corrections to classical dynamics. For more general systems, using suitable semi-classical states one may be able to find horizontal sections which are preserved by the quantum Hamiltonian flow to a desired accuracy (e.g. in an \hbar expansion). The effective Hamiltonian governing this flow—the expectation value of the quantum Hamiltonian operator in the chosen states, calculated to the desired accuracy—is generally different from the classical Hamiltonian. In this case, dynamics generated by the effective Hamiltonian provides systematic quantum corrections to the classical dynamics [24] (see also [25, 26, 33]).

This procedure has been explicitly carried out in LQC for various matter sources [24, 82]. For a massless scalar field, the leading order quantum corrections are captured in the following effective Hamiltonian constraint [82]:

$$C_{\text{eff}} = -\frac{6}{\gamma^2 \mu_o^2} |p|^{\frac{1}{2}} \sin^2(\mu_o c) + 8\pi G B(p) p_\phi^2 \quad (\text{A1})$$

where $B(p)$ is the eigenvalue of $\widehat{1/|p|^{3/2}}$ operator given by (4.3). ¹⁰ For $|\mu| \gg \mu_o$, $B(p)$ can be approximated as

$$B(p) = \left(\frac{6}{8\pi\gamma\ell_{\text{Pl}}^2} \right)^{3/2} |\mu|^{-3/2} \left(1 + \frac{5}{128} \frac{\mu_o^2}{\mu^2} + O\left(\frac{\mu_o^4}{\mu^4}\right) \right). \quad (\text{A2})$$

The leading order term is $1/p^{3/2}$, thus $B(p)$ quickly approaches its classical value for $|\mu| \gg \mu_o$, corrections being significant only in the ‘genuinely quantum region’ in the vicinity of $\mu = 0$. *From now on, we will ignore the quantum corrections to $B(p)$.*

To obtain the equations of motion, we need the effective Hamiltonian \mathcal{H}_{eff} . As usual it is obtained simply by a rescaling of C_{eff} which gives \mathcal{H}_{eff} the dimensions of energy and ensures that the matter contribution to it is the standard matter Hamiltonian:

$$\mathcal{H}_{\text{eff}} = \frac{C_{\text{eff}}}{16\pi G} = -\frac{3}{8\pi G \gamma^2 \mu_o^2} |p|^{1/2} \sin^2(\mu_o c) + \frac{p_\phi^2}{2p^{3/2}}. \quad (\text{A3})$$

Then, the Hamilton’s equation for \dot{p} become:

$$\dot{p} = \{p, \mathcal{H}_{\text{eff}}\} = -\frac{8\pi\gamma G}{3} \frac{\partial \mathcal{H}_{\text{eff}}}{\partial c} = \frac{2|p|^{1/2}}{\gamma\mu_o} \sin(\mu_o c) \cos(\mu_o c). \quad (\text{A4})$$

Further, since the Hamiltonian constraint implies that \mathcal{H}_{eff} of (A3) vanishes, we have:

$$\sin^2(\mu_o c) = \frac{8\pi\gamma^2 \mu_o^2 G}{6|p|^2} p_\phi^2 \quad (\text{A5})$$

which on using Eq.(A4) provides the *modified Friedmann equation* for the Hubble parameter H :

$$H^2 \equiv \frac{\dot{p}^2}{4p^2} = \frac{8\pi G}{3} \rho \left(1 - \frac{\rho}{\rho_{\text{crit}}} \right), \quad \text{where} \quad \rho_{\text{crit}} = \left(\frac{3}{8\pi G \gamma^2 \mu_o^2} \right)^{3/2} \frac{\sqrt{2}}{p_\phi}. \quad (\text{A6})$$

¹⁰ In the literature, eigenvalues $B(p)$ often contain a half-integer j , a parameter representing a quantization ambiguity. In view of the general consistency arguments advanced in [84], we have set its value to its minimum, i.e. $j = 1/2$.

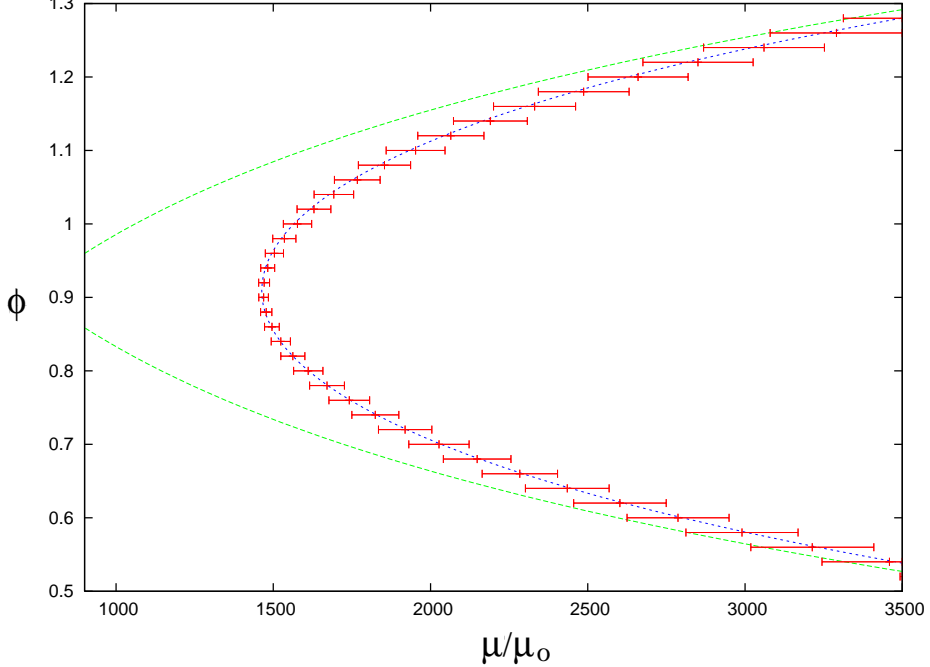


FIG. 17: Expectation values (and dispersions) of $\widehat{|\mu|_\phi}$ are plotted near the bounce point, together with classical and effective trajectories (fainter and darker dots, respectively). While the classical description fails in this region, the effective description provides an excellent approximation to the exact quantum evolution. In this plot, $p_\phi = 3000$ and $\varepsilon = 2\mu_o$.

To obtain the dynamical trajectory, we also need the Hamilton's equation for ϕ ,

$$\dot{\phi} = \{\phi, \mathcal{H}_{\text{eff}}\} = \frac{p_\phi}{p^{3/2}}. \quad (\text{A7})$$

By combining Eq. (A4) and (A7) we obtain the effective equation of motion in the μ - ϕ plane:

$$\frac{d\mu}{d\phi} = \sqrt{\frac{16\pi G}{3}} \left(1 - \frac{\rho}{\rho_{\text{crit}}}\right)^{1/2} \mu. \quad (\text{A8})$$

The classical Friedmann dynamics results if we set $\rho_{\text{crit}} = \infty$. Eqs. (A6) and (A8) suggest that the LQC effects significantly modify the Friedmann dynamics once the matter density reaches a critical value, ρ_{crit} . In the classical dynamics, the Hubble parameter H can not vanish (except in the trivial case with $p_\phi = 0$). In the modified dynamics, on the other hand, H vanishes at $\rho = \rho_{\text{crit}}$. At this point, the Universe bounces. Thus, the bounce predicted by Eq.(A6) has its origin in quantum geometry. (The critical value μ at which this bounce occurs is given by $\mu_{\text{crit}} = (\sqrt{6/8\pi G\hbar^2}) p_\phi \mu_o$.) As pointed out in the main text, a physical limitation of the present framework is that if p_ϕ is chosen to be sufficiently large, the critical density ρ_{crit} can be small.

To obtain the effective equations, several approximations were made [24, 82] which are violated in the deep Planck regime. Nonetheless, the resulting picture of the bounce is consistent with the detailed numerical analysis. In fact, within numerical errors the trajectory

$$\mu(\phi) = \frac{1}{2} \left(\exp \left(\sqrt{\frac{16\pi G}{3}}(\phi - \phi_o) \right) + D(p_\phi) \exp \left(-\sqrt{\frac{16\pi G}{3}}(\phi - \phi_o) \right) \right) \quad (\text{A9})$$

obtained by integrating Eq (A8) approximates the expectation values of $\widehat{\mu}_\phi$ quite well. (As in the main text, $D(p_\phi) = \mu_o^2 p_\phi^2 / 12\pi G \hbar^2$). An illustrative plot of this generic behavior is shown in Fig. 17. Therefore, in retrospect, this analysis can be taken as a justification for the validity of the approximation throughout the evolutionary history of semi-classical states used in this paper. However, by its very nature, the effective description can not reproduce the interesting features exhibited by quantum states captured in Figs. 13-16.

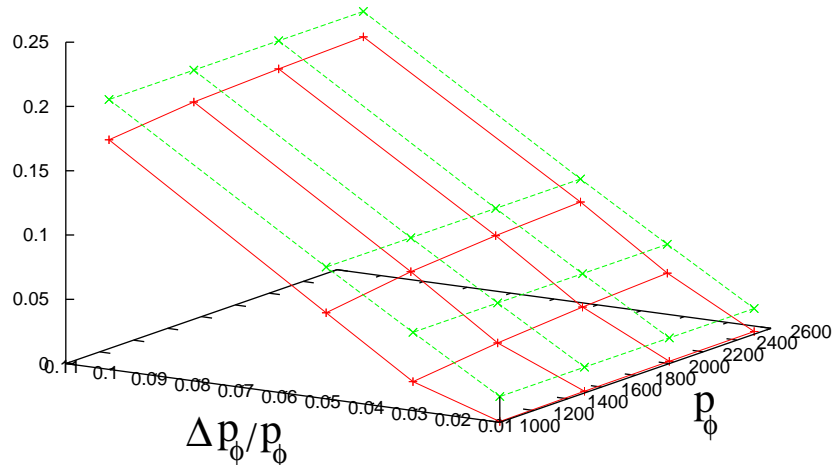


FIG. 18: The darker ‘lattice’ show the difference between final and initial relative spreads $\Delta\mu/\mu$ for states obtained by evolving initial data of *Method II*. The upper, fainter ‘lattice’ shows the heuristic bound $\delta\mu/\mu$ given by Eq (A10).

However, the effective description can be used to provide an intuitive understanding of the behavior of various uncertainties discovered through numerical analysis. Let us first note that the position of the bounce point depends linearly on the value of p_ϕ . Next, consider two near-by solutions with slightly different p_ϕ which asymptote to the same WDW solution for the expanding branch in the distant future. We wish to know the way in which $(\delta\mu/\mu)(\phi) := ((\mu_1 - \mu_2)/\mu_2)(\phi)$ changes in the backward evolution as the two wave functions asymptote to WDW solutions in the distant past. This relative difference can be found using Eq (A9) and is given by

$$\frac{\delta\mu}{\mu} = 2 \frac{\delta p_\phi}{p_\phi} + \left(\frac{\delta p_\phi}{p_\phi} \right)^2, \quad (\text{A10})$$

where δp_ϕ is the difference between values of p_ϕ of the two classical trajectories. A heuristic estimate on the relative difference in μ can be compared with the relative dispersion $\Delta\mu/\mu$

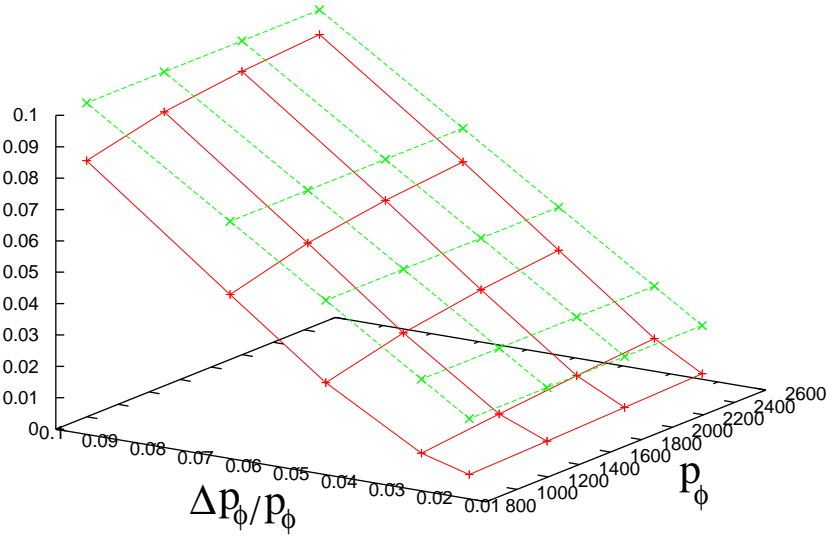


FIG. 19: The darker ‘lattice’ show the difference between final and initial relative spreads $\Delta\mu/\mu$ for states obtained by evolving initial data of *Method III*. The upper, fainter ‘lattice’ shows the heuristic bound $\delta\mu/\mu$ given by Eq (A12).

obtained from the *Method II* in the ϕ evolution of section V B. It turns out that estimate in Eq (A10) provides a reasonably good upper bound to the relative dispersion found numerically (see Fig. 18). A similar comparison can be made for *Method III* of section V B. In this case the corresponding solution to Eq (A8) is

$$\mu(\phi) = \frac{1}{2} \left(D(p_\phi)^{-1/2} \exp \left(\sqrt{\frac{16\pi G}{3}}(\phi - \phi_o) \right) + D(p_\phi)^{1/2} \exp \left(-\sqrt{\frac{16\pi G}{3}}(\phi - \phi_o) \right) \right) \quad (\text{A11})$$

with relative difference

$$\frac{\delta\mu}{\mu} = \frac{\delta p_\phi}{p_\phi} . \quad (\text{A12})$$

A comparison with the relative dispersions in numerical analysis is shown in Fig. 19. As in the case of construction of coherent states via *Method II*, above estimate serves as an upper bound for relative dispersions computed by numerical analysis.

Finally, in the numerical analysis an important issue concerns with the behavior of dispersions of our Dirac observables $\hat{\mu}_\phi$ and \hat{p}_ϕ and the product $\Delta\phi\Delta p_\phi$. Intuitive understanding of our numerical results of Fig. 16 can be gained by casting Eq. (A8) in the form

$$\Delta\phi = \sqrt{\frac{3}{16\pi G}} \left(1 - \frac{\rho}{\rho_{\text{crit}}} \right)^{-1/2} \frac{\Delta\mu}{\mu} . \quad (\text{A13})$$

Since $\Delta\mu/\mu$ can be determined numerically, we can then estimate $\Delta\phi$ throughout the evolution. The factor $\left(1 - \frac{\rho}{\rho_{\text{crit}}} \right)^{-1/2}$ is approximately equal to unity for $\rho \ll \rho_{\text{crit}}$ or equivalently

for $\mu \gg \mu_{\text{crit}}$. However near the bounce point, $\left(1 - \frac{\rho}{\rho_{\text{crit}}}\right)^{-1/2} \gg 1$. In *Method II* and *Method III* of constructing initial states described in Sec. VB 2, this change compensates the corresponding decrease in $\Delta\mu/\mu$ and leads to a nearly constant value of $\Delta\phi$. However, for *Method I*, since $\Delta\mu/\mu$ increases monotonically, the fluctuation $\Delta\phi$ increases significantly near the bounce point.

APPENDIX B: ISSUES IN NUMERICAL ANALYSIS

In this Appendix we will spell out the way in which the WDW limit of the eigenfunctions of Θ were found.

Consider a general eigenfunction \underline{e}_ω of Θ (for $\omega^2 \geq \pi G/3$). It is always a linear combination of basis functions $\underline{e}_{|k|}, \underline{e}_{-|k|}$ (where $k^2 = 3/(16\pi G)\omega^2 - 1/16$) defined in Eq. (3.5). For later convenience, let us express the linear combination as:

$$\underline{e}_\omega = r^+ e^{i(\beta+\alpha)} \underline{e}_{|k|} + r^- e^{i(\beta-\alpha)} \underline{e}_{-|k|}, \quad (\text{B1})$$

where r_\pm, α, β are real numbers. Since each $\underline{e}_{\pm|k|}$ is a product of an ‘amplitude’ $|\mu|^{1/4}/4\pi$ and a ‘phase’ $e^{\pm i|k|\ln|\mu|}$, it is natural to rescale \underline{e}_ω :

$$\tilde{\underline{e}}_\omega(\mu) := 4\pi|\mu|^{-1/4} \underline{e}_\omega. \quad (\text{B2})$$

In terms of coefficients defined in (B1), we have

$$\tilde{\underline{e}}_\omega(\mu) = e^{i\beta} ((r^+ + r^-) \cos(\alpha + |k|\ln|\mu|) + i(r^+ - r^-) \sin(\alpha + |k|\ln|\mu|)). \quad (\text{B3})$$

The values of $\tilde{\underline{e}}_\omega(\mu)$ trace out an ellipse on the complex plane, parameterized by $\ln|\mu|$. The length of semi-major and semi-minor axis of this ellipse is equal to, respectively

$$r^+ + r^- = \sup_\mu |\tilde{\underline{e}}_\omega| \quad |r^+ - r^-| = \inf_\mu |\tilde{\underline{e}}_\omega|, \quad (\text{B4})$$

whereas the phase α is related to positions of maxima of $\tilde{\underline{e}}_\omega$ as follows

$$|\underline{e}_\omega| = r^+ + r^- \Leftrightarrow \alpha + |k|\ln|\mu| = n\pi, \quad n \in \mathbb{Z}. \quad (\text{B5})$$

The remaining phase β is just the phase of $\tilde{\underline{e}}_\omega$ at maximum. The sign of $(r^+ - r^-)$ is, on the other hand, determined by direction of the rotation of the curve as μ increases.

The method specified above allows us to calculate the decomposition in \underline{e}_k basis of a function \underline{e}_ω specified in the form of numerical data (i.e. array of values at sufficiently large domain). The same algorithm can be applied to identify the WDW limit of any eigenfunction of the LQC operator Θ . Indeed given an eigenfunction $e_\omega(\mu)$ supported on the lattice $\mathcal{L}_{|\varepsilon|}$ (or $\mathcal{L}_{-|\varepsilon|}$) one can again define $\tilde{\underline{e}}_\omega$ analogously to \underline{e}_ω and find its (local) extrema for large μ . (For definiteness, we restrict our consideration to finding the limit on the positive μ side, however this method can be used of course also for the negative μ domain.) Next, the positions of extrema and values of $\tilde{\underline{e}}_\omega$ at them can be used to calculate coefficients $r^+ \pm r^-, \alpha, \beta$ at each extremum independently. If $\tilde{\underline{e}}_\omega \rightarrow \underline{e}_\omega$ then these coefficients form sequences $(\{r^+ + r^-\}_i, \{r^+ - r^-\}_i, \{\alpha\}_i, \{\beta\}_i)$ which converge to the analogous coefficients corresponding to \underline{e}_ω as $\mu \rightarrow \infty$. Finding the WDW limit of $\tilde{\underline{e}}_\omega$ reduces then to finding the limit of $(\{r^+ + r^-\}_i, \{r^+ - r^-\}_i, \{\alpha\}_i, \{\beta\}_i)$.

In actual numerical work the following method was used:

- After given eigenfunction e_ω was calculated using (4.6) the positions of extrema $\{\mu\}_i$ were found.
- Around the extrema the function e_ω supported on $\mathcal{L}_{|\varepsilon|}$ (or $\mathcal{L}_{-|\varepsilon|}$) was extended to neighborhoods of $\{\mu\}_i$ via polynomial interpolation. Then the positions and values of extrema were recalculated with use of this extension. This allowed us to construct sequences converging to the WDW limit much more quickly than the ones constructed in the first step. The motivation for this construction is the expectation that for sufficiently large μ the values of e_ω at $\mathcal{L}_{|\varepsilon|}$ should be good estimates of its WDW limit (being regular function defined on entire \mathbb{R}^+).
- Extrema found in previous step were next used to calculate sequences $(\{r^+ + r^-\}_i, \{r^+ - r^-\}_i, \{\alpha\}_i, \{\beta\}_i)$ in a way analogous to that specified by Eqs. (B4) and (B5) and in the description below them.
- Finally the limits of coefficients at $1/\mu \rightarrow 0$ were calculated by polynomial extrapolation.

APPENDIX C: AN ALTERNATE PHYSICAL HILBERT SPACE

In this Appendix we will construct a physical Hilbert space $\mathcal{H}'_{\text{phy}}$ in LQC which is qualitatively different from the spaces $\mathcal{H}^\varepsilon_{\text{phy}}$ constructed in section IV B. In its features, it interpolates between these and the Hilbert space $\mathcal{H}^{\text{wdw}}_{\text{phy}}$ of section III B. For completeness, we will first explain why a new representation of the algebra of Dirac observables can arise, then summarize the results and finally compare and contrast them with those obtained in sections III B and IV B. The first part is somewhat technical but we have organized the presentation such that the readers can go directly to the summary without loss of continuity.

Let us begin by recalling the situation for a general system with a single constraint C . In the refined version of Dirac quantization [35], one introduces an auxiliary Hilbert space \mathcal{H}_{aux} , and represents the constraint by a self-adjoint operator \hat{C} on it. The technically difficult task is to choose a dense sub-space Φ of \mathcal{H}_{aux} such that for all $f, g \in \Phi$,

$$(\Psi_f| := \int_{-\infty}^{\infty} d\lambda \langle e^{-i\lambda\hat{C}} f | \quad (C1)$$

is a well-defined element of Φ^* , such that the action $(\Psi_f|g)$ of $(\Psi_f| \in \Phi^*$ on $|g\rangle \in \Phi$ yields a Hermitian scalar product on the space of solutions $(\Psi_f|$ to the quantum constraint (see, e.g. [34, 35, 83]). Results in section IV B were obtained using $L^2(\mathbb{R}_{\text{Bohr}}, B(\mu) d\mu_{\text{Bohr}}) \otimes L^2(\mathbb{R}, d\phi)$ for \mathcal{H}_{aux} , and the space of rapidly decreasing functions $f(\mu, \phi)$ in this \mathcal{H}_{aux} for Φ . In the LQC literature, Φ is sometimes called Cyl and Φ^* is taken to be its algebraic dual, denoted by Cyl*.

The construction given above is rather general. For the model under consideration, we can extend this construction by using an entirely different subspace of Φ^* for the auxiliary Hilbert space. This is possible because by duality the action of \hat{C} can be extended to all of Φ^* . Let us set $\mathcal{H}'_{\text{aux}} := L^2(\mathbb{R}^2, B(\mu) d\mu d\phi)$. This is a subspace of Φ^* because each $\Psi \in \mathcal{H}'_{\text{aux}}$ defines a linear map from Φ to \mathbb{C} :

$$(\Psi|f\rangle := \sum_{\mu} \int_{-\infty}^{\infty} d\phi B(\mu) \bar{\Psi}(\mu, \phi) f(\mu, \phi) \quad \forall \Psi \in \mathcal{H}'_{\text{aux}} \quad (C2)$$

where the sum over μ converges because $f \in \Phi$ has support only on a countable number of points on the μ -axis and a rapid fall-off. The dual action of \hat{C} on $\mathcal{H}'_{\text{aux}}$ can now be calculated: Since

$$\begin{aligned} (\Psi | \hat{C} f \rangle = \sum_{\mu} \int_{-\infty}^{\infty} d\phi B(\mu) \bar{\Psi} \left[\frac{\partial^2 f}{\partial \phi^2} + [B(\mu)]^{-1} (C^+(\mu) f(\mu + 4\mu_o, \phi) \right. \\ \left. + C^o(\mu) f(\mu, \phi) + C^-(\mu) f(\mu - 4\mu_o)) \right] \end{aligned} \quad (\text{C3})$$

it follows from the definitions of $C^\pm(\mu)$ that

$$\begin{aligned} (\hat{C} \Psi)(\mu, \phi) &= \frac{\partial^2 \Psi}{\partial \phi^2} + [B(\mu)]^{-1} (C^+(\mu) \Psi(\mu + 4\mu_o, \phi) + C^o(\mu) \Psi(\mu, \phi) + C^-(\mu) \Psi(\mu - 4\mu_o)) \\ &\equiv \left[\frac{\partial^2 f}{\partial \phi^2} + \Theta \right] \Psi(\mu, \phi) \end{aligned} \quad (\text{C4})$$

It is straightforward to verify that \hat{C} is self-adjoint on $\mathcal{H}'_{\text{aux}}$. Therefore, we can carry out group averaging on $\mathcal{H}'_{\text{aux}}$ and obtain a new physical Hilbert space. As in the WDW theory of section III B, there are two superselected sectors. We will work with the positive frequency sector and denote it by $\mathcal{H}'_{\text{phy}}$. The Dirac observables \hat{p}_ϕ and $\widehat{\mu|_{\phi_o}}$ on Φ act by duality on $\mathcal{H}'_{\text{aux}}$ and descend naturally to $\mathcal{H}'_{\text{phy}}$.

The final results can be summarized as follows. The new physical Hilbert space $\mathcal{H}'_{\text{phy}}$ is the space of functions $\Psi(\mu, \phi)$ satisfying the positive frequency equation: $-i\partial_\phi \Psi = \sqrt{\Theta} \Psi$, with finite norm:

$$\|\Psi\|_{\text{phy}}'^2 = \int_{\phi=\phi_o} d\mu B(\mu) |\Psi(\mu, \phi)|^2 \quad (\text{C5})$$

and the action of the Dirac observables is the standard one:

$$\widehat{\mu|_{\phi_o}} \Psi(\mu, \phi) = e^{i\sqrt{\Theta}(\phi-\phi_o)} \mu \Psi(\mu, \phi_o), \quad \text{and} \quad \hat{p}_\phi \Psi(\mu, \phi) = -i\hbar \frac{\partial \Psi(\mu, \phi)}{\partial \phi}. \quad (\text{C6})$$

Note that the final physical theory is different from both the WDW theory of III B and the ‘standard’ LQC theory of IV B. Since the inner product (C5) involves an integral rather than a sum, states $\Psi(\mu, \phi)$ now have support on continuous intervals of the μ -axis as in the WDW theory, rather than on a countable number of points as in LQC. However, the states satisfy the LQC type positive frequency equation $-i\partial_\phi \Psi = \sqrt{\Theta} \Psi$, where the operator on the right is the square-root of a *difference* operator rather than of a differential operator, and the measure determining the inner product also involves $B(\mu)$ from LQC rather than $\underline{B}(\mu)$ from the WDW theory. Thus, the dynamical operator is the same as in LQC. *In particular, as in section V, the quantum states exhibit a big bounce.* However, since typical states are continuous on the μ -axis, the spectrum of the Dirac observable $\widehat{\mu|_{\phi_o}}$ is now continuous. In essence, the states $\Psi(\mu, \phi)$ have support on 2-d *continuous* regions of the $\mu - \phi$ plane as in the WDW theory but their dynamics is dictated by a *difference* operator as in LQC. When the cosmological constant is non-zero, the analog of this physical Hilbert space appears to be a natural home to analyze the role of the Kodama state in quantum cosmology [68].

In the literature on ‘polymer representations’, non-relativistic quantum mechanics of point particles and the quantum theory of a Maxwell theory have been discussed in some

detail[45, 85]. In the first case, the standard Schrödinger Hilbert space $L^2(\mathbb{R}, dx)$, and in the second case, the standard Fock space turned out to be subspaces of Cyl^* which were especially helpful for semi-classical analysis. The present auxiliary Hilbert space $\mathcal{H}'_{\text{aux}} \subset \Phi^*$ is completely analogous to these. Therefore the resulting $\mathcal{H}'_{\text{phy}}$ may be more useful for semi-classical considerations. Indeed, since it does not refer to any ε , no coarse graining is required to carry out the semi-classical analysis. Therefore the analog of this construction may well be useful in more general contexts in full LQG.

- [1] A. Ashtekar and J. Lewandowski, Background independent quantum gravity: A status report, *Class. Quant. Grav.* **21**, R53-R152 (2004), [arXiv:gr-qc/0404018](https://arxiv.org/abs/gr-qc/0404018).
- [2] C. Rovelli *Quantum Gravity*, (CUP, Cambridge, 2004).
- [3] T. Thiemann, *Introduction to Modern Canonical Quantum General Relativity* (CUP, Cambridge, at press).
- [4] M. Gasperini and G. Veneziano, The pre-big bang scenario in string cosmology, *Phys. Rept.* **373**, 1 (2003) [arXiv:hep-th/0207130](https://arxiv.org/abs/hep-th/0207130).
- [5] J. Khoury, B. A. Ovrut, P. J. Steinhardt, N. Turok, The Ekpyrotic Universe: Colliding Branes and the Origin of the Hot Big Bang, *Phys. Rev. D* **64** (2001) 123522 [hep-th/0103239](https://arxiv.org/abs/hep-th/0103239).
- [6] J. Khoury, B. A. Ovrut, N. Seiberg, P. J. Steinhardt, N. Turok, From Big Crunch to Big Bang, *Phys. Rev. D* **65** (2002) 086007 [hep-th/0108187](https://arxiv.org/abs/hep-th/0108187).
- [7] R. Brustein and G. Veneziano, The Graceful Exit Problem in String Cosmology, *Phys. Lett.* **B329**, 429 (1994) [arXiv:hep-th/9403060](https://arxiv.org/abs/hep-th/9403060).
- [8] S. J. Rey, Back reaction and graceful exit in string inflationary cosmology, *Phys. Rev. Lett.* **77**, 1929-1932 (1996), [arXiv:hep-th/9605176](https://arxiv.org/abs/hep-th/9605176).
- [9] R. Brustein and R. Madden, Graceful exit and energy conditions in string cosmology, *Phys. Lett.* **B410**, 110 (1997) [arXiv:hep-th/9702043](https://arxiv.org/abs/hep-th/9702043);
A Model of Graceful Exit in String Cosmology, *Phys. Rev. D* **57**, 712-724 (1998), [arXiv:hep-th/9708046](https://arxiv.org/abs/hep-th/9708046).
- [10] R. Kallosh, L. Kofman, A. D. Linde, A. A. Tseytin, BPS branes in cosmology, *Phys. Rev. D* **64**, 123524 (2001) [hep-th/0106241](https://arxiv.org/abs/hep-th/0106241).
- [11] T. Padmanabhan, J. V. Narlikar, Quantum conformal fluctuations in a singular space-time, *Nature* **295**, 677 (1982).
- [12] M. Bojowald, Loop quantum cosmology, *Liv. Rev. Rel.* **8**, 11 (2005), [arXiv:gr-qc/0601085](https://arxiv.org/abs/gr-qc/0601085).
- [13] M. Bojowald, Absence of singularity in loop quantum cosmology, *Phys. Rev. Lett.* **86**, 5227-5230 (2001), [arXiv:gr-qc/0102069](https://arxiv.org/abs/gr-qc/0102069), Isotropic loop quantum cosmology, *Class. Quantum Grav.* **19**, 2717-2741 (2002), [arXiv:gr-qc/0202077](https://arxiv.org/abs/gr-qc/0202077).
- [14] A. Ashtekar, M. Bojowald, J. Lewandowski, Mathematical structure of loop quantum cosmology, *Adv. Theo. Math. Phys.* **7**, 233-268 (2003), [gr-qc/0304074](https://arxiv.org/abs/gr-qc/0304074).
- [15] A. Ashtekar, T. Pawłowski and P. Singh, Quantum Nature of the Big Bang, *Phys. Rev. Lett.* **96**, 141301 (2006). [arXiv:gr-qc/0602086](https://arxiv.org/abs/gr-qc/0602086).
- [16] M. Bojowald and F. Hinterleitner, Isotropic loop quantum cosmology with matter, *Phys. Rev. D* **66**, 104003 (2002), [arXiv:gr-qc/0207038](https://arxiv.org/abs/gr-qc/0207038).
- [17] F. Hinterleitner and S. Major, Isotropic loop quantum cosmology with matter II: The Lorentzian constraint, *Phys. Rev. D* **68**, 12403 (2003), [arXiv:gr-qc/0309035](https://arxiv.org/abs/gr-qc/0309035).
- [18] M. Bojowald, G. Date and K. Vandersloot, Homogeneous loop quantum cosmology: The role

of the spin connection, *Class. Quantum Grav.* **21**, 1253-1278 (2005), [arXiv:gr-qc/0311004](https://arxiv.org/abs/gr-qc/0311004).

[19] M. Bojowald, Non-singular black holes and degrees of freedom in quantum gravity, *Phys. Rev. Lett.* **95**, 061301 (2005), [arXiv:gr-qc/0506128](https://arxiv.org/abs/gr-qc/0506128).

[20] A. Ashtekar and M. Bojowald, Quantum geometry and the Schwarzschild singularity, *Class. Quant. Grav.* **2** (2006) 391-411, [arXiv:gr-qc/0509075](https://arxiv.org/abs/gr-qc/0509075).

[21] M. Bojowald, Inflation from quantum geometry, *Phys. Rev. Lett.* **89**, 261302 (2002), [arXiv:gr-qc/0206054](https://arxiv.org/abs/gr-qc/0206054).

[22] M. Bojowald and G. Date, Quantum suppression of the genral chaotic behavior close to cosmological singularities *Phys. Rev. Lett.* **92**, 071302 (2004), [arXiv:gr-qc/0311003](https://arxiv.org/abs/gr-qc/0311003).

[23] S. Tsujikawa, P. Singh and R. Maartens, Loop quantum gravity effects on inflation and the CMB, *Class. Quantum Grav.* **21**, 5767-5775 (2004), [arXiv:astro-ph/0311015](https://arxiv.org/abs/astro-ph/0311015).

[24] J. Willis, On the low energy ramifications and a mathematical extension of loop quantum gravity, Ph.D. Dissertation, The Pennsylvania State University (2004); A. Ashtekar, M. Bojowald and J. Willis, Corrections to Friedmann equations induced by quantum geometry, IGPG preprint (2004).

[25] G. Date and G. M. Hossain, Genericity of inflation in isotropic loop quantum cosmology, *Phys. Rev. Lett.* **94**, 011301 (2005), [arXiv:gr-qc/0407069](https://arxiv.org/abs/gr-qc/0407069).

[26] G. Date and G. M. Hossain, Genericity of big bounce in isotropic loop quantum cosmology, *Phys. Rev. Lett.* **94**, 011302 (2005), [arXiv:gr-qc/0407074](https://arxiv.org/abs/gr-qc/0407074).

[27] M. Bojowald, R. Maartens and P. Singh, Loop quantum gravity and the cyclic universe, *Phys. Rev. D* **70**, 083517 (2004), [arXiv:hep-th/0407115](https://arxiv.org/abs/hep-th/0407115).

[28] S. Hofmann and O. Winkler, The spectrum of fluctuations in inflationary quantum cosmology, [arXiv:astro-ph/0411124](https://arxiv.org/abs/astro-ph/0411124).

[29] J. E. Lidsey, Early universe dynamics in semi-classical loop quantum cosmology, *JCAP* **0412**, 007 (2004), [arXiv:gr-qc/0411124](https://arxiv.org/abs/gr-qc/0411124).

[30] G. Date, Absence of Kasner singularity in the effective dynamics of loop quantum cosmology, *Phys. Rev. D* **71**, 127502 (2005), [arXiv:gr-qc/05005002](https://arxiv.org/abs/gr-qc/05005002).

[31] G. M. Hossain, Primordial density perturbations in effective loop quantum cosmology, *Class. Quantum Grav.* **22**, 2511-2532 (2005), [arXiv:gr-qc/0411012](https://arxiv.org/abs/gr-qc/0411012).

[32] P. Singh, Effective state metamorphosis in semi-classical loop quantum cosmology, *Class. Quantum Grav.* **22**, 4203-4216 (2005), [arXiv:gr-qc/0502086](https://arxiv.org/abs/gr-qc/0502086).

[33] P. Singh and K. Vandersloot, Semi-classical states, effective dynamics and classical emergence in loop quantum cosmology, *Phys. Rev. D* **72**, 084004 (2005), [arXiv:gr-qc/0507029](https://arxiv.org/abs/gr-qc/0507029).

[34] D. Marolf, Refined algebraic quantization: Systems with a single constraint [arXiv:gr-qc/9508015](https://arxiv.org/abs/gr-qc/9508015);
 Quantum observables and recollapsing dynamics, *Class. Quant. Grav.* **12** (1995) 1199-1220 [arXiv:gr-qc:9404053](https://arxiv.org/abs/gr-qc:9404053)
 Observables and a Hilbert space for Bianchi IX, *Class. Quant. Grav.* **12** (1995) 1441-1454 [arXiv:gr-qc:9409049](https://arxiv.org/abs/gr-qc:9409049)
 Almost ideal clocks in quantum cosmology: A brief derivation of time, *Class. Quant. Grav.* **12** (1995) 2469-2486 [arXiv:gr-qc:9412016](https://arxiv.org/abs/gr-qc:9412016).

[35] A. Ashtekar, J. Lewandowski, D. Marolf, J. Mourão and T. Thiemann, Quantization of diffeomorphism invariant theories of connections with local degrees of freedom *Jour. Math. Phys.* **36** 6456-6493 (1995).

[36] J. Brunnemann and T. Thiemann, On(cosmological) singularity avoidance in loop quantum gravity, [arXiv:gr-qc/0505032](https://arxiv.org/abs/gr-qc/0505032)

[37] A. Ashtekar, T. Pawłowski and P. Singh, Quantum nature of the Big Bang: An analytical and numerical investigation, II (IGPG pre-print).

[38] J. Lewandowski, A. Okolow, H. Sahlmann and T. Thiemann, Uniqueness of diffeomorphism invariant states on holonomy flux algebras, [arXiv:gr-qc/0504147](https://arxiv.org/abs/gr-qc/0504147).

[39] C. Fleischhack, Representations of the Weyl algebra in quantum geometry, [arXiv:math-ph/0407006](https://arxiv.org/abs/math-ph/0407006).

[40] A. Ashtekar and J. Lewandowski, Representation theory of analytic holonomy algebras, in *Knots and Quantum Gravity*, ed J. Baez, (Oxford U. Press, Oxford, 1994).

[41] J. C. Baez, Generalized measures in gauge theory, *Lett. Math. Phys.* **31**, 213-223 (1994).

[42] D. Marolf and J. Mourão, On the support of the Ashtekar-Lewandowski measure, *Commun. Math. Phys.* **170**, 583-606 (1995).

[43] A. Ashtekar and J. Lewandowski, Projective techniques and functional integration, *Jour. Math. Phys.* **36**, 2170-2191 (1995).

[44] A. Ashtekar and J. Lewandowski, Differential geometry on the space of connections using projective techniques *Jour. Geo. & Phys.* **17**, 191-230 (1995)

[45] A. Ashtekar, S. Fairhurst and J. Willis, Quantum gravity, shadow states, and quantum mechanics, *Class. Quantum Grav.* **20**, 1031-1062 (2003), [arXiv:gr-qc/0207106](https://arxiv.org/abs/gr-qc/0207106).

[46] A. Ashtekar and J. Lewandowski, Quantum theory of geometry I: Area operators, *Class. Quant. Grav.* **14** A55–A81 (1997).

[47] Thiemann, T. (1996) Anomaly-free formulation of non-perturbative, four-dimensional Lorentzian quantum gravity, *Phys. Lett.* **B380**, 257–264; (1998)
Quantum spin dynamics (QSD), *Class. Quant. Grav.* **15** 839–873; (1998)
QSD V : Quantum gravity as the natural regulator of matter quantum field theories, *Class. Quant. Grav.* **15**, 1281–1314.

[48] W. Kaminski, personal communication to AA (November 2005).

[49] C. Kiefer, Wave packets in minisuperspace, *Phys. Rev. Rev.* **D38**, 1761-1772 (1988).

[50] J. B. Hartle and D. Marolf, Comparing formulations of generalized quantum mechanics for reparametrization-invariant systems, *Phys. Rev.* **D56**, 6247-6257 (1997) [arXiv:gr-qc/9703021](https://arxiv.org/abs/gr-qc/9703021).

[51] A. Ashtekar, *Lectures on non-perturbative canonical gravity*, Notes prepared in collaboration with R. S. Tate (World Scientific, Singapore, 1991), Chapter 10.

[52] A. Ashtekar and R. S. Tate, An algebraic extension of Dirac quantization: Examples, *Jour. Math. Phys.* **35** 6434–6470 (1994).

[53] J. Louko and C. Rovelli, *J. Math. Phys.* **D41**, 132-155 (2000), [arXiv:gr-qc/9907004](https://arxiv.org/abs/gr-qc/9907004).

[54] I. M. Gel'fand and G. E. Shilov, *Generalized functions*, Volume 4, translated by M. E. Mayer (Academic Press, New York and London, 1967)

[55] A. Ashtekar, J. C. Baez, A. Corichi and K. Krasnov, Quantum geometry and black hole entropy, *Phys. Rev. Lett.* **80** 904–907 (1998).

[56] A. Ashtekar, J. C. Baez and K. Krasnov, Quantum geometry of isolated horizons and black hole entropy, *Adv. Theo. Math. Phys.* **4** 1–95 (2000).

[57] T. Thiemann, The phoenix project: Master constraint program for loop quantum gravity, [arXiv:gr-qc/0305080](https://arxiv.org/abs/gr-qc/0305080); T. Thiemann and B. Dittrich, Testing the master constraint program for loop quantum gravity I. General Framework, *Class. Quantum. Grav.* **23** 1025-1066 (2006).

[58] R. Stephens, G. 't Hooft and B. F. Whiting, Black hole evaporation without information loss, *Class. Quant. Grav.* **11**, 621 (1994), [arXiv:gr-qc/9310006](https://arxiv.org/abs/gr-qc/9310006).

[59] C. Rovelli, Time In Quantum Gravity: Physics Beyond The Schrödinger Regime, *Phys. Rev.*

D **43**, 442 (1991).

[60] A. Ashtekar and J. Stachel, eds *Conceptual problems of Quantum Gravity* (Birkhäuser, Boston, 1988).

[61] K. Kuchar, Time and Interpretations of Quantum Gravity, in Proc 4th Canadian Conf on "General Relativity and Relativistic Astrophysics", G. Kunstatter, D. Vincent, J. Williams eds (World Scientific Singapore 1992).

[62] C. J. Isham, Canonical Quantum Gravity and the Problem of Time, in "Integrable systems, quantum groups and quantum field theories", eds. LA Ibort and MA Rodriguez, Salamanca (Kluwer, London, 1993), [arXiv:gr-qc/9210011](https://arxiv.org/abs/gr-qc/9210011).

[63] T. Padmanabhan, A definition for time in Quantum Cosmology, *Pramana* **35**, L199 (1990); Y. Ohkuwa, Semiclassical time variable in cosmology with a massless scalar field (KEK preprint, 1995).

[64] J. Greensite, Ehrenfest's Principle In Quantum Gravity, *Nucl. Phys. B* **351**, 749 (1991).

[65] T. Brotz and C. Kiefer, Ehrenfest's Principle and the Problem of Time in Quantum Gravity, *Nucl. Phys. B* **475**, 339 (1996) [arXiv:gr-qc/9602033](https://arxiv.org/abs/gr-qc/9602033).

[66] J. D. Brown and K. Kuchar, Dust as a standard of space and time in canonical gravity, *Physical Review* **D51**, 5600–5629 (1995); [arXiv:gr-qc/9409001](https://arxiv.org/abs/gr-qc/9409001).

[67] L. Smolin, Time, measurement and information loss in quantum cosmology, [arXiv:gr-qc/9001016](https://arxiv.org/abs/gr-qc/9001016)

[68] S. Alexander, J. Malecki and L. Smolin, Quantum gravity and inflation, *Phys. Rev.* **D70** 044025 (2004), [arXiv:hep-th/0309045](https://arxiv.org/abs/hep-th/0309045);
J. Malecki, Inflationary quantum cosmology: General framework and exact Bianchi I solution, *Phys. Rev.* **D70** 084040 (2004).

[69] J. D. Bekenstein, Nonsingular general-relativistic cosmologies, *Phys. Rev. D* **11**, 2072 (1975).

[70] J. V. Narlikar, T. Padmanabhan, Creation-field cosmology: A possible solution to singularity, horizon, and flatness problems, *Phys. Rev. D* **32**, 1928 (1985).

[71] V. Mukhanov, R. Brandenberger, A Nonsingular Universe, *Phys. Rev. Lett.* **68**, 1969 (1992).

[72] G. N. Felder, A. V. Frolov, L. Kofman and A. V. Linde, Cosmology with negative potentials, *Phys. Rev. D* **66**, 023507 (2002) [arXiv:hep-th/0202017](https://arxiv.org/abs/hep-th/0202017)

[73] Y. Shtanov and V. Sahni, Bouncing braneworlds, *Phys. Lett. B* **557**, 1 (2003), [arXiv:gr-qc/0208047](https://arxiv.org/abs/gr-qc/0208047).

[74] S. Mukherji and M. Peloso, Bouncing and cyclic universes from brane models *Phys. Lett. B* **547**, 297 (2002), [arXiv:hep-th/0205180](https://arxiv.org/abs/hep-th/0205180).

[75] J. L. Hovdebo and R. C. Myers, Bouncing braneworlds go crunch!, *JCAP* **0311**, 012 (2003), [arXiv:hep-th/0308088](https://arxiv.org/abs/hep-th/0308088).

[76] M. Bojowald, Spherically symmetric quantum geometry: Hamiltonian constraint, *Class.Quant.Grav.* **23** 2129–2154 (2006), [arXiv:gr-qc/0511108](https://arxiv.org/abs/gr-qc/0511108)

[77] T. Hertog and G. Horowitz, Holomorphic description of ADS cosmologies, *JHEP* 0504, 005 (2005), [arXiv:hep-th/0503071](https://arxiv.org/abs/hep-th/0503071).

[78] M. Bojowald, H. H. Hernandez and H. A. Morales-Tecotl, Perturbative degrees of freedom in loop quantum gravity: Anisotropies, *Class. Quant. Grav.*, **18** L117–L127 (2001) [arXiv:gr-qc/0511058](https://arxiv.org/abs/gr-qc/0511058).

[79] J. B. Hartle and S. W. Hawking, Wave Function Of The Universe, *Phys. Rev. D* **28**, 2960 (1983).

[80] N. Dadhich, Singularity: Is Raychaudhuri equation required once again, to appear in: *Raychaudhuri Memorial Volume*.

- [81] A. Ashtekar and T. Schilling, Geometrical formulation of quantum mechanics, In: *On Einstein's path*, A. Harvey, ed (Springer-Verlag, New York, 1998); [arXiv:gr-qc/9706069](https://arxiv.org/abs/gr-qc/9706069); T. Schilling, Geometry of quantum mechanics, Ph.D. Dissertation, Penn State (1996), <http://cgpg.gravity.psu.edu/archives/thesis/index.shtml>
- [82] V. Taveras, IGPG preprint (2006)
- [83] A. Ashtekar, L. Bombelli and A. Corichi, Semiclassical states for constrained systems, Phys. Rev. **D72**, 025008 (2005) [gr-qc/0504052](https://arxiv.org/abs/gr-qc/0504052).
- [84] A. Perez, On the regularization ambiguities in loop quantum gravity, Phys. Rev. D **73** (2006) 044007, [arXiv:gr-qc/0509118](https://arxiv.org/abs/gr-qc/0509118).
- [85] A. Ashtekar and J. Lewandowski, Relation between polymer and Fock excitations, Class. Quant. Grav. **18** L117-L128 (2001), [arXiv:gr-qc/0107043](https://arxiv.org/abs/gr-qc/0107043).